Received: 17 March 2023 | Revised: 15 July 2023 | Accepted: 8 August 2023

DOI: 10.1002/ar.25310

RESEARCH ARTICLE

The Anatomical Record WILEY

The fossil record of appendicular muscle evolution in Synapsida on the line to mammals: Part II—Hindlimb

Peter J. Bishop[1,2] | **Stephanie E. Pierce**[1]

[1]Museum of Comparative Zoology and Department of Organismic and Evolutionary Biology, Harvard University, Cambridge, Massachusetts, USA

[2]Geosciences Program, Queensland Museum, Brisbane, Queensland, Australia

Correspondence
Peter J. Bishop, Museum of Comparative Zoology and Department of Organismic and Evolutionary Biology, Harvard University, Cambridge, MA, USA.
Email: pbishop@fas.harvard.edu

Funding information
William F. Milton Fund, Harvard University; United States National Science Foundation, Grant/Award Numbers: DEB-1754459, EAR-2122115

Abstract

This paper is the second in a two-part series that charts the evolution of appendicular musculature along the mammalian stem lineage, drawing upon the exceptional fossil record of extinct synapsids. Here, attention is focused on muscles of the hindlimb. Although the hindlimb skeleton did not undergo as marked a transformation on the line to mammals as did the forelimb skeleton, the anatomy of extant tetrapods indicates that major changes to musculature have nonetheless occurred. To better understand these changes, this study surveyed the osteological evidence for muscular attachments in extinct mammalian and nonmammalian synapsids, two extinct amniote outgroups, and a large selection of extant mammals, saurians, and salamanders. Observations were integrated into an explicit phylogenetic framework, comprising 80 character–state complexes covering all muscles crossing the hip, knee, and ankle joints. These were coded for 33 operational taxonomic units spanning >330 Ma of tetrapod evolution, and ancestral state reconstruction was used to evaluate the sequence of muscular evolution along the stem lineage from Amniota to Theria. The evolutionary history of mammalian hindlimb musculature was complex, nonlinear, and protracted, with several instances of convergence and pulses of anatomical transformation that continued well into the crown group. Numerous traits typically regarded as characteristically "mammalian" have much greater antiquity than previously recognized, and for some traits, most synapsids are probably more reflective of the ancestral amniote condition than are extant saurians. More broadly, this study highlights the utility of the fossil record in interpreting the evolutionary appearance of distinctive anatomies.

KEYWORDS

evolution, fossils, hindlimb, mammal, musculature, synapsid

1 | INTRODUCTION

Among extant tetrapods, mammals are distinctive for the breadth of locomotor strategies that they employ in almost every environment (Biewener & Patek, 2018). Underpinning this functional diversity was a shift in stance and gait within Synapsida, away from the "sprawled" posture inferred as ancestral for all amniotes to the "erect" posture characteristic of terrestrial therians. Changes in locomotor function involved substantial anatomical transformation in the limbs and vertebral column of synapsids, and much of this is documented by an

exceptionally rich fossil record spanning >320 Ma (Kemp, 1982, 2005, 2016). Study of the synapsid fossil record indicates that, on the line with mammals, the forelimb skeleton underwent a more profound set of changes compared to that of the hindlimb, including reduction or loss of most bones of the pectoral girdle, alteration of the glenoid to become a ventrally oriented cup, and development of a novel sternal complex (e.g., Bendel et al., 2022; Guignard et al., 2019a; Jenkins & Parrington, 1976; Jenkins, 1971; Kemp, 1980b; Lai et al., 2018; Romer, 1922). This is paralleled by a greater diversity in musculoskeletal adaptations and functions in the forelimb of extant mammals compared to the hindlimb (Polly, 2007).

Despite its less dramatic history of skeletal evolution, the mammalian hindlimb is nevertheless highly distinctive among extant tetrapods in terms of its muscular anatomy. This is especially true in the proximal limb, such that hypotheses of muscle and bone surface homology have had a long history of flux (Diogo et al., 2016; Jenkins, 1971; Jones, 1979; Parrington, 1961; Romer, 1922, 1924). Moreover, the hindlimb is crucial as the primary propulsive organ during terrestrial locomotion in most species (Alexander, 2006; Biewener & Patek, 2018). How this critical role was maintained during substantial postural evolution on the line to mammals, and throughout their subsequent ecological radiation, is a key question remaining to be answered. With rare exceptions, decades of prior studies of hindlimb functional evolution in nonmammalian synapsids have featured mostly qualitative and correlative (rather than causative and mechanistic) appraisals of the relationship between musculoskeletal anatomy and function (Bakker, 1971; Blob, 2001; Boonstra, 1955b, 1967; Colbert, 1948; Fröbisch, 2006; Gregory, 1926; Guignard et al., 2018; Jenkins, 1971; Kemp, 1978, 1980a, 1980b, 1982, 1985; King, 1981a, 1981b, 1985; Preuschoft et al., 2022; Ray, 2006; Ray & Chinsamy, 2003; Sullivan et al., 2013). This has hampered attempts to understand how anatomy and mechanics facilitated or constrained locomotor evolution on the line to mammals, and indeed at times has contributed to paradoxical interpretations of "erect" hindlimb posture but "sprawled" forelimb posture in various species (Abbott, 2019; Guignard et al., 2018; Jenkins, 1970, 1971; Kemp, 1980a, 1982; King, 1981a; Ray, 2006).

Understanding the deep evolutionary history of the musculature of the mammalian hindlimb can provide key context for investigating the origins of its distinctive musculoskeletal anatomy, and how this influenced locomotor biomechanics across profound functional and ecological change. In a similar fashion to the companion study on the forelimb (Bishop & Pierce, 2023), the present study draws upon the fossil record of nonmammalian synapsids, integrating osteological data with the anatomy of extant tetrapods in an explicit phylogenetic framework (Burch, 2014; Hutchinson, 2001a, 2001b, 2002; Molnar et al., 2018, 2020; Witmer, 1995) to infer the evolution of hindlimb musculature through time, focusing on muscles crossing the hip, knee, and ankle. Adopting a fossil-rich approach can help overcome obstacles imposed by stark disparities between the anatomies of extant taxa, a problem that is particularly prevalent in studies of nonmammalian synapsids. In addition to charting the evolution of hindlimb musculature on the line to mammals, the present study lays the foundation for the rigorous, phylogenetically informed reconstruction of hindlimb anatomy and function in extinct species, paving the way toward a more comprehensive understanding of locomotor evolution within Synapsida.

2 | MATERIALS AND METHODS

The present study follows the same approach as outlined in the companion study on the synapsid forelimb (Bishop & Pierce, 2023). The scope of taxa considered here, their assumed phylogenetic relationships, and their representation as operational taxonomic units (OTUs) for the purpose of phylogenetic analysis is illustrated in Figure 1.

2.1 | Source of data

For extant taxa, information on the anatomy of salamanders (Caudata, representing lissamphibians as an amniote outgroup) was derived from published literature accounts including Mivart (1869), Perrin (1893), Davison (1895), Wilder (1912), Francis (1934), Schaeffer (1941a), Ashley-Ross (1992), Walthall and Ashley-Ross (2006), and Diogo and Molnar (2014). Three principal saurian groups were included: Rhynchocephalia (i.e., *Sphenodon*), Squamata, and Crocodylia. Studies of *Sphenodon* that were consulted include Perrin (1895), Osawa (1897), Gregory and Camp (1918), and Byerly (1925), with additional details sourced from Schaeffer (1941a), Hutchinson (2001a, 2001b, 2002), and Russell and Bauer (2008). Studies of squamates that were consulted include De Vis (1884), Perrin (1893), Romer (1922), Schaeffer (1941a), Snyder (1954), Brinkman (1980b), Landsmeer (1990), Russell (1993), Dilkes (1999), Zaaf et al. (1999), Russell and Bauer (2008), Anzai et al. (2014), and Dick and Clemente (2016), with additional details sourced from Hutchinson (2001a, 2001b, 2002). Crocodylians were used to represent Archosauria; avian hindlimb anatomy is highly derived, whereas the anatomy of extant crocodylians is inferred to closely reflect

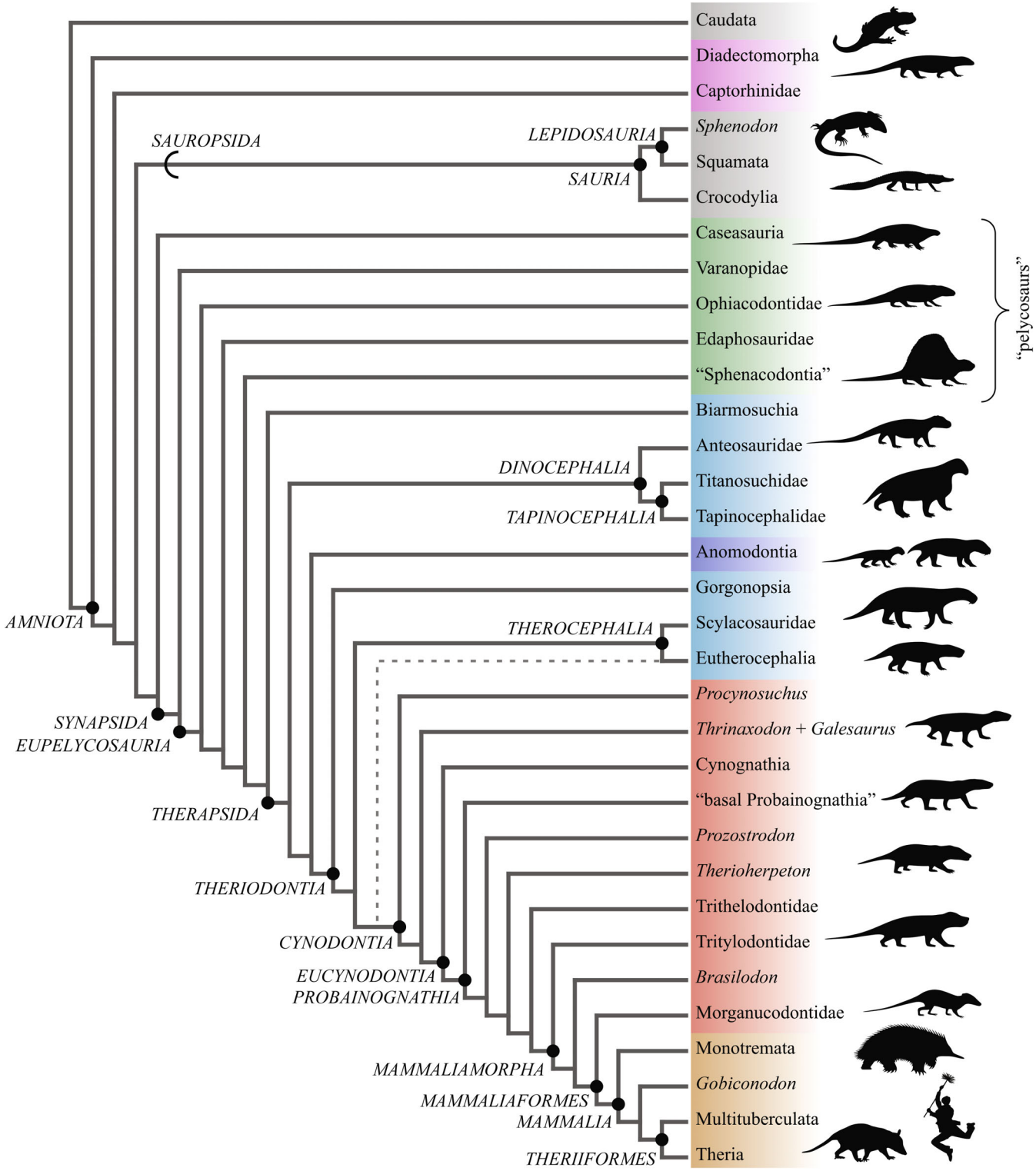

FIGURE 1 Phylogenetic interrelationships of operational taxonomic units used for character state mapping in the study, following Bishop and Pierce (2023). Key clades are labeled, and major groups referred to in subsequent figures are indicated by different colors. Note that "Sphenacodontia" as coded here is a paraphyletic taxon comprising all nontherapsid sphenacodontians, and that "basal Probainognathia" is a paraphyetic taxon comprising all probainognathian cynodonts more basal than *Prozostrodon*. The term "pelycosaur" refers to any nontherapsid synapsid. For the purposes of this study, "Scylacosauridae" includes both lycosuchid and scylacosaurid therocephalians. Note that Sauropsida is a far more inclusive clade than Sauria, although in the present study, both are represented by extant saurian lineages only. The dashed line indicates an alternative topology that was considered here, where eutherocephalians are more closely related to cynodonts than other therocephalians.

the condition plesiomorphic for Archosauria in most respects (Gatesy, 1999; Hutchinson, 2001a, 2001b, 2002; Hutchinson & Gatesy, 2000). Consulted literature included Romer (1923), Brinkman (1980a), Cong et al. (1998), Hutchinson (2001a, 2001b, 2002), Otero et al. (2010), Suzuki et al. (2011), Allen et al. (2015), and Hattori and Tsuihiji (2021). In some instances, the anatomy of testudines, although derived in many respects, provided additional perspective on Archelosauria as a whole (Walker, 1973; Zug, 1971). Within mammals, studies on monotremes that were consulted include Coues (1871), Westling (1889), Gregory and Camp (1918), Walter (1988a), and Gambaryan et al. (2002). Information on therian anatomy was drawn from studies of basal marsupials and placentals with a "generalized" quadrupedal anatomy, including Murie and Mivart (1865), Coues and Wyman (1872), MacCormick (1887), Romer (1922), Le Gros Clark (1924), Le Gros Clark (1926), Elftman (1929), Greene (1935), Rinker (1954), Barbour (1963), Brannen (1979), George (1977), Stein (1981), Stein (1986), Diogo and Molnar (2014), Warburton et al. (2015), and Charles et al. (2016).

The osteology of extinct taxa was investigated through extensive first-hand observation and/or photography of fossil material; abbreviations used herein for institutional collections are as follows: AMNH: American Museum of Natural History, New York, USA; BP: Evolutionary Studies Institute, University of the Witwatersrand, Johannesburg, South Africa; BSPG: Bayerische Staatssammlung für Paläontologie und Geologie, Munich, Germany; CGS: Council for Geosciences, Pretoria, South Africa; FMNH: Field Museum of Natural History, Chicago, USA; GPIT: Paläontologische Sammlung, Eberhard Karls Universität, Tübingen, Germany; MACN: Museo Argentino de Ciencias Naturales "Bernardino Rivadavia," Buenos Aires, Argentina; MCZ: Museum of Comparative Zoology, Harvard University, Cambridge, USA; MNC, Museum für Naturkunde, Chemnitz, Germany; NHCC: National Heritage Conservation Commission, Lusaka, Zambia; NHMUK: Natural History Museum, London, UK; NMQR: National Museum, Bloemfontein, South Africa; NMT: National Museum of Tanzania, Dar es Salaam, Tanzania; PVL: Instituto Miguel Lillo (Paleovertebrados), Universidad Nacional de Tucumán, Tucumán, Argentina; RC: Rubidge Collection, Wellwood, Graaf-Reinet, South Africa; SAM: Iziko South African Museum, Cape Town, South Africa; TM: Ditsong National Museum of Natural History, Pretoria, South Africa; UCMP: Museum of Paleontology, University of California, Berkeley, USA; UFRGS: Departamento de Paleontologia e Estratigrafia, Instituto de Geociências, Universidade Federal do Rio Grande do Sul, Porto Alegre, Brazil; UMZC: University Museum of Zoology, Cambridge, UK; USNM: National Museum of Natural History, Smithsonian Institution, Washington, DC, USA.

Study of fossil material was supplemented with reference to the published literature including Williston (1911), Simpson and Elftman (1928), Haughton (1929), Watson (1931), Boonstra (1934), Broili and Schröder (1935), Romer and Price (1940), Schaeffer (1941b), Broom (1947), Young (1947), Colbert (1948), Brink and Kitching (1951), Boonstra (1955a), Attridge (1956), Kühne (1956), Cox (1959), Watson (1960), Parrington (1961), Bonaparte (1963), Boonstra (1964), Boonstra (1965), Fox and Bowman (1966), Cruickshank (1967), Cys (1967), Jenkins (1971), Sigogneau and Tchudinov (1972), Jenkins and Parrington (1976), Cluver (1978), Kemp (1978, 1980a, 1980b), Brinkman (1981b), King (1981a, 1981b), Krause and Jenkins (1983), Tchudinov (1983), King (1985), Sun and Li (1985), DeFauw (1986), Kemp (1986), Jenkins and Schaff (1988), Sigogneau-Russell (1989), Sumida (1989), Rougier (1993), Kielan-Jaworowska and Gambaryan (1994), Rubidge et al. (1994), King (1996), Rubidge and Hopson (1996), Bonaparte and Barberena (2001), Holmes (2003), Berman et al. (2004), Maisch et al. (2004), Martin (2005), Martinelli et al. (2005), Sues and Jenkins (2006), Fourie and Rubidge (2007), Hurum and Kielan-Jaworowska (2008), Fourie and Rubidge (2009), Liu and Powell (2009), Campione and Reisz (2010), De Oliveira et al. (2010), Fröbisch and Reisz (2011), Kammerer et al. (2013), Sullivan et al. (2013), Yuan et al. (2013), Sumida et al. (2014), Spindler (2016), Gaetano et al. (2017), Sidor and Hopson (2017), Liu et al. (2017), Wynd et al. (2017), Guignard et al. (2018), Butler et al. (2019), Guignard et al. (2019a), Guignard et al. (2019b), Berman et al. (2020), Mocke et al. (2020), and Werneburg et al. (2022).

Inferred homologies of muscles across crown tetrapods, particularly within amniotes, follow those outlined by previous studies (Table 1; Diogo & Molnar, 2014; Diogo et al., 2016; Romer, 1922). These hypotheses are based on topographic similarities of origin, insertion, and spatial relationships with respect to adjacent musculature and other soft tissues; patterns of embryological development; and innervation.

2.2 | Phylogenetic analysis of muscle evolution

An explicit phylogenetic approach was used to document osteological evidence of muscle attachment, and to rigorously analyze the pattern of muscle evolution along the mammalian stem lineage. A full description of the methodology used is outlined in the companion paper (Bishop & Pierce, 2023; see also Supporting Information Appendix 3 of that paper), and is briefly summarized here.

To formalize variation in muscle attachments across the taxa considered, character–state complexes were

TABLE 1 Homology scheme used here for muscle correspondences across extant taxa, with names (and abbreviations) used in this study.

Muscle	Caudata	*Sphenodon*	Squamata	Crocodylia	Monotremata	Theria
Iliotibialis	IT, anterior head	IT, anterior head	IT, anterior head	Three heads (IT1–3)	Rectus femoris (RF)	Rectus femoris (RF)
	IT, posterior head	IT, posterior head	IT, posterior head		Gluteus maximus (GMAX)	Gluteus maximus (GMAX) anteriorly, femorococcygeus (FCOC) posteriorly
Ambiens		AMB	AMB	Two heads: AMB1 and AMB2	AMB ("gracilis anterior" of Gambaryan et al., 2002)	Sartorius (SART)
Femorotibialis		FMT	Femorotibialis exterus (FMTE) and internus (FMTI)	Femorotibialis exterus (FMTE) and internus (FMTI)	Vastus lateralis (VL) and medialis (VM)	VL and VM in marsupials, with additional head in placentals (vastus intermedia, VI)
Iliofemoralis	IF	IF	IF	IF	Two heads in *Tachyglossus* (gluteus medius [GMED] and minimus [GMIN]), single head in *Ornithorhynchus* (GMED)	≥3 heads: gluteus minimus (GMIN), gluteus medius (GMED) and piriformis (PIR)
Puboischiofemoralis internus	PIFI	PIFI anterior and posterior heads	PIFI 1–3 (subdivision variable)	PIFI 1–2	Iliopsoas (ILPS), in part	Iliacus (ILC) and psoas major (PSO), in part; sometimes fused into singular iliopsoas (ILPS)
Puboischiofemoralis externus	PIFE	PIFE	PIFE	Three heads (PIFE 1, 2, 3)	Obturator externus (OBEX) and quadratus femoris (QF)	Obturator externus (OBEX) and quadratus femoris (QF)
Iliofibularis	ILFB	ILFB	ILFB	ILFB		Tenuissimus (TEN), often absent
Flexor tibialis internus 1	"Ischioflexorius," comprising proximal and distal bellies	FTI1	FTI1	"FTI1"	Semimembranosus (SMEM), with anterior and posterior heads	Semimembranosus (SMEM), sometimes with two heads

TABLE 1 (Continued)

Muscle		Caudata	*Sphenodon*	Squamata	Crocodylia	Monotremata	Theria
	2	longitudinally separated by tendon	FTI2, superficial and deep heads	FTI2, superficial and deep heads	"FTI3"	Biceps femoris (BICF), singular	Biceps femoris (BICF), sometimes with two heads
	3				"FTI4"		
Flexor tibialis externus			FTE	FTE	FTE	Semitendinosus (STEN), with vertebral (anterior) and ischiadic (posterior) heads	Semitendinosus (STEN), with vertebral (anterior) and ischiadic (posterior) heads
Puboischiotibialis		PIT	PIT	PIT	Two heads, PIT and FTI2	Gracilis (GRA)	Gracilis (GRA), sometimes bipartite
Pubotibialis		PUT	PUT	PUT		Pectineus (PECN), in part	Pectineus (PECN), in part
						Adductor longus (ADDL), in part	Adductor longus (ADDL), in part
Adductor femoris		ADD	ADD	ADD	Two heads, ADD1 and ADD2	Adductor magnus (ADDM)	Adductor magnus (ADDM) and brevis (ADDB); placentals can possess additional heads
Ischiotrochantericus		ISTR	ISTR	ISTR	ISTR	ISTR (GEM?)	obturator internus (OBIN)
							gemellus (GEM), typically with superior and inferior subdivisions
Caudofemoralis		CF	Two heads: longus (CFL) and brevis (CFB)	Two heads: longus (CFL) and brevis (CFB)	Two heads: longus (CFL) and brevis (CFB)	CF	CF
Gastrocnemius	externus	"flexor primordialis communis"	GE, superifical and deep subdivisions	GE, superifical and deep subdivisions	GE	Gastocnemius lateralis (GL)	Gastocnemius lateralis (GL)
							Soleus (SOL)
						Plantaris (PLA)	Plantaris (PLA)

(Continues)

TABLE 1 (Continued)

Muscle		Caudata	*Sphenodon*	Squamata	Crocodylia	Monotremata	Theria
	internus		GI, tibial, and fibular subdivisions	GI	GI	Gastrocnemius medialis (GM)	Gastrocnemius medialis (GM)
Flexor digitorum longus			FDL, three or four subdivisions	FDL, variable levels of subdivision	FDL	FDL	FDL
Flexor digitorum brevis		FDB	FDB	FDB	FDB, superficial and deep heads	FDB	FDB
Flexor hallucis longus			FHL, partially differentiated from FDL?		FHL		FHL
Extensor digitorum longus		EDL	EDL	EDL	EDL	EDL	EDL, subdivided into some marsupials
Extensor digitorum brevis		EDB	EDB	EDB	EDB	EDB	EDB "extra peroneal heads," including tertius, digiti terti quarti, and quinti
Extensor hallucis longus			EHL	EHL	EHL	EHL	EHL
Tibialis anterior		Bipartite: "extensor cruris tibialis" and "extensor tarsi tibialis"	TA	TA	TA	TA	TA
Peroneus	longus	"Extensor cruris et tarsi fibularis"	Singular head	PL	PL	PL	PL, bipartite in some taxa
	brevis			PB	PB	PB	PB
Pronator profundus		PP	PP	PP	PP	Tibialis posterior (TP)	Tibialis posterior (TP)
Popliteus		Only IC has previously been recognized (two possibly fused?)	POP	POP	POP	POP	POP
Interosseus cruris			IC	IC	IC, sometimes inseparable from POP proximally	IC (absent in *Ornithorhynchus*)	IC, sometimes inseparable from POP proximally

Note: This table omits several muscles found in the salamander hindlimb (i.e., femorofibularis, flexores accessories lateralis et medialis, caput longum musculorum contrahentium; see Diogo & Molnar, 2014) which have no clear equivalent in amniotes. Further work is needed to resolve the homologies of these muscles, but for the purposes of the current study, they will be tentatively treated as salamander apomorphies. Gray cells denote the absence of a muscle.

created and codified for a dense sample of (mostly suprageneric) OTUs spanning from basal synapsids to extant mammals, in addition to several outgroups; a total of 33 OTUs were coded. The construction of character–state complexes considered both taxic and transformational perspectives to homology (Patterson, 1982), allowing for transformational hypotheses to be incorporated and tested. For practical reasons, the broad phylogenetic scope of this study typically necessitated the adoption of a broad taxonomic resolution in defining the OTUs, and the adoption of a broad anatomical resolution in the construction and coding of character–state complexes. For example, the highly diverse nonmammalian synapsid clade Anomodontia was represented as a single unit, and coding emphasized the states observed in more basal (especially nondicynodont) members. See Supporting Information Appendix S1 for a list of taxa that contributed to the coding of suprageneric OTUs and Supporting Information Appendix S2 for the taxon–character matrix developed.

Following the coding of character states, these were used to explore trait evolution via ancestral state reconstruction (ASR). A single primary "consensus" tree topology was used (Figure 1), although as in the companion study, two variants were considered, one with a monophyletic Therocephalia and one with Eutherocephalia more closely related to Cynodontia than Scylacosauridae (see Bishop & Pierce, 2023). ASRs were computed using both maximum parsimony and maximum likelihood methods (Maddison & Maddison, 2021; Paradis et al., 2004). Branch lengths used in maximum likelihood were derived from the results of a Bayesian phylogenetic analysis (Ronquist et al., 2012) considering both forelimb (Bishop & Pierce, 2023) and hindlimb characters together. The results of maximum likelihood ASR were used to quantitatively examine character evolution along the stem lineage, by recognizing a change in state when the likelihood of an alternate state equaled or exceeded a predefined threshold of 0.75. Applying this approach in both the root-up and tip-down directions can bracket the latest and earliest nodes (respectively) at which a state transition likely occurred, and the average of both was used to compute the number of node-specific state changes along the stem lineage. As per the companion study, the effect of missing data on the detection of state changes was evaluated by comparing the number of inferred state changes for each node against the proportion of missing data in the immediate vicinity of that node (for details, see Bishop & Pierce, 2023).

3 | RESULTS

A total of 80 character complexes were devised for all the muscles crossing the hip, knee, and ankle (see also Supporting Information Appendix S2). In a similar fashion to Hutchinson (2002), the characters and states for each muscle or muscle group are presented below, sequentially addressing the number of muscle heads, the origin(s), and the insertion(s). The states for each character are outlined, and pertinent notes of discussion or justification are presented in a "Remarks" section immediately following. Square brackets are used to denote osteological correlates of muscle attachment. Only if such osteological correlates were observed in fossils was a given extinct OTU coded numerically in the phylogenetic analysis, otherwise, it was coded as unknown ("?").

For clarity, a consistent set of anatomical terms are employed to describe the spatial positioning of attachments on the bones (Figure 2). For the femur, four homologous bone surfaces (Hutchinson, 2001a) are recognized across the sample of taxa, defined with respect to the femoral condyles, avoiding issues due to differences in femoral head orientation (i.e., medial inclination, anteversion) and limb posture. These surfaces are recognized such that the femur is oriented vertically and with the axis of the distal femoral condyles running left-to-right, thus presenting anterior, posterior, medial, and lateral aspects (Figure 2b). Terms describing attachments on the tibia and fibula are used as if the two bones were articulated naturally, and with the crus oriented vertically and its extensor surface pointing forwards; this gives anterior, posterior, medial (tibial-ward) and lateral (fibular-ward) aspects. Lastly, terms describing attachments on the pes assume that the entire pes is straightened out and oriented horizontally with the digits pointing forward; this gives dorsal, ventral (plantar-ward), medial (digit I-ward), and lateral (digit V-ward) aspects. Note that these terms of reference do not necessarily correspond to an in-life relative positioning of the femur, crus, or pes.

On another terminological note, the muscles involved have typically received different names in the herpetological versus mammalian literature, even if there is no doubt as to homology (abbreviations outlined in Table 1). Given this historical precedent, and the profound anatomical transformation that occurred along the mammalian stem lineage, use of a single name for a given muscle will hamper communication. No one name will work well for all purposes; using a herpetological name for a cynodont may be confusing for mammal specialists, and likewise using a mammalian name for a "pelycosaur" may be confusing for early amniote specialists. As a compromise, the muscle is initially referred to using its herpetological name, but when it exhibits a more "mammalian" manifestation, the mammalian name is used instead. So, for example, when the ambiens shifts its origin to the anterior ilium, it "becomes" the sartorius. This approach does not distinguish between plesiomorphic and apomorphic

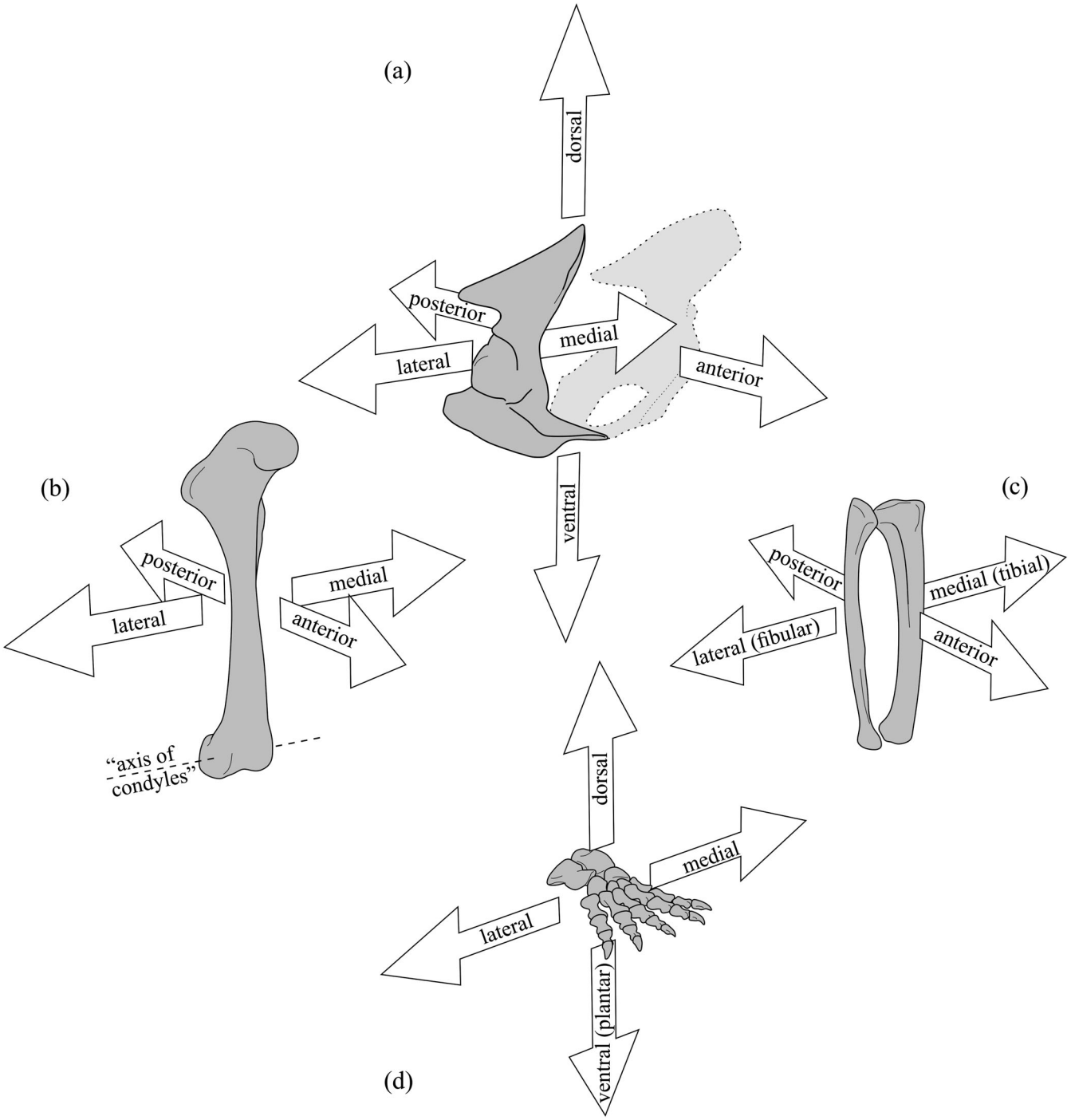

FIGURE 2 Convention of terms used in this study to describe anatomical positioning of each bone, shown with a cynodont pelvis (a), femur (b), crus (c), and pes (d) as an example. In this and all subsequent figures, bones are illustrated from the right side of the body.

states, providing a neutral means to communicate character evolution.

Schematic summaries of changes in gross osteology from basal synapsids through to crown mammals are presented for the pelvis (Figure 3), femur (Figure 4), crus (Figure 5), and pes (Figure 6). These provide a broader skeletal context for the subsequent figures that focus on the evidence for specific muscles, and also illustrate major trends in skeletal transformation on the line to mammals. Abbreviations used for key anatomical landmarks in the text and figures are as follows: 3Tr = third trochanter, 4Tr = fourth trochanter, Ast = astragalus, AvTr = "anteroventral trochanter" of Jenkins (1971), Cal = calcaneum, CnCr = cnemial crest, Epi = epipubis,

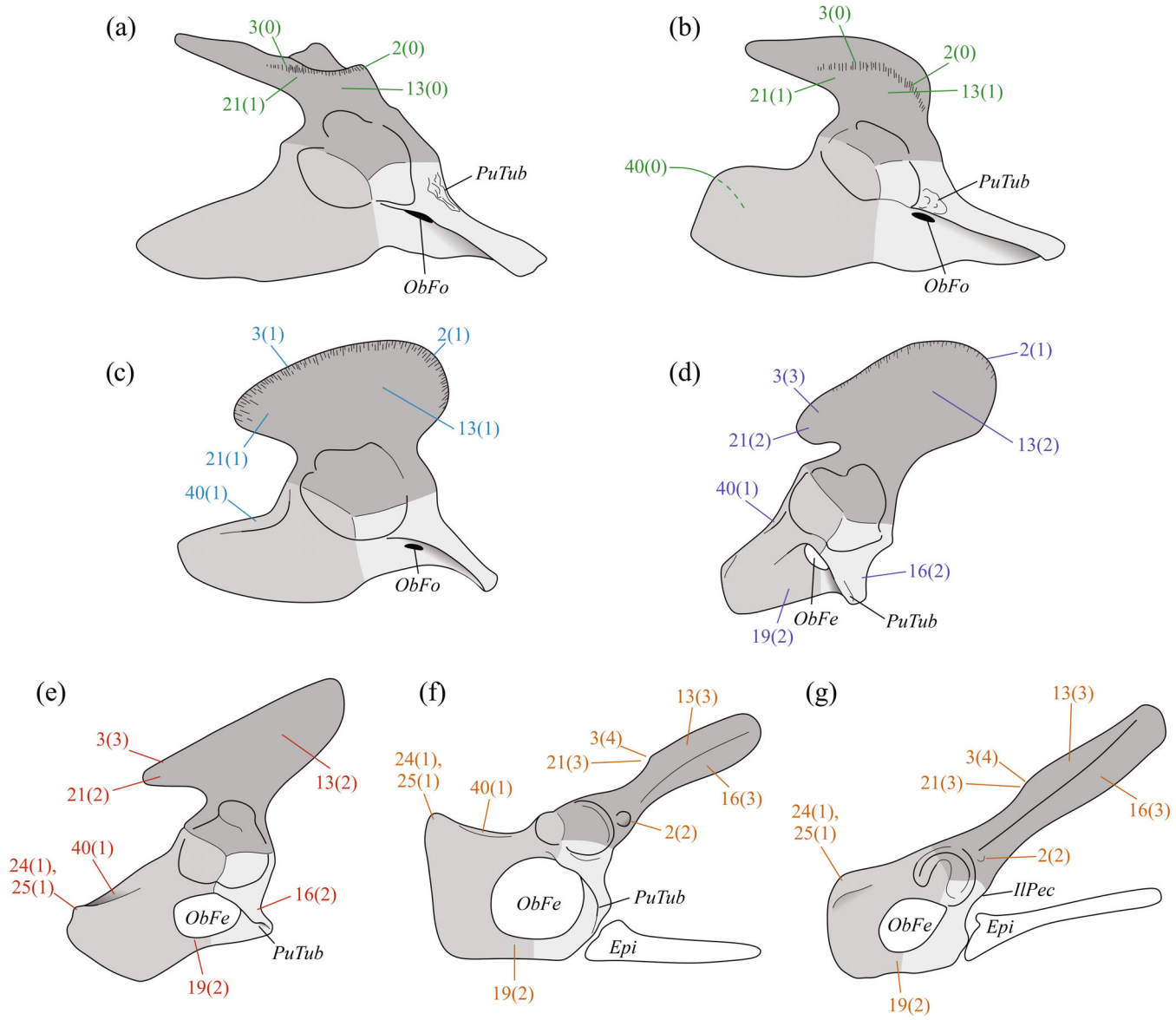

FIGURE 3 Summary of the evolution of pelvic morphology within Synapsida. (a) Basal synapsid (amniote). (b) Sphenacodontian "pelycosaur". (c) Therapsid. (d) Permian bidentalian dicynodont. (E) Eucynodont. (f) Crown mammal. (g) Therian. Pelves are shown in lateral view (not to scale); dark gray = ilium, medium gray = ischium, light gray = pubis. Individual pelves are not necessarily based on a single taxon, but rather are indicative of the stage in synapsid evolution that they represent, and as such are based on numerous literature sources and first-hand observation of numerous specimens. In this and subsequent figures, features corresponding to muscle character–state combinations with explicit osteological correlates are indicated, with the font and line color used indicative of the major taxonomic group (cf. Figure 1).

FibFac = fibular facet on calcaneum; FiTu = fibular tubercle, GrTr = greater trochanter, I–V = digits I–V, IlPec = iliopectineal process, IncTub = incipient tuber on the heel of the calcaneum, InTr = internal trochanter, IsTu = ischiadic tuberosity, LeTr = lesser trochanter, ObFe = obturator fenestra, ObFo = obturator foramen, Pat = patella, PerSh = peroneal shelf, PopFos = popliteal fossa, PosRid = posterolateral ridge of femur, PuTub = pubic tubercle; SusTal = sustentaculum tali; Tub = proper tuber on the heel of the calcaneum. In all figures, bones are illustrated as from the right side of the body.

3.1 | Iliotibialis (IT, Figure 7): Characters 1–5

1. Number of heads

0. Two; degree of subdivision variable
1. Three [three separate regions of scarring on dorsal ilium]
2. Three, posterior head subdivided to give gluteus maximus (GMAX) anteriorly and femorococcygeus (FCOC) posteriorly

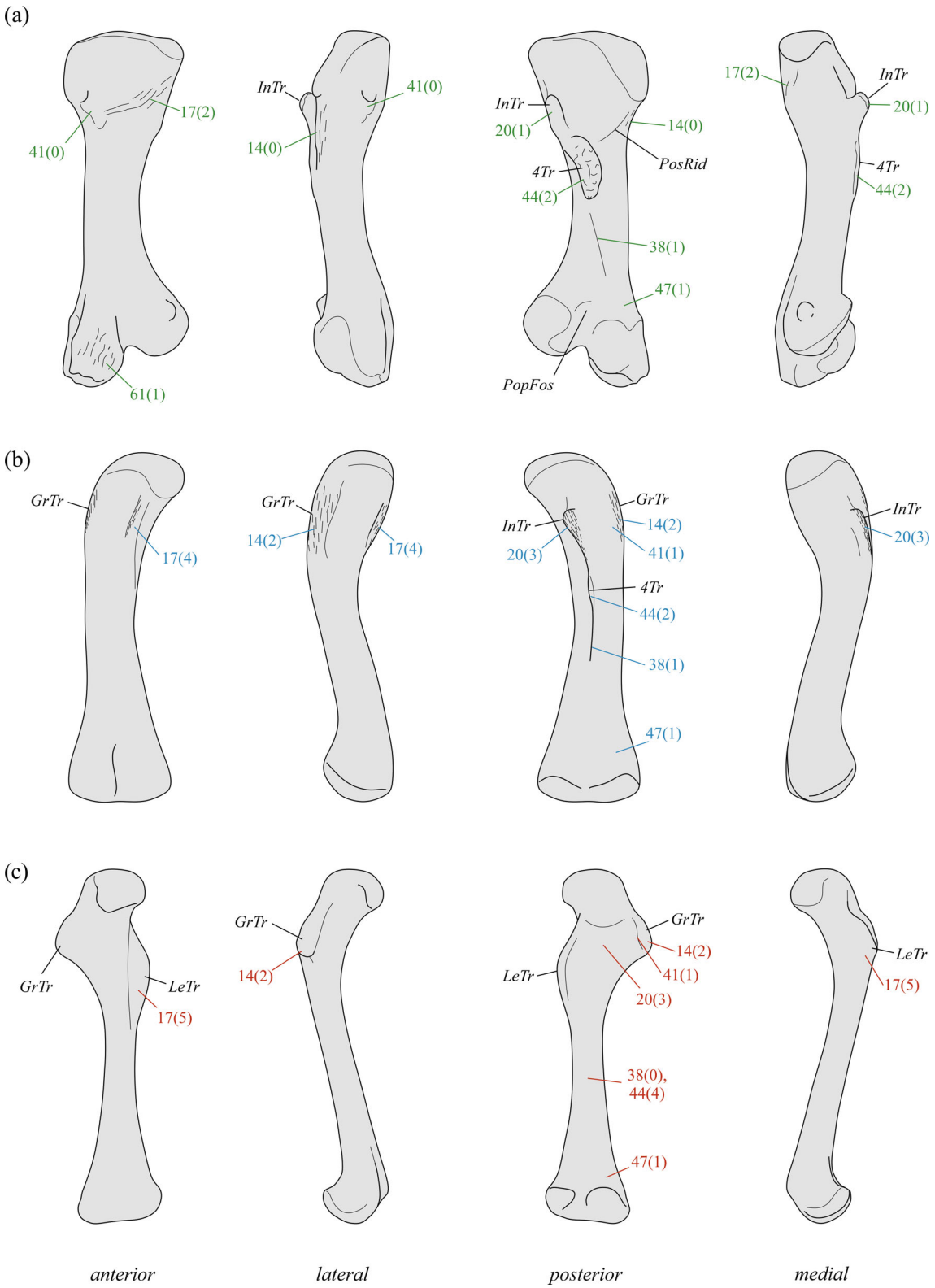

FIGURE 4 Summary of the evolution of femoral morphology within Synapsida. (a) "Pelycosaur". (b) Therapsid. (c) Eucynodont. (d) Crown mammal. (e) Therian. Individual femora (not to scale) are not necessarily based on a single taxon, but rather are indicative of the stage in synapsid evolution that they represent, and as such are based on numerous literature sources and first-hand observation of numerous specimens.

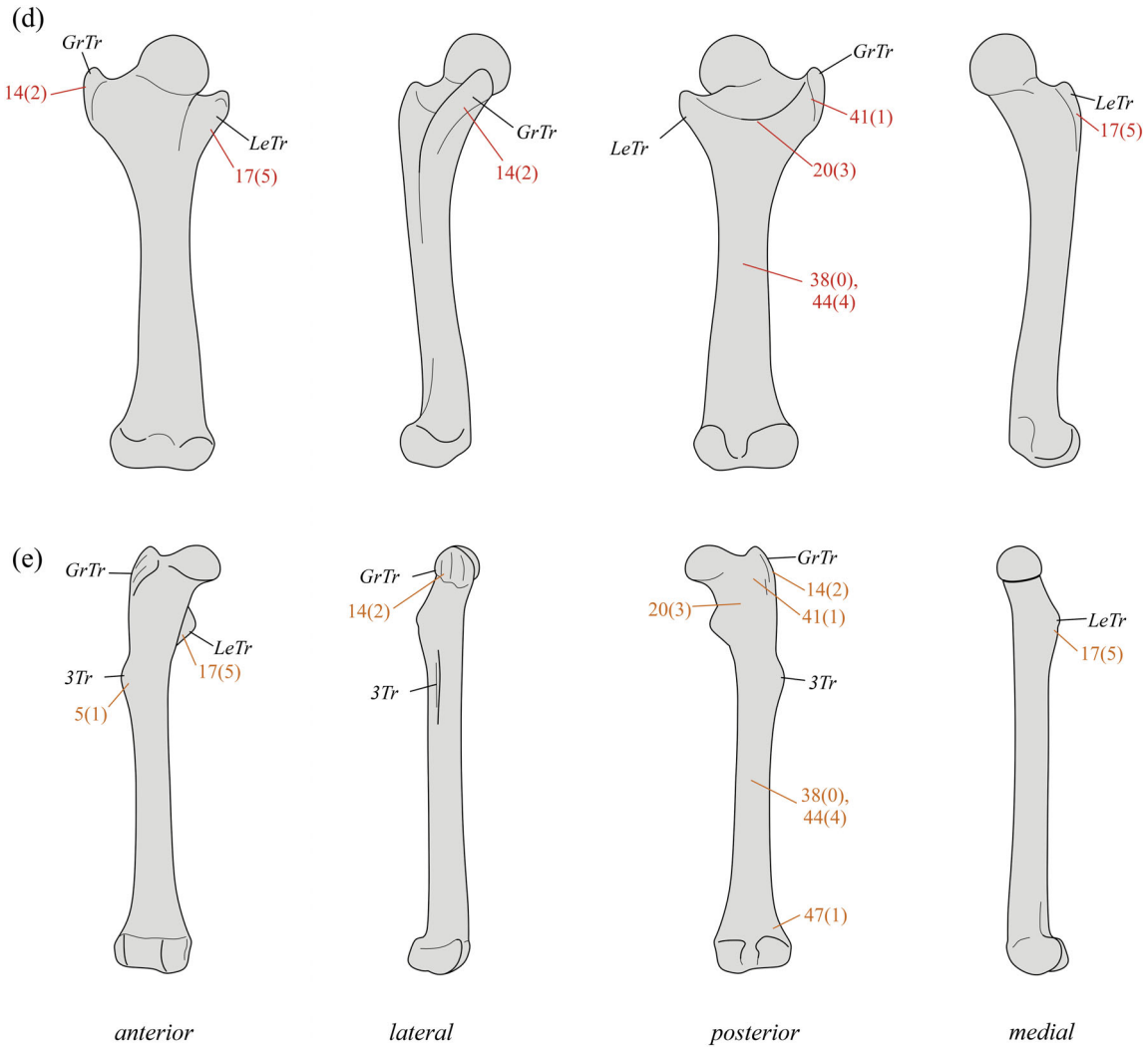

FIGURE 4 (Continued)

Remarks—The homology of the three heads of Crocodylia (Archosauria) with the two heads of nonarchosaur amniotes remains unclear, but is not immediately relevant to the present study. Although salamanders possess two IT heads, they lack femorotibiales or an AMB; the homology between the salamander IT and at least parts of the latter muscles in amniotes is uncertain and in need of further scrutiny (Diogo & Molnar, 2014).

2. Origin of "anterior head"

0. Anterolateral dorsal ilium, superficial to iliofemoralis [rugose transverse line or ridge on lateral surface]
1. Anterolateral dorsal ilium, superficial to iliofemoralis [rugose/thickened dorsal rim]
2. Base of ilium immediately anterior to acetabulum [scar or tubercle = rectus femoris (RF)]

Remarks—In crocodylians, this character is coded simply for the anterior part of the heads' collective area of origin, ignoring the precise origins of each separate head.

Romer (1922, pp. 559–560) first espoused a hypothesis of iliac evolution in early amniotes, involving the dorsal shift of a "transverse line" and concomitant repositioning of dorsal hip and axial musculature. Plesiomorphically, this transverse line was a long ridge situated on the lateral surface and below the dorsal margin of the bone (Figure 7a, arrows; also Figure 3a); the line itself demarcated the dorsal limit of the thigh muscles' origin, above which the ilium served as attachment for epaxial musculature. Over time, this ridge shifted dorsally to form the dorsal margin of the bone, and the dorsalmost ilium "folded over" to face medially (lying above the sacral attachments), such that the entire lateral surface of the ilium dorsal to the acetabulum now served as the origin for thigh muscles, and the attachment of epaxial

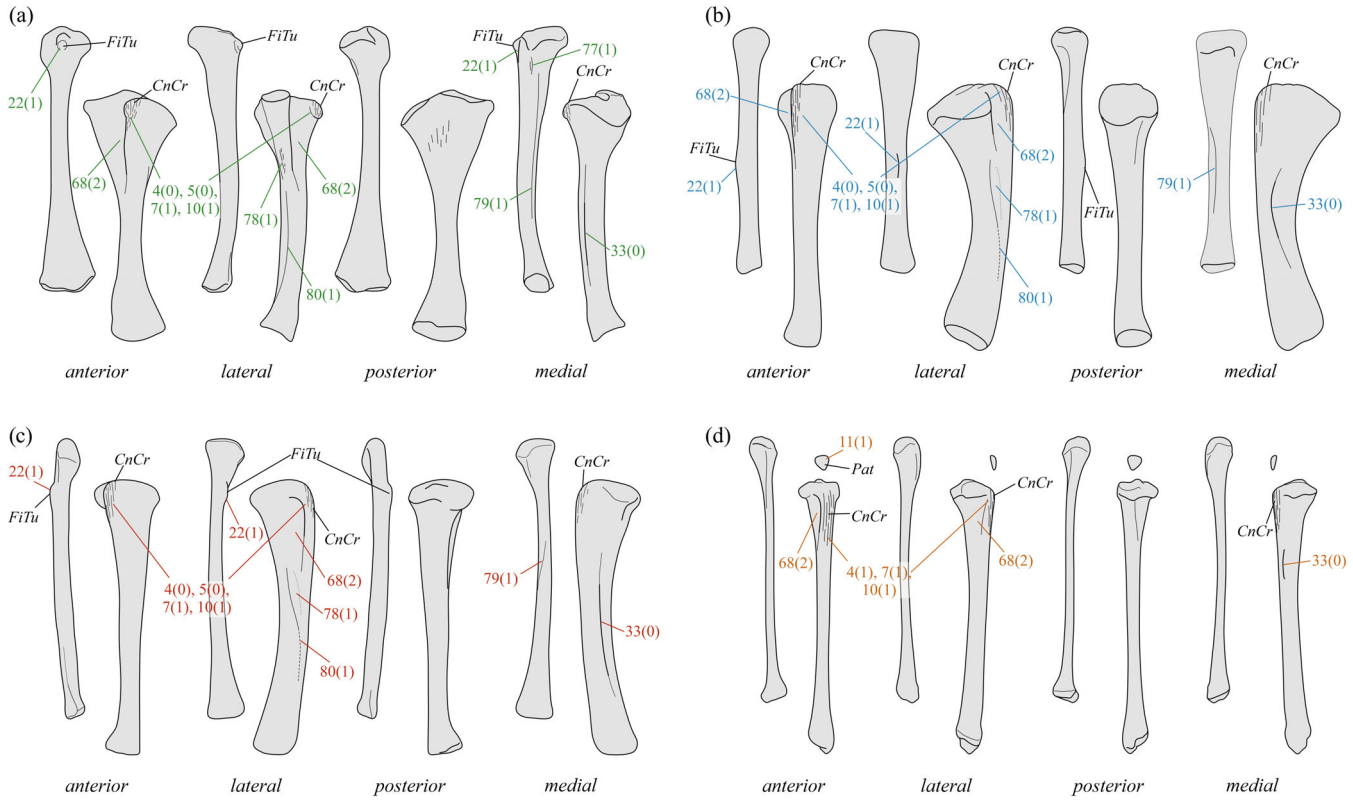

FIGURE 5 Summary of the evolution of crural morphology within Synapsida. (a) "Pelycosaur". (b) Therapsid. (c) Eucynodont. (d) Therian. Each panel shows the tibia (lower row) and fibula (upper row). Individual bones (not to scale) are not necessarily based on a single taxon, but rather are indicative of the stage in synapsid evolution that they represent, and as such are based on numerous literature sources and first-hand observation of numerous specimens.

musculature was restricted to the medial surface only. Romer (1922) contended that this transformation was completed in forms such as the sphenacodont *Dimetrodon*, and thus in the present scheme, these ought to be coded as state 1. However, examination of abundant material of edaphosaurids and (nontherapsid) sphenacodontians shows that a transverse line of fibrous scarring persists on the lateral iliac surface, below the dorsal margin of the bone (Figure 7b,c, arrows, also Figure 3b), even though a raised ridge is no longer present. Hence, even in these forms, dorsal migration of the thigh musculature is inferred to not have been fully completed, thus being coded as state 0; dorsal migration was likely completed around the base of Therapsida (Figure 7d; Supporting Information Appendix S3).

3. Origin of "posterior head"

0. Posterolateral dorsal ilium, superficial to iliofemoralis [rugose transverse line or ridge on lateral surface]
1. Posterolateral dorsal ilium, superficial to iliofemoralis [rugose/thickened dorsal rim]
2. Anterolateral dorsal ilium, partly anterior and superficial to iliofemoralis
3. Posterolateral dorsal ilium and adjacent sacral or caudal vertebrae [postacetabular iliac blade reduced]
4. Sacral and/or proximal caudal and/or posteriormost lumbar vertebrae [postacetabular iliac blade lost]

Remarks—It is hypothesized that as the postacetabular iliac blade became reduced in cynodonts and ultimately lost entirely in mammaliaforms, the origin of the posterior IT head shifted onto the neural spines and/or transverse processes of neighboring vertebrae to become the mammalian GMAX (i.e., states 1 → 3 → 4; Supporting Information Appendix S3). Whether this was also coincident with the subdivision into separate GMAX and FCOC is uncertain at present. State 2 captures the apomorphic condition observed in extant *Sphenodon* (Osawa, 1897).

4. Insertion of "anterior head"

0. Anteroproximal tibia via common "triceps" tendon [tuberosity on proximal cnemial crest]
1. Anteroproximal tibia via common "triceps" tendon, patella, and patellar ligament [tuberosity and ossified patellar sesamoid]

Remarks—The insertion of the "triceps" musculature (iliotibiales, femorotibiales, and ambiens, or their homologues) onto the cnemial crest of the anteroproximal tibia is almost ubiquitous across tetrapods. Its inference in fossil species (for both characters 4 and 5) is thus well supported even when the proximal tibia is poorly ossified and scarring per se is absent—a level I′ inference in the scheme of Witmer (1995).

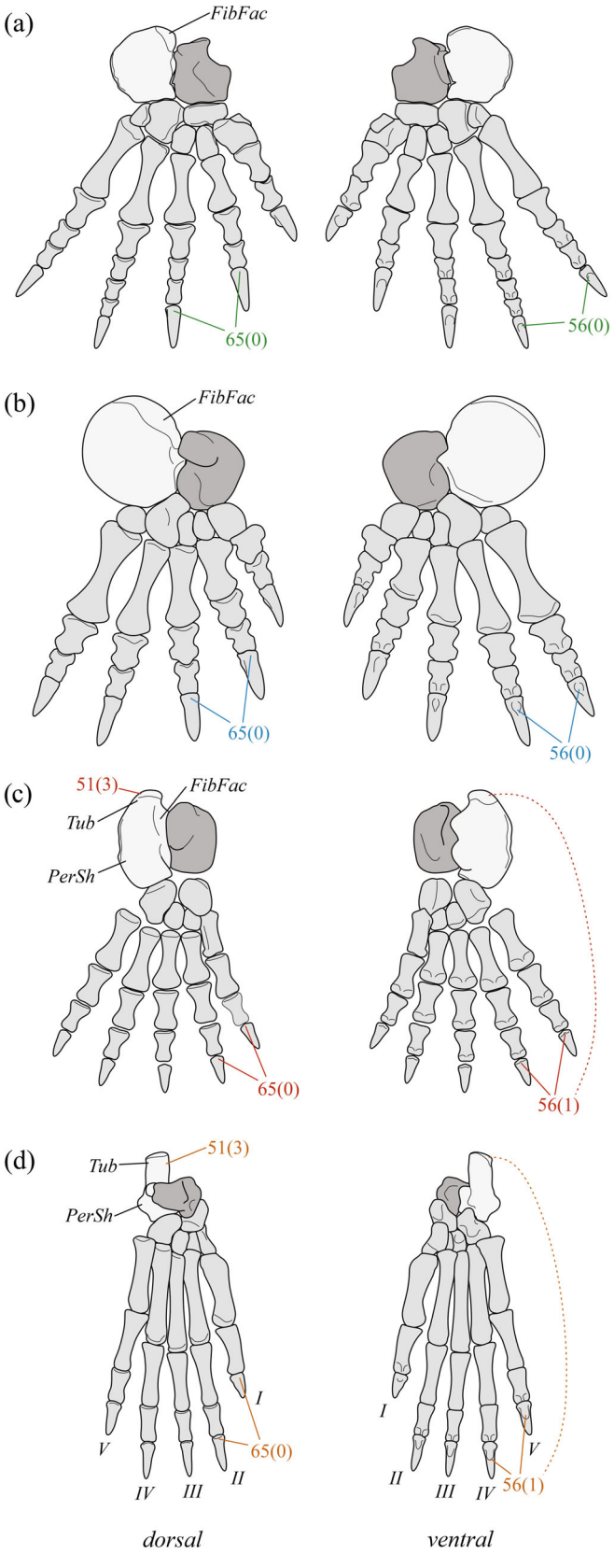

5. Insertion of "posterior head(s)"

0. Anteroproximal tibia via common "triceps" tendon [tuberosity on proximal cnemial crest]
1. Lateral aspect of femoral shaft [tuberosity or crest]
2. Lateral aspect of femoral shaft [large process, "third trochanter"]
3. Lateral aspect of femoral shaft, from base of greater trochanter to more distal parts

Remarks—Uniquely among amniotes, on the line to mammals, the posterior head shifted away from the knee to insert on the lateral femoral shaft. This coincides with the appearance of a crest (state 1, such as in monotremes and multituberculates) or trochanter (state 2, typical of crown therians; Figure 4e), although such processes have also been lost numerous times, including in stem therians (e.g., Jäger et al., 2019; Jenkins & Schaff, 1988; Rougier, 1993), most marsupials and some derived placental clades (state 3; Sargis, 2002). Complicating the picture, in some rodents (Greene, 1935; Rinker, 1954; Stein, 1986), tupaiids (Le Gros Clark, 1924, 1926), and didelphids (Coues & Wyman, 1872), the FCOC inserts on the lateral patella and surrounding soft tissues of the knee, despite a third trochanter often being present. Hence, the existence of the third trochanter in fossil species does not unequivocally indicate a complete shift in insertion (from knee to femur), only that such a shift has commenced.

In large dicynodonts, especially kannemeyeriiforms, the greater trochanter (see below) is often expanded distally along the lateral aspect of the femur, which Parrington (1961) suggested may represent an incipient third trochanter. However, there is no phyletic continuity between the dicynodont structure and the condition observed in extant taxa, with the earliest recognizable third trochanter occurring in Mammaliaformes (Martin,

FIGURE 6 Summary of the evolution of pedal morphology within Synapsida. (a) "Pelycosaur"; (b) Therapsid; (c) Cynodont; (d) Therian. Each panel shows the pes in dorsal (left) and ventral (right) views; dark gray tarsal = astragalus, light gray tarsal = calcaneum. Individual pedes (not to scale) are not necessarily based on a single taxon, but rather are indicative of the stage in synapsid evolution that they represent, and as such are based on numerous literature sources and first-hand observation of numerous specimens. Among other things, note the increasing symmetry of the pes in more crownward taxa.

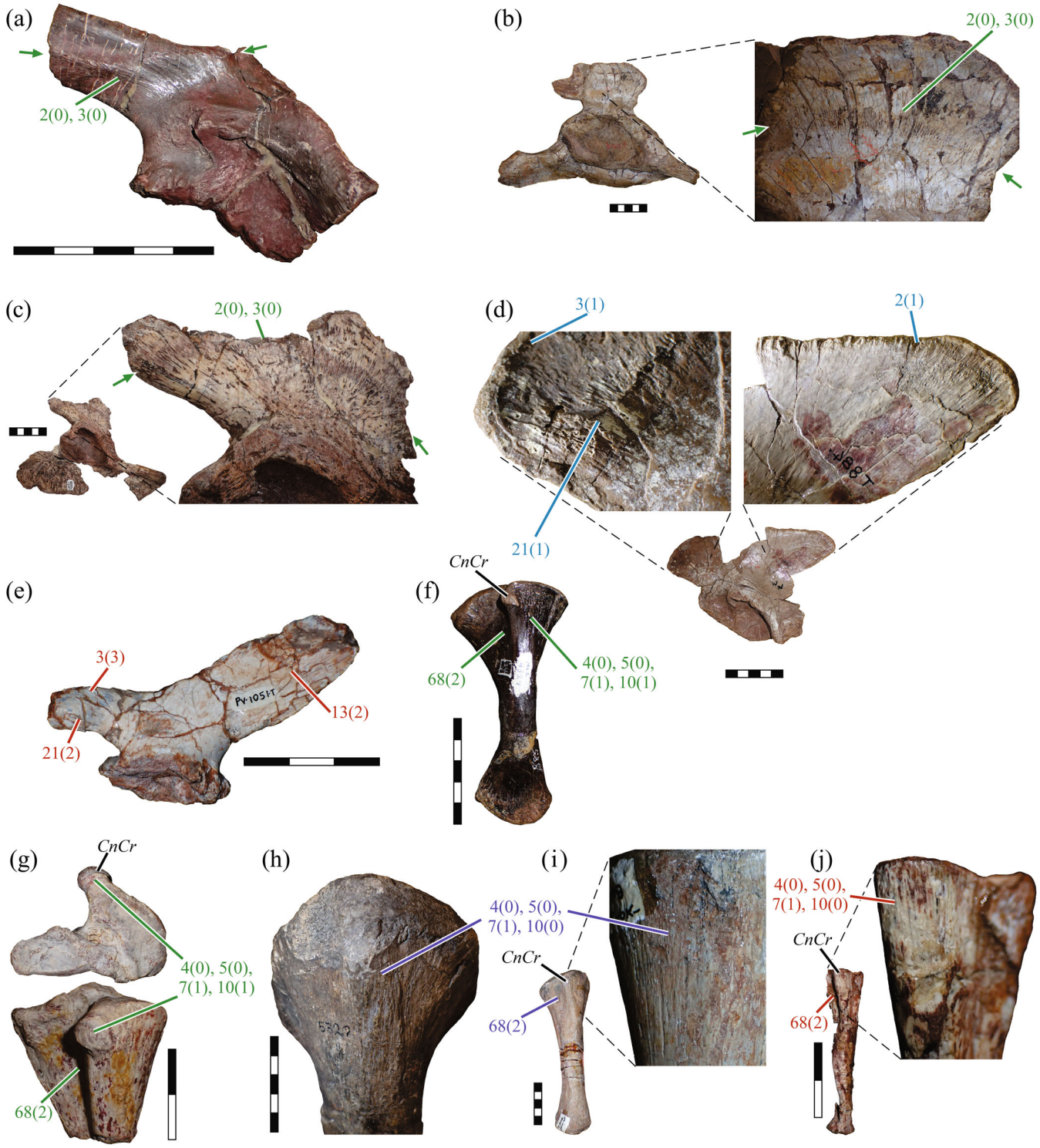

FIGURE 7 Osteological evidence of iliotibialis musculature attachment in synapsids. (a) MCZ VPRA-4857 *Ophiacodon mirus* (Ophiacodontidae) ilium in lateral view. (b) AMNH FARB 4006 *Lupeosaurus kayi* (Edaphosauridae) pelvis in lateral view, with focus on ilium. (c) UCMP 83524 *Sphenacodon ferox* (Sphenacodontia) pelvis in lateral view, with inset focused on ilium. (d) UMZC T.884 Gorgonopsia indet. pelvis in lateral view, with insets focused on anterior and posterior ilium. (e) UFRGS-PV-1051-T *Trucidocynodon riograndensis* (basal probainognathian) ilium in lateral view. (f) MCZ VPRA-4324 *Edaphosaurus boanerges* (Edaphosauridae) tibia in anterior view. (g) MCZ VPRA-1112 *Dimetrodon* sp. (Sphenacodontia) proximal tibia in proximal (above) and anterior (below) views. (h) AMNH FARB 5322 *Moschops capensis* (Tapinocephalidae) proximal tibia in anterior view. (i) SAM-PK-2348 cf. *Dicynodon* sp. (Dicynodontia) tibia in anterior view, with inset focused on cnemial crest. (j) UFRGS-PV-0248-T *Prozostrodon brasiliensis* tibia in anterior view, with inset focused on cnemial crest. Unless otherwise indicated, all scale bars in this and the following figures are in increments of centimeters.

2005). Failing the test of congruence (Patterson, 1982), these structures must be regarded as nonhomologous. To that end, the structure in dicynodonts should not be referred to as a third trochanter, and moreover, it is unlikely to have represented a similar muscular anatomy to that observed in extant mammals.

3.2 | Ambiens (AMB): Characters 6 and 7

6. Origin

0. Absent
1. Lateral aspect of anterior pubis, anteroventral to acetabulum
2. Anterior iliopubic symphysis and medial proximal pubis
3. Anterolateral apex of ilium and/or immediately adjacent iliopubic ligament (sartorius, SART)

Remarks—It is unclear whether the pubic tubercle of sauropsids is homologous with the iliopectineal process of mammals. Basal amniotes, including "pelycosaurs," possess a distinct rugosity anteroventral to the acetabulum, in a similar position to the tubercle of sauropsids, and the two have been previously considered as homologous (Romer, 1922; PuTub, Figure 3a,b). Some therapsids (dicynodonts, therocephalians, and cynodonts) also typically possess a tubercle or swelling on the pubis anteroventral to the acetabulum, at the apex of the laterally everted (but anteroposteriorly foreshortened) pubic apron (Figure 3d–f). Topologically, this places it closer to the distal extremity of the pubis, but the iliopectineal process of crown mammals is more proximally sited on the pubis, near the iliac peduncle (e.g., Elftman, 1929; Gambaryan et al., 2002; Figure 3g, IlPec). Indeed, at least one tritylodontid cynodont appears to possess both a pubic tubercle distally and an iliopectineal process proximally (Sullivan et al., 2013), implying nonhomology by conjunction (Patterson, 1982). Further complicating matters, in addition to the AMB, other muscles attach to this region of the pubis in extant tetrapods (pubotibialis and quadratus lumborum in nonmammals, pectineus, psoas minor, and potentially others in mammals), but the topological relationships of these other muscles' attachments with respect to the pubic tubercle or iliopectineal process, with each other, and with the AMB origin are labile.

In light of this unresolved complexity, rugosities or processes on the anteroventral pubis are here recognized principally as osteological correlates for attachment of the iliopubic ligament and abdominal musculature, rather than any particular appendicular muscle, since the former relationship appears highly stable across amniotes. The presence of a pubic tubercle in a fossil species (regardless of its location) should not be taken as an unambiguous indicator of the presence of the AMB, only its general location, and as such all extinct OTUs are presently coded as unknown ("?").

7. Insertion

0. Absent
1. Anteroproximal tibia via common "triceps" tendon [tuberosity on proximal cnemial crest]
2. Medioproximal tibia and surrounding tissues

3.3 | Femorotibialis (FMT, Figure 8): Characters 8–10

8. Number of heads

0. Absent
1. One
2. Two, one medial (internus/FMTI or vastus medialis/VM) and one lateral (externus/FMTE or vastus lateralis/VL)
3. Three, vasti medialis, lateralis, and intermedia (VI)

9. Origin

0. Absent
1. Much of lateral, anterior, and medial femoral shaft; proximally it is always more lateral to insertion of puboischiofemoralis internus (or homologue)

Remarks—The topological relationships of the FMT origin (s) with respect to the attachments of other muscles on the femur is somewhat labile, especially the iliofemoralis (or homologue). Consistently, however, the FMT originates laterally to the insertion of puboischiofemoralis internus (or homologue). Unlike archosaurs (Hutchinson, 2001a), the femora of synapsids mostly lack intermuscular lines that demarcate the boundaries of individual FMT attachment areas; two probable exceptions to this generality have been observed in a dinocephalian and cynodont, and are illustrated in Figure 8 (arrows).

10. Insertion

0. Absent
1. Anteroproximal tibia via common "triceps" tendon [tuberosity on proximal cnemial crest]

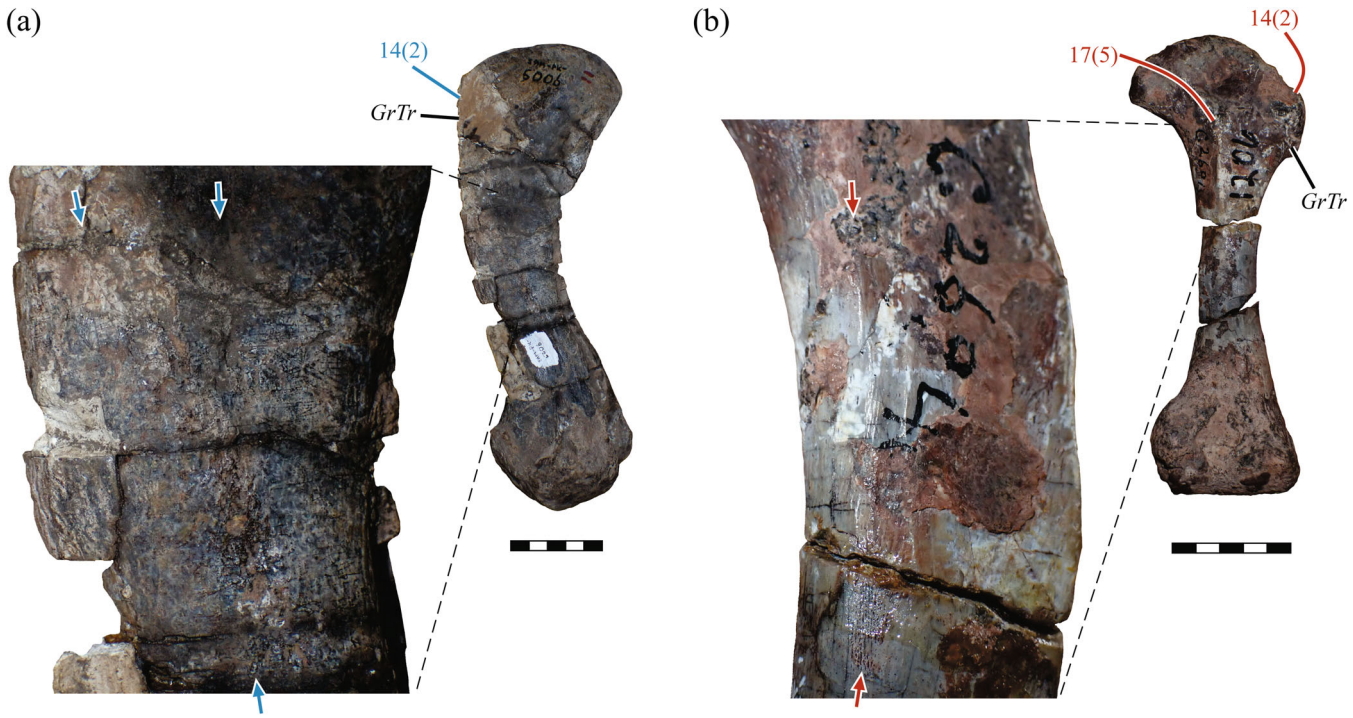

FIGURE 8 Osteological evidence of femorotibialis musculature attachment in synapsids. (a) SAM-PK-5006 *Struthiocephalus whaitsi* (Tapinocephalidae) femur in anterolateral view, inset illustrating diffuse longitudinal band of mottled surface texture that may indicate an intermuscular division within the femorotibiales. (b) NMQR 1206 *Diademodon tetragonus* (Cynognathia) femur (whole bone in posterior view, inset in medial view), illustrating possible femorotibial intermuscular line.

3.4 | Patella: Character 11

11. Ossified patellar sesamoid in "triceps" tendon

0. Absent
1. Present, with more deeply developed "patellar sulcus" on anterodistal femur

Remarks—Occasionally the depression between the medial and lateral condyles on the anterodistal femur of nonmammalian synapsids has been referred to as a "patellar sulcus" or "patellar groove." Yet, an ossified patella is only known among crown mammals, and its patchy phylogenetic distribution implies multiple independent origins within Mammalia (Samuels et al., 2017). It is possible that some nonmammalian synapsids may have possessed a fibrocartilaginous patelloid, but the present character explicitly codes for an *ossified* sesamoid. Recognizing whether an ossified sesamoid was present is complicated by the possibility that a small bone such as this could be lost during preservation, even in otherwise well-preserved specimens. As a counterpoint, it is worth noting that the pisiform, a small sesamoid in the wrist of amniotes, is very frequently preserved in various nonmammalian synapsid fossils (see Bishop & Pierce, 2023). In the present study, if sufficient numbers of articulated specimens were known for a given extinct OTU, and all lacked ossified patellae, it was felt justifiable to view absence in the fossils as indicative of true absence in life, permitting an explicit coding of state 0.

3.5 | Iliofemoralis (IF, Figures 9 and 10): Characters 12–14

12. Number of heads

0. One
1. Two, gluteus medius (GMED) and minimus (GMIN)
2. At least three, gluteus medius, gluteus minimus and piriformis (PIR); or more

Remarks—Monotremes exhibit a simple bipartite subdivision (state 1), whereas therians exhibit a wide diversity in subdivision; in addition to those listed in state 2 above, there may also be the gluteus profundus or quartus, tensor fascia lata or scansorius. Ostensibly, the more complex pattern of subdivisions captured by state 2 was derived from the simpler arrangement of state 1. However, since

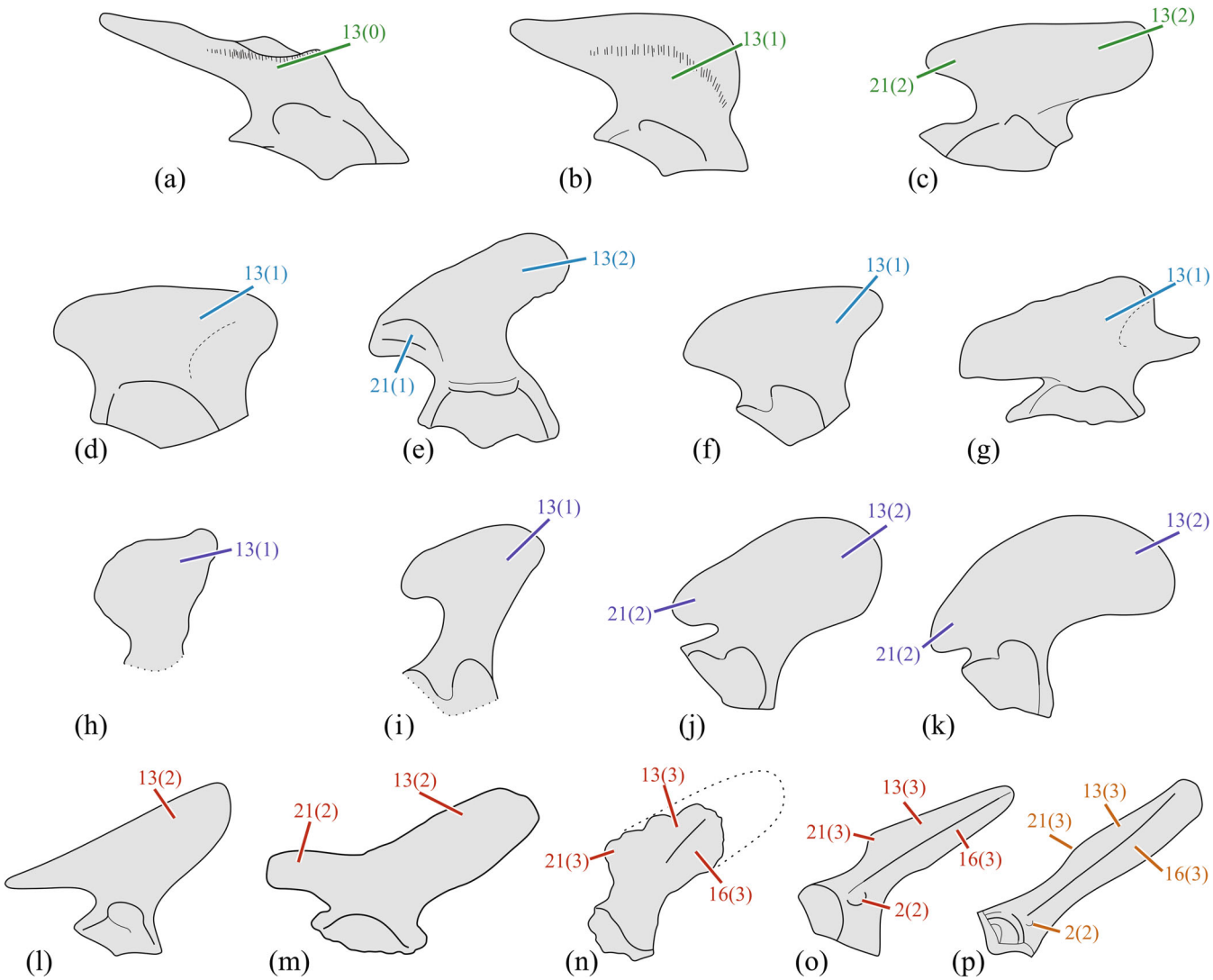

FIGURE 9 Changes in iliac proportions in Synapsida on the line to mammals, illustrated with key representative taxa. (a) The ophiacodontid *Ophiacodon retroversus* (based primarily on FMNH UC 458). (b) The sphenacodontid *Dimetrodon* spp. (based on numerous specimens). (c) The aberrant varanopid *Mycterosaurus smithae* (after Romer & Price, 1940). (d) The basal therapsid *Biarmosuchus tener* (after Tchudinov, 1983). (e) The dinocephalian *Titanosuchus* sp. (based primarily on SAM-PK-K249, with added detail from Boonstra, 1955). (f) A typical gorgonopsian (based on numerous specimens, and Kemp, 1982). (g) The eutherocephalian *Regisaurus jacobi* (based on BP/1/5394 and Kemp, 1978). (h) The basal anomodont *Patronomodon nyaphulii* (based on NMQR 3000). (i) The basal dicynodont *Eodicynodon oosthuizeni* (based on NMQR 3155, with added detail from Rubidge et al., 1994). (j) The bidentalian dicynodont *Oudenodon bainii* (based primarily on NHMUK PV R.4607). (k) The kannemeyeriiform dicynodont *Kannemeyeria simocephalus* (based on numerous specimens). (l) The cynognathian eucynodont *Massetognathus pascuali* (based primarily on MCZ VPRA-3691). (m) The probainognathian eucynodont *Trucidocynodon riograndensis* (based on UFRGS-PV-1051-T). (n) The derived probainognathian *Prozostrodon brasiliensis* (based on UFRGS-PV-0248-T; specimen is incomplete, dotted lines show inferred complete extent of bone). (o) The tritylodont *Oligokyphus* sp. (after Kuhne, 1956). (p) Extant opossum *Didelphis* sp. Bones are not to scale. Changes in the proportions of the ilium, both anterior and posterior to the acetabulum, indicate changes in the size and location of attachments of the iliofemoralis and iliofibularis musculature.

only monotremes exhibit state 1, and only therians exhibit state 2, this is of little relevance for charting iliofemoralis evolution on the line to crown mammals. No osteological evidence has yet been recognized as indicating how or when iliofemoral subdivision first occurred in nonmammalian synapsids, although it is possibly linked with the progressive expansion in the muscle's origin in association with preacetabular iliac expansion.

13. Origin

0. Lateral or posterolateral ilium, immediately dorsal to acetabulum [ilium swept posteriorly, lacking anterior expansion]
1. Lateral surface of ilium, dorsal and anterodorsal to acetabulum [ilium expanded anteriorly and dorsally to form modest blade]

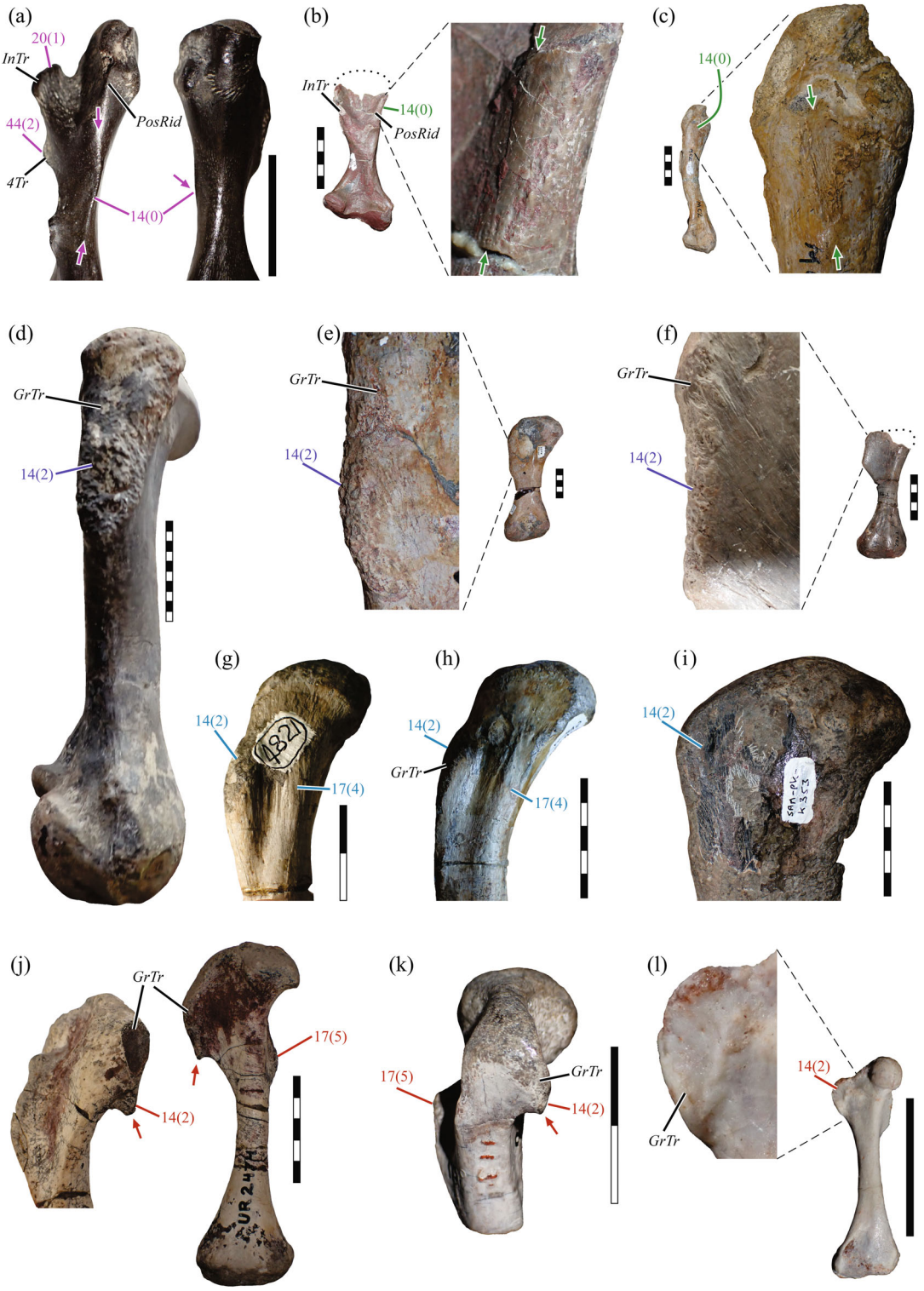

FIGURE 10 Osteological evidence of iliofemoralis musculature insertion on the femur in synapsids. (a) USNM PAL 768796 cf. *Captorhinus* (Captorhinidae), in lateral and anterior views, showing faint ridge of attachment (arrows). (b) MCZ VPRA-4856 *Ophiacodon mirus* (Ophiacodontidae), in posterior view (enlarged inset in posterolateral view). (c) MCZ VPRA-2863 *Dimetrodon limbatus* (Sphenacodontia), in lateral view. (d) GPIT-PV-30792 *Stahleckeria potens* (Dicynodontia) in lateral view. (e) SAM-PK-2348 cf. *Dicynodon* sp. in anterior view. (f) UMZC T.987 *Oudenodon* sp. (Dicynodontia) in anterior view. (g) TM 4821 Gorgonopsia indet. in anterior view. (h) SAM-PK-K8077 Gorgonopsia indet. in anterior view. (i) SAM-PK-K353 Lycosuchidae indet. in anterior view. (j) FMNH UR 2474 Cynodontia indet. (?cynognathid) in lateral and anterior views. (k) UMZC T.976 Cynodontia indet. in lateral view. (l) UFRGS-PV-1043-T *Brasilodon quadrangularis* in anterior view. Note the pendant distal projection of the greater trochanter in (k) and (j) (arrows).

2. Most of lateral surface of preacetabular ilium [greatly expanded preacetabular blade]
3. Most of iliac blade dorsal to iliac spine [longitudinal ridge on lateral surface], and possibly also adjacent sacral and caudal vertebrae

Remarks—The anterior expansion of the ilium has historically been recognized as one of the hallmarks of therapsids. Further development into a massive blade-like structure (state 2) occurs independently in at least two other lineages in addition to cynodonts (Figure 9; Supporting Information Appendix S3). Among dinocephalians, anteosaurids possess a modest expansion (state 1; e.g., Orlov, 1958), but pronounced iliac expansion is widespread in tapinocephalians (Figure 9e; Boonstra, 1955a). Among anomodonts, modest iliac development is observed in *Eodicynodon* and more basal forms (Figure 9h,i; Fröbisch & Reisz, 2011; Rubidge & Hopson, 1996; Rubidge et al., 1994), but more derived taxa exhibit progressively enlarged preacetabular iliac blades, especially prominent in kannemeyeriiforms (Figure 9k; Ray, 2006). Importantly, modest anterior expansion (state 1) is also seen in edaphosaurids and nontherapsid sphenacodontians (Figure 9b; Romer & Price, 1940; Spindler, 2016), indicating that transformation of the iliofemoralis commenced prior to the appearance of Therapsida. There are also instances of convergence in iliac evolution among other early amniotes, both within and beyond Synapsida; preacetabular iliac expansion is observed in caseid caseasaurs (state 1; Berman et al., 2020; Romer & Price, 1940), the varanopid *Mycterosaurus* (state 2, Figure 9c; Romer & Price, 1940), the araeoscelidian *Petrolacosaurus* (state 1; Peabody, 1952) and pareiasaurs (states 1 or 2; Turner et al., 2015; Van den Brandt et al., 2021). In a similar fashion to the posterior head of the IT (character 3), it is hypothesized that an expansion of the origin of the IF onto neighboring vertebrae was associated with the diminishment and eventual loss of the postacetabular ilium, in tandem with the preacetabular iliac blade becoming more rod-like on the line to mammals.

14. Insertion

0. Posterolateral aspect of nonapical part of internal trochanter (InTr), base of posterolateral ridge (PosRid) and fossa, or adjacent femoral shaft [trochanter with drawn-out base, posterolateral ridge, and intervening fossa]
1. Lateral to craniolateral aspect of femoral shaft [internal trochanter absent, flat surface]
2. Lateral to anterolateral proximal femur on the greater trochanter (GrTr) [trochanter, rugosities, or fibrous scarring]

Remarks—In some large, well-preserved "pelycosaur" femora, the posterolateral aspect of the PosRid exhibits fine scarring texture which can creep up onto the lateral surface (Figure 10b,c). Due to the oblique orientation of the proximal femur when articulated in the acetabulum (the InTr directed essentially ventrally in global space), the posterolateral ridge would have faced as much posteriorly as ventrally, and possibly even somewhat dorsally. This is suggestive of an IF insertion around the "waist" of the femoral head, comparable to the location observed in extant lepidosaurs and salamanders, rather than an extended insertion of the puboischiofemoralis externus, as interpreted for archosauriforms (Hutchinson, 2001a).

The generally conservative nature of proximal femoral structure across "pelycosaurs" implies a relatively consistent pattern of insertion throughout these taxa. However, the basalmost therapsids known from postcranial material (e.g., Boonstra, 1965; Orlov, 1958; Seeley, 1894; Sigogneau & Tchudinov, 1972; Tchudinov, 1983) already display a marked transformation of the proximal femoral structure compared to sphenacodontian "pelycosaurs." In addition to a more medially inclined head, the GrTr is developed laterally (Figures 4b,c and 10d–l) and the posterior surface topography simplified, involving a reduction in depth and distal extent of the InTr, and subduing or loss of the PosRid and fossa structure (see also character 20 below). The InTr has also shifted laterally to occupy a more central position on the posterior face of the bone (cf. Romer, 1924). These structural transformations are consistent with the IF shifting its insertion laterally onto the GrTr, in association with other muscular changes, as outlined below. The role of the IF evidently gained increased importance in eucynodonts, where the GrTr is laterally and proximally expanded (Figure 4c), even gaining a distally pendant form (Figure 10j,k).

3.6 | Puboischiofemoralis internus (PIFI, Figures 9–12): Characters 15–17

15. Number of heads

0. One
1. Two
2. Three

Remarks—The PIFI has a complex evolutionary history on the line to mammals, involving partial fusion with the ancestral pubotibialis, which probably renders it impossible to identify a one-to-one correspondence between its subdivisions in extant mammals and sauropsids. The present character's formulation is purely taxic in its

treatment of homology, principally intended to capture structural diversity within each lineage.

16. Origin

0. Medial (dorsal/internal) surface of much of puboischiadic plate and symphysis, extending from anterior pubis to anterior ischium, as well as inner surface of obturator foramen
1. Medial surface of ilium, proximal pubis, and posteriormost dorsal vertebrae [puboischiadic plate reduced]
2. Dorsal medial pubis and/or ventral medial ilium [pubis reduced and rotated posteriorly, and/or depression on medial pubis/ilium]
3. Fossa on iliac blade ventral to iliac spine [iliac fossa, ilium rod-like and trihedral], plus centra and transverse processes of posteriormost dorsal (lumbar) and anterior sacral vertebrae

Remarks—Romer (1922) suggested that the dorsal migration of the PIFI on the line to mammals is signaled, at least in part, by the reduction of its ancestral osseous origin (pubis). A similar scenario was subsequently hypothesized for archosaurs (Hutchinson, 2001a, 2001b, 2002). Romer's transformational hypothesis is well supported by the results of ASR (Supporting Information Appendix S3). Under maximum likelihood, the transition to state 1 was not formally detected on the stem lineage when therocephalian monophyly was assumed (i.e., transformation of $0 \rightarrow 2 \rightarrow 3$), but it was detected when assuming therocephalian paraphyly (i.e., $0 \rightarrow 1 \rightarrow 2 \rightarrow 3$; Supporting Information Appendix S3). From a purely geometric perspective, state 1 is ostensibly the evolutionary intermediate between states 0 and 2.

Kemp (1978) suggested that the PIFI originated from the lateral surface of the preacetabular ilium in the eutherocephalian *Regisaurus jacobi*, citing a fossa in BP/1/5394 (Figure 11a, dashed white line); a similarly sited, shallow fossa seems to be quite common throughout eutherocephalians (Figure 11b–e, between arrows). It is unclear if this fossa demarcates the attachment of a particular muscle, PIFI or otherwise, rather than being a structural consequence of the large anterodorsal processes (and associated ridges) characteristic of the group (i.e., a "spandrel"; Gould & Lewontin, 1979). The significance of the anterodorsal processes remains to be investigated, but they may have been involved with attachment of epaxial or costal musculature (e.g., iliocostalis). A discrete fossa is also present on the lateral surface of the anteroventral preacetabular iliac blade in a specimen of the dicynodont *Dicynodontoides* (Figure 11f, arrows). In the cynognathian *Luangwa drysdalli*, Kemp (1980a) suggested that the *medial* surface of the (laterally flaring) preacetabular iliac blade seen in NHMUK PV R.36995 possibly served as the origin for the PIFI in this taxon,

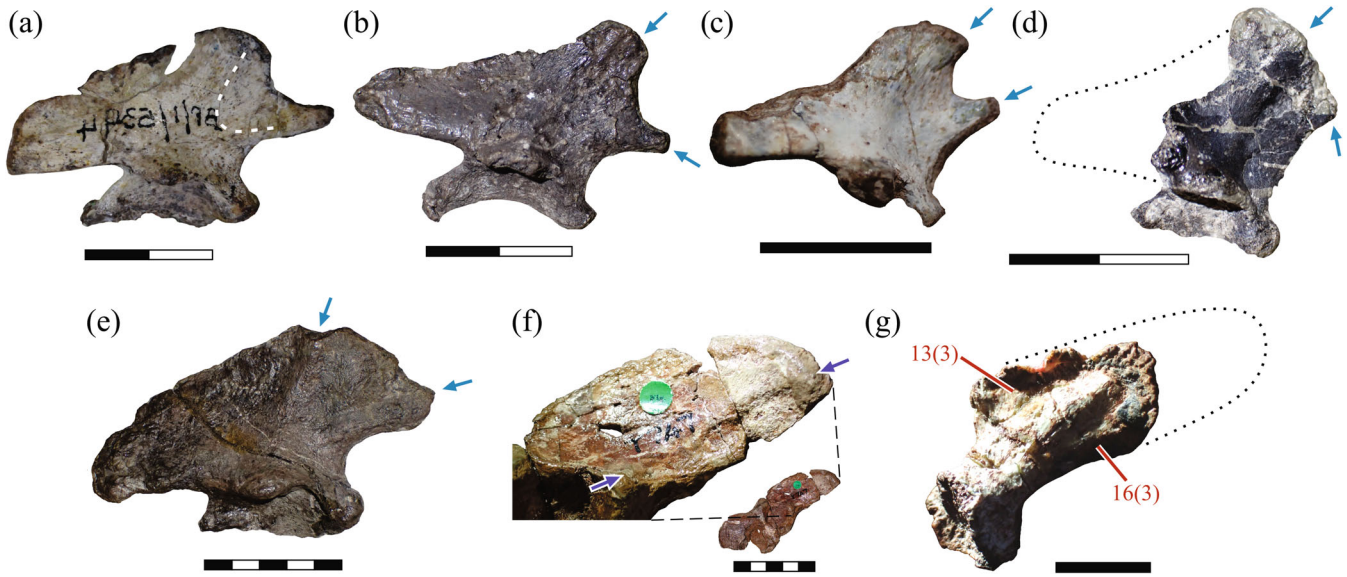

FIGURE 11 Putative osteological evidence of puboischiofemoralis musculature origin from the ilium in synapsids. (a) BP/1/5394 *Regisaurus jacobi*; (b) BP/1/3973 *Olivierosuchus parringtoni* (Botha-Brink et al., 2014; Eutherocephalia); (c) SAM-PK-K11543 *Scaloposaurus constrictus*; (d) BP/1/4335 cf. *Tetracynodon darti*; (e) NMQR 3351 *Moschorhinus kitchingi*; (f) UMZC T.747 *Dicynodontoides nowacki* (Dicynodontia) pelvis; enlarged inset shows shallow ventral fossa on ilium (between arrows). (g) UFRGS-PV-0248-T *Prozostrodon brasiliensis*. All specimens are shown in lateral view. In (a), the dashed line demarcates the fossa of attachment as interpreted by Kemp (1978), and a similar fossa is observed in many other eutherocephalian ilia between the two anterior processes (arrows in b–e).

arguing that the very reduced and posteriorly swept pubis offered little area for osseous attachment, necessitating an iliac origin. First-hand examination of the specimen shows the "fine striations" on this region of the bone to be indistinguishable from typical growth structures observed elsewhere on this and other elements. Although not refuted, Kemp's interpretation nevertheless is currently weakly supported by the osteological and phylogenetic evidence available. Presently the earliest-diverging synapsids that show convincing evidence of a PIFI origin from the ilium are the probainognathian cynodonts *Prozostrodon* (Figures 9n and 11g; Guignard et al., 2018) and *Therioherpeton* (Bonaparte & Barberena, 2001). The preacetabular iliac blade in both taxa is gently convex laterally, with a longitudinal ridge dividing incipient gluteal and iliac fossae (dorsally and ventrally, respectively; state 3), and this structural arrangement can be continually traced through to the "trihedral" iliac shape of crown mammals.

17. Insertion

0. Medial to posteromedial femur, between insertions of puboischiofemoralis externus (PIFE, on InTr) and IF, covering much of femur
1. Medial proximal femur, medial to IF insertion
2. Anterior to anteromedial proximal femur, bounded laterally and distally and separated from IF and FMT [rugose line]
3. Anteromedial and anterolateral proximal femur [multiple discrete scars]
4. Anteromedial proximal femur [longitudinally oriented, linear rugose area or process]
5. Anterior and anterolateral aspect of lesser trochanter (LeTr), sited medially or posteromedially on proximal femur [trochanter]

Remarks—The evolution of the PIFI's insertion on the line to mammals has historically been a subject of disagreement, stemming principally from debate over the possible homology between the InTr of nonmammalian, nonarchosaur tetrapods and the LeTr of extant mammals (Gregory & Camp, 1918; Guignard et al., 2019a; Jenkins, 1971; Kemp, 1978, 1980b; Parrington, 1961; Romer, 1922, 1924; Sues, 1986). As the InTr is at least plesiomorphically the principal site of insertion of the PIFE musculature, the issue of PIFI evolution is intimately tied to the evolution of the PIFE. Here the pure observations of purported PIFI scarring are documented, with the broader significance of these observations for understanding the evolution of PIFI and PIFE musculature explored in the Discussion.

As previously noted (e.g., Holmes, 2003; Romer, 1922; Romer & Price, 1940), a variety of stem and early crown amniotes exhibit a rugose line or linear patch of scars on the anterior to anteromedial femur, running diagonally across the anterior femur toward the large tubercle for the ischiotrochantericus (state 2; Figure 12a–c, between arrows). A longitudinally oriented scar or ridge in this region of the femur has hitherto been documented in a handful of therapsids (state 4; Boonstra, 1964; Fourie & Rubidge, 2007; Kemp, 1978, 1980b; Parrington, 1961; Romer, 1924; Rubidge et al., 2019), which was interpreted by Parrington (1961) and Kemp (1978) as denoting the insertion of the PIFI. First-hand examination shows that this scarring morphology is far more widespread than previously appreciated, being a consistent topographical feature on the femur of dinocephalians, gorgonopsians, scylacosaurids, and eutherocephalians (Figures 10g,h and 12d,e,g–o). It is also evident in the basal dicynodont *Eodicynodon* (Figure 12f) and *Charassognathus*, the oldest and most primitive known cynodont (Figure 12p; see also Discussion). Kemp (1980b) recognized "scarring" in this region of the femur in another primitive cynodont, *Procynosuchus delaharpeae*, but examination of his material (NHMUK PV R.37054) shows that the bone surface here is damaged and not reliably interpretable. Examination of RC 92 *Procynosuchus delaharpeae* via photographs and a high-fidelity cast (USNM PAL 410206) also shows no evidence of scarring on this region of the femur. However, scarring is clearly evident on the femora of the large taxa *Cynognathus* and *Diademodon* (Figure 12q–s). In all other cynodonts examined (including mammaliaforms), the only evidence of muscle insertion is the posteromedially situated LeTr (state 5; Figure 12t,u).

3.7 | Puboischiofemoralis externus (PIFE, Figures 13–15): Characters 18–20

18. Number of heads

0. One
1. Two
2. Three

Remarks—As with character 15, this character is primarily intended to capture structural diversity within each lineage. Given the generally poor (if any) differentiation of the PIFE in lepidosaurs or salamanders, it is unclear if any of the subdivisions in Crocodylia (PIFE 1, 2, and 3) can actually be equated with those of Mammalia (obturator externus/OBEX and quadratus femoris/QF).

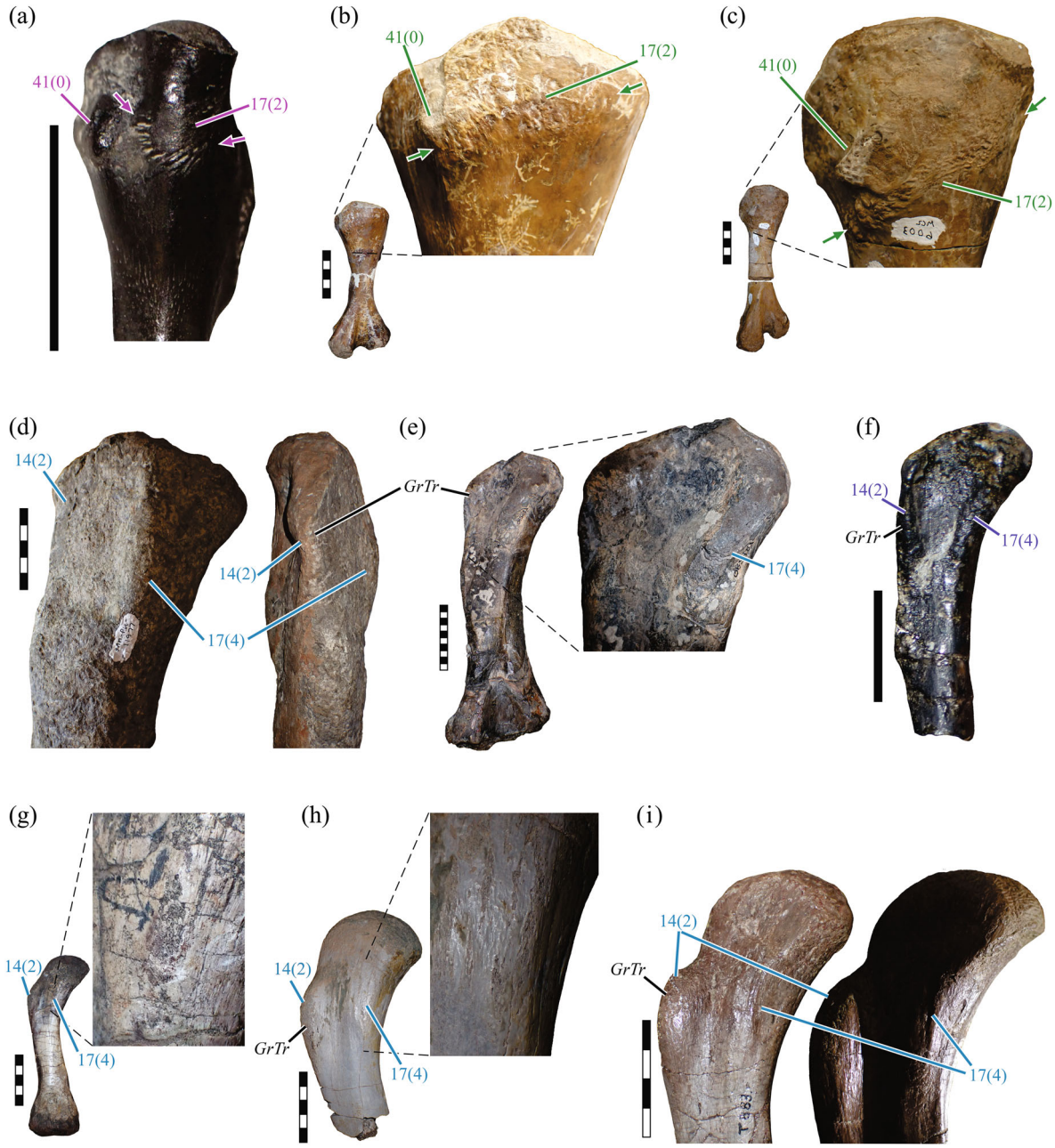

FIGURE 12 Osteological evidence of puboischiofemoralis internus musculature insertion on the femur in synapsids. (a) USNM PAL 768796 cf. *Captorhinus* (Captorhinidae), in anterior view. (b) MCZ VPRA-3296 *Ophiacodon retroversus* (Ophiacodontidae) in anterior view. (c) MCZ VPRA-6003 *Dimetrodon limbatus* (Sphenacodontia) in anterior view. (d) SAM-PK-11977a *Anteosaurus magnificus* (Anteosauridae) in anterior (left) and lateral (right) views. (e) NMQR 2987 *Tapinocaninus pamelae* (Tapinocephalidae) in anterior view. (f) NMQR 3155 *Eodicynodon oosthuizeni* (Dicynodontia) in anterior view. (g) GPIT-PV-31579 "*Scymnognathus*" *parringtoni* (Gorgonopsia) in anterior view. (h) SAM-PK-K10696 Gorgonopsia indet. in anterior view. (i) UMZC T.883 Gorgonopsia indet. in anterior view, right element on the left, left element (mirrored) on the right. (j) SAM-PK-11557 Scylacosauridae indet. in anterior view. (k) SAM-PK-K12051 *Alopecognathus* sp. (Scylacosauridae) in anterior view. (l) UMZC T.994 Whaitsiidae indet. (Eutherocephalia) in anterior view. (m) UMZC T.369 *Ericiolacerta parva* (Eutherocephalia) in anterior view. (n) UCMP 78396 *Tetracynodon darti* (Eutherocephalia) in anterior view. (o) BP/1/2468 *Ictidosuchops* sp. (Eutherocephalia) in anterior view. (p) SAM-PK-K10369 *Charassognathus gracilis* (Cynodontia) in anterior view. (q) NMHUK R.2571 *Cynognathus crateronotus* (Cynognathia) in anterior view, inset in medial view. (r) BP/1/1675 cf. *Cynognathus* in anterior view, inset in medial view. (s) UCMP 63529 cf. *Diademodon* sp. (Cynognathia) in anterior view. (t) MCZ VPRA-3801 *Massetognathus pascuali* (Cynognathia) in posterior view. (u) AMNH FARB 7656 Tritylodontidae indet. in posterior view. Arrows in (a)–(c) delimit a linear band of scarring, and those in (t) and (u) indicate margin of "intertrochanteric fossa."

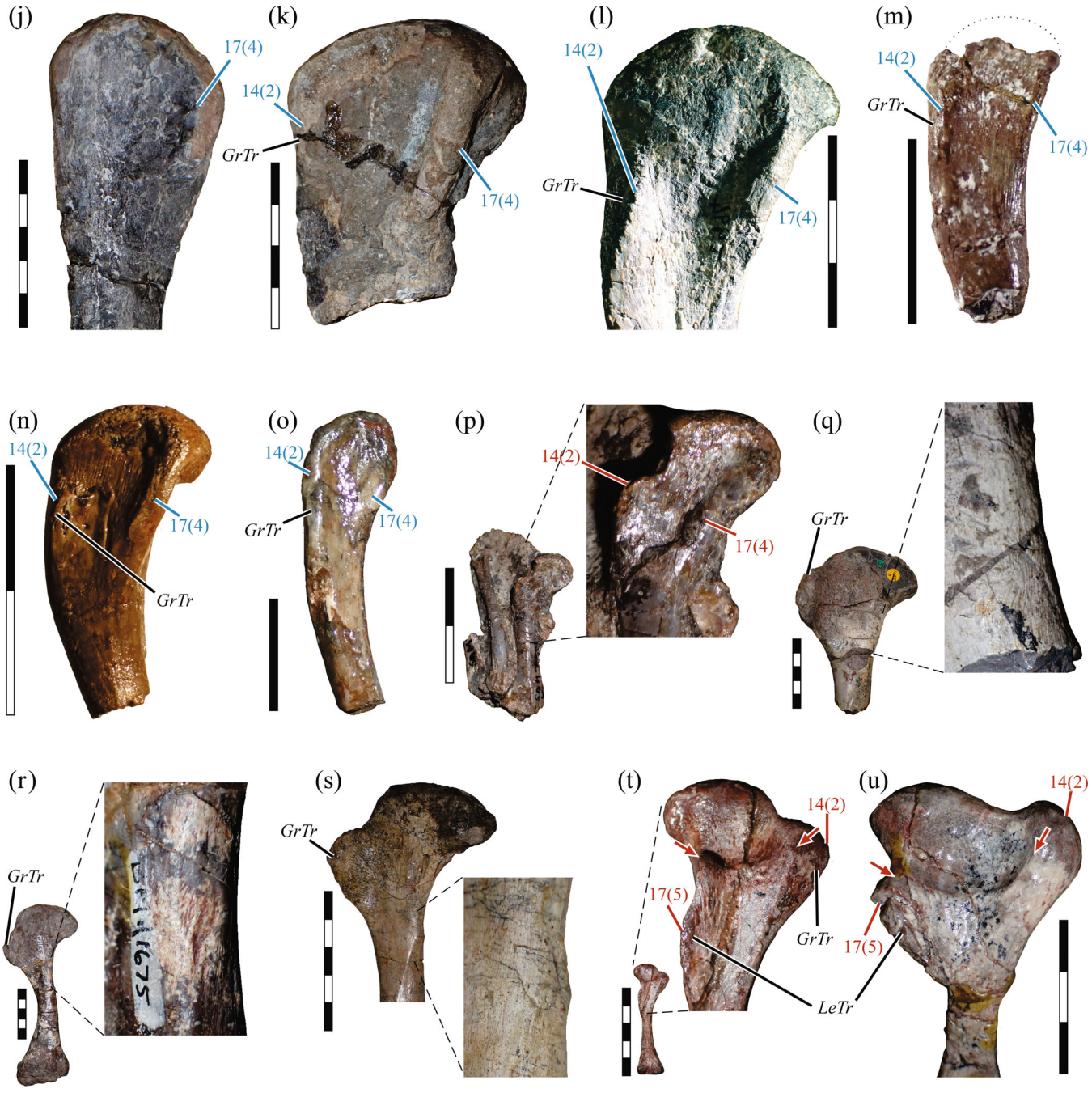

FIGURE 12 (Continued)

19. Origin

0. Much of ventral (lateral, outer) surface of puboischiadic plate and symphysis, including obturator foramen
1. Anteromedial and/or posterolateral pubis, lateral ischium [reduction of puboischiadic plate]
2. Much of lateral surface of pubis and ischium surrounding obturator foramen (anteriorly, ventrally, and posteriorly) [reduction of pubis, obturator foramen enlargement]

Remarks—Broad conservatism across extant tetrapods implies that the general locus of the PIFE's origin(s) was stable throughout synapsid evolution, being centered on the lateral surface of the puboischiadic plate. However, the size and morphology of the plate itself changed markedly on the line to mammals (Figure 3a–c,e–g). The pubis progressively reduced and rotated posteriorly, and the obturator foramen, originally piercing solely the pubis, enlarged and moved posteriorly to form an expanded fenestra situated between the pubis and ischium. The present

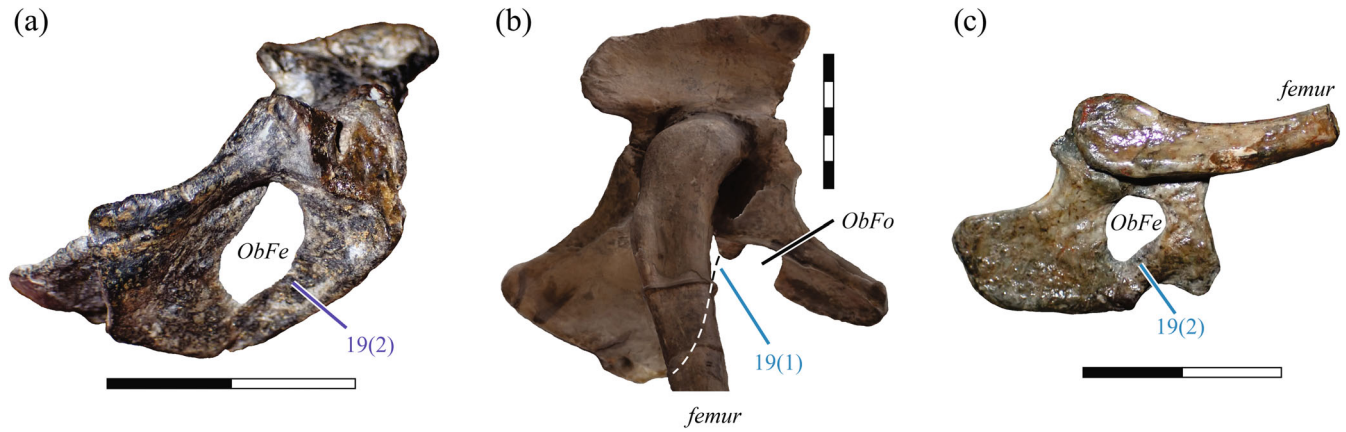

FIGURE 13 Modifications to the puboischiadic plate in therapsids. (a) The basal dicynodont *Eodicynodon oosthuizeni* (NMQR 3155) in ventrolateral view, showing the reduced pubis (characteristic of dicynodonts) and enlarged obturator fenestra (apomorphic to *Eodicynodon*). (b) The gorgonopsian *Lycaenops ornatus* (AMNH FARB 2240) in lateral view, showing the obturator foramen communicating ventrally to the space between ischium and pubis; image produced from a photocomposite made of the mounted skeleton. (c) The baurioid eutherocephalian *Ictidosuchops* sp. (BP/1/2468) in ventral view, showing the well-developed obturator fenestra characteristic of eutherocephalians.

character formulation captures these changes, but ignores superficially similar changes in other amniote groups, such as the development of the thyroid fenestra in lepidosaurs (Hutchinson, 2001b), which is not homologous to the obturator foramen, since the latter remains enclosed by the pubis and co-exists with the thyroid fenestra.

Superimposed upon the above general phyletic trend were a number of clade-specific variations. Among anomodonts, considerable reduction of the pubis had already occurred by the origin of dicynodonts, as evidenced by *Eodicynodon* (Figure 13a; Rubidge et al., 1994), and this was carried to an extreme in *Dicynodontoides* (Cox, 1959; King, 1985). In nondicynodont anomodonts, the obturator foramen remains contained wholly in the pubis, although its size is variable (Brinkman, 1981b; Fröbisch & Reisz, 2011), whereas in dicynodonts the foramen shifted posteriorly to lie along the puboischiadic suture. Typically the foramen remained small, although in *Eodicynodon* a large fenestra exists instead (Figure 13a; Rubidge et al., 1994). In gorgonopsians, exceedingly few specimens are known with a complete or near-complete pubis (e.g., *Gorgonops torvus* SAM-PK-K10585, K10591; *Lycaenops ornatus* AMNH FARB 2240), but it appears that the pubis was reduced in many taxa, whereby its articulation with the ischium occurred only around the acetabulum, creating an enlarged obturator foramen that communicated ventrally with the space between pubis and ischium (Figure 13b; Colbert, 1948; Tatarinov, 2004). At a gross structural level, this is similar to the condition in crocodylians, and thus gorgonopsians are tentatively coded as state 1 here. Notably, scylacosaurid therocephalians possess sizeable puboischiadic plates with small obturator foramina piercing the pubis (Boonstra, 1964; Fourie & Rubidge, 2009), whereas in eutherocephalians (Figure 13c) and cynodonts (Figure 3e), the pubis is reduced in size and the obturator foramen enlarged into a fenestra situated between the pubis and ischium (state 2).

In extant monotremes, Gambaryan et al. (2002) identified an "adductor brevis" as originating from much of the puboischiadic plate ventral to the obturator fenestra, with their OBEX occupying a rather small origin. Yet, the insertion of their adductor brevis was sited quite proximally on the posterior femur, among the insertions of the OBEX and QF, and proximal to the insertion of the caudofemoralis. Elsewhere among extant amniotes, the insertion of the adductor brevis (or its homologue) is always distal to that of the OBEX and QF (or their homologues); see also character 38 below. A likely explanation is that the "adductor brevis" of Gambaryan et al. is actually a subdivision of the OBEX; indeed, Gregory and Camp (1918) interpreted the OBEX origin to include much the same area of the puboischiadic plate as observed by Gambaryan et al. for their "adductor brevis."

20. Insertion

0. Apex of InTr and surrounding femoral bone surface medially, laterally, and distally [trochanter]
1. Apex of InTr on posteromedial proximal femur and fossa lateral to this (can include multiple discrete areas) [trochanter, posterolateral ridge, and intervening fossa]
2. Posterolateral proximal femur, proximal to insertion of caudofemoralis and origin of FMT, posterior to ischiotrochantericus insertion [rugose surface; InTr lost, fourth trochanter (4Tr) present]
3. Apex of InTr and surrounding area on posterior femoral surface [trochanter reduced, no posterolateral ridge or intervening fossa]

4. Posteroproximal femur, between GrTr and LeTr or more distally [smooth surface, LeTr on posteromedial margin of femur]

Remarks—As with the PIFI, important observations are documented here but an examination of the broader issues of femoral trochanter identity, homology, and evolution within Synapsida is left for the Discussion. Note that this study explicitly avoids using the term "intertrochanteric fossa" to describe the fossa characteristic of the posterior proximal femur of basal amniotes (contra Romer & Price, 1940). The fossa formed between the InTr and PosRid is not phylogenetically continuous with the intertrochanteric fossa of extant therians (i.e., fails the test of congruence, and hence not homologous), which is probably apomorphic for Theria (Romer, 1924) or a more inclusive clade. Although archosaurs are highly apomorphic for this character (state 2), the condition in testudines is quite comparable to state 1 (Walker, 1973; Zug, 1971).

A well-developed InTr is characteristic of stem and early crown amniotes, including "pelycosaurs," but it is characteristically reduced in therapsids (Figures 4a,b and 10a). A reduced InTr is retained alongside a subdued ridge and fossa in several dinocephalian femora of uncertain affinity from the middle Permian of Russia (Efremov, 1954; Seeley, 1894). A large InTr is present in association with a low ridge and fossa in the basal anomodont *Patranomodon* (state 1, Figure 14b; Rubidge & Hopson, 1996), but the proximal posterior femur of dicynodonts is considerably simplified, typically presenting a flat, featureless surface (state 4). However, occasionally large or well-preserved dicynodont femora exhibit a small rugose area or bump on the posteromedial surface, distal to the head, which is here interpreted as a vestigial InTr (state 3, Figure 14c–f). The manifestation of the InTr in gorgonopsians is variable (Figure 15). Typically it is present as a longitudinal ridge terminating proximally in a low apex (e.g., Figure 15a), but in some taxa (e.g., *Lycaenops ornatus* AMNH FARB 2240, *Cyonosaurus longiceps* SAM-PK-K10428) it is reduced to little more than a longitudinal patch of scarred surface texture (e.g., Figure 15d). In a handful of specimens collected in Tanzania and Zambia (UMZC and NHCC collections), a short ridge occurs on the posterior face of the femoral head around the level of the GrTr, in line with and proximal to the InTr (Figure 15e–g), which may denote a second discrete attachment of the PIFE. Parrington (1961) suggested that in one such specimen that preserved two apices (UMZC T.883), the distal of the two served as the insertion of the caudofemoral musculature, thus being homologous to the fourth trochanter (see character 44). While caudofemoral musculature is presumably inserted in this general region of the femur, the inconsistent manifestation of scarring on the posterior surface among gorgonopsians prevents the recognition of unambiguous, homologous osteological correlates of any additional muscles.

3.8 | Iliofibularis (ILFB, Figures 9 and 16): Characters 21 and 22

21. Origin

0. Posterior aspect of ilium, posterior to IF
1. Lateral aspect of posterior ilium, posterior to IF origin, and deep to IT origin [postacetabular iliac blade]
2. Posterolateral iliac blade and adjacent sacral or caudal vertebrae [postacetabular iliac blade reduced]
3. Transverse processes of anterior caudal vertebrae, deep to posterior IT head(s) [postacetabular iliac blade greatly reduced or absent entirely]
4. Absent

Remarks—In a similar fashion to the posterior head of the IT (character 3), it is hypothesized that as the postacetabular iliac blade became reduced in probainognathian cynodonts, and then lost in mammaliaforms, the origin of the iliofibularis shifted onto the neighboring caudal vertebrae to become the tenuissimus (TEN). The muscle has subsequently become greatly reduced in size, or even lost, in many extant mammals. Convergent reduction in the postacetabular iliac blade also occurred in dicynodonts (e.g., Cox, 1959; King, 1985; Ray, 2006; Figure 16g) and some derived cynognathians (Figure 16n), suggesting that at least a similar shift in origin had occurred in these taxa, if not an actual reduction in muscle size (see also next character). Many tapinocephalian dinocephalians possess a strongly developed, laterally projecting ridge on the postacetabuluar ilium, which probably signifies the attachment of the ILFB (Figure 9e; Boonstra, 1955a). The postacetabular iliac blade of sphenacodontids sometimes bears a series of longitudinal striations (Romer & Price, 1940; see also Figure 16c), which may signify ILFB attachment, but the possibility cannot be excluded that this alternatively represents the attachment of iliocaudalis musculature instead.

22. Insertion

0. Posterior proximal fibula
1. Lateral to anterolateral fibula [rugosity, ridge or tubercle]
2. Lateral distal crural fascia, deep to biceps femoris insertion (no direct osteological attachment)
3. Absent

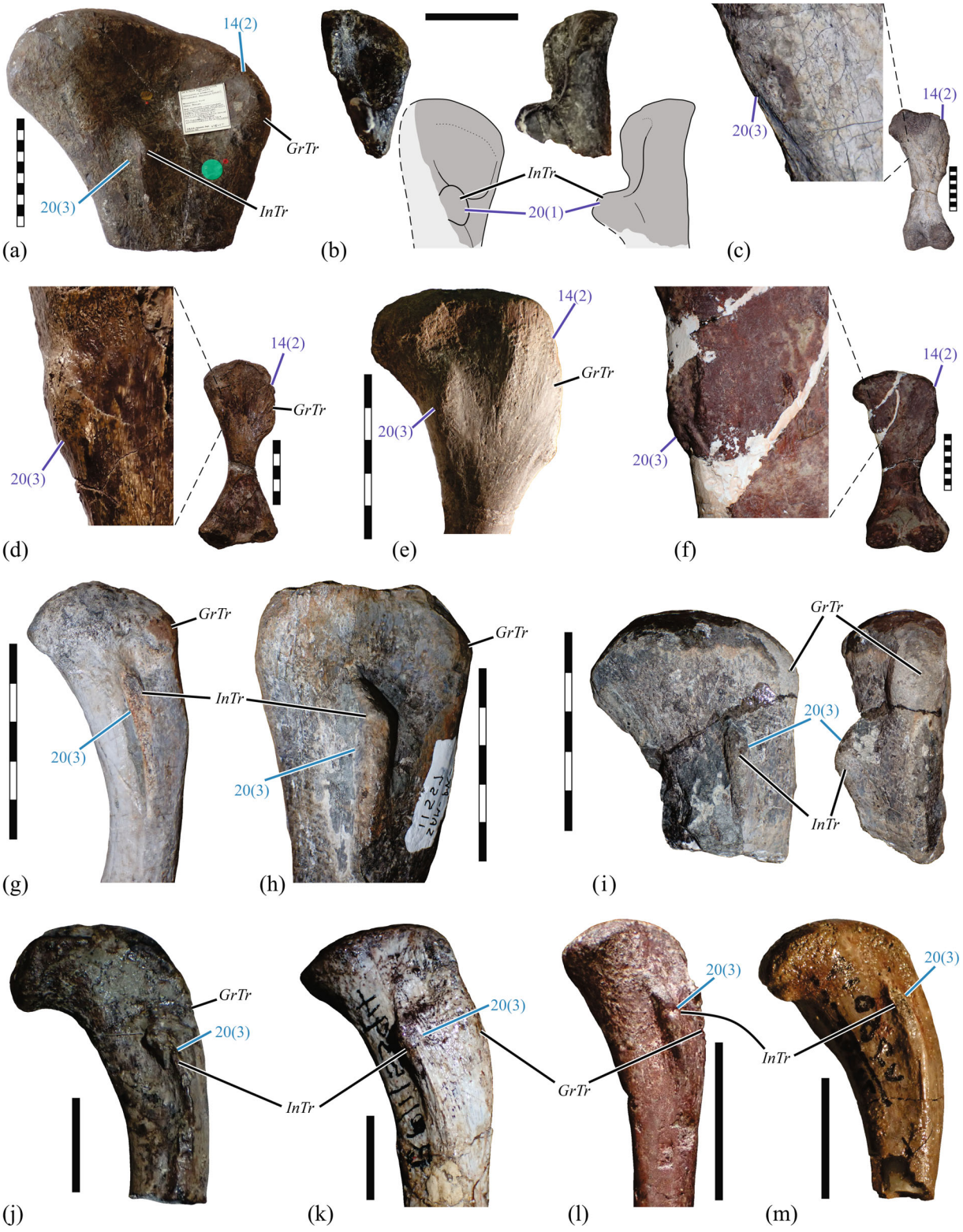

FIGURE 14 Osteological evidence of puboischiofemoralis externus musculature insertion on the femur in noncynodont therapsids. (a) NHMUK PV R.43523 *Tapinocephalus atherstonei* (Tapinocephalidae) in posterior view. (b) NMQR 3000 *Patranomodon nyaphulii* (basal anomodont) in posterior (left) and lateral (right) views, along with interpretive illustrations of the complete morphology of the proximal femur. (c) NMQR 1478 *Aulacephalodon bainii* (Dicynodontia) in posterior view. (d) NHMUK PV R.37374 Dicynodontia indet. in posterior view. (e) TM 4557 *Lystrosaurus* sp. (Dicynodontia) in posterior view. (f) BP/1/4450 *Kannemeyeria* sp. (Dicynodontia) in posterior view. (g) SAM-PK-K11200 Scylacosauridae indet. in posterior view. (h) SAM-PK-11557 Scylacosauridae indet. in posterior view. (i) SAM-PK-K12051 *Alopecognathus* sp. (Scylacosauridae) in posterior and lateral views. (j) NMQR 3375 *Theriognathus microps* (Eutherocephalia) in posterior view. (k) BP/1/5394 *Regisaurus jacobi* (Eutherocephalia) in posterior view. (l) UMZC T.837 *Scaloposaurus constrictus* (Eutherocephalia) in posterior view. (m) UCMP 78396 *Tetracynodon darti* (Eutherocephalia) in posterior view.

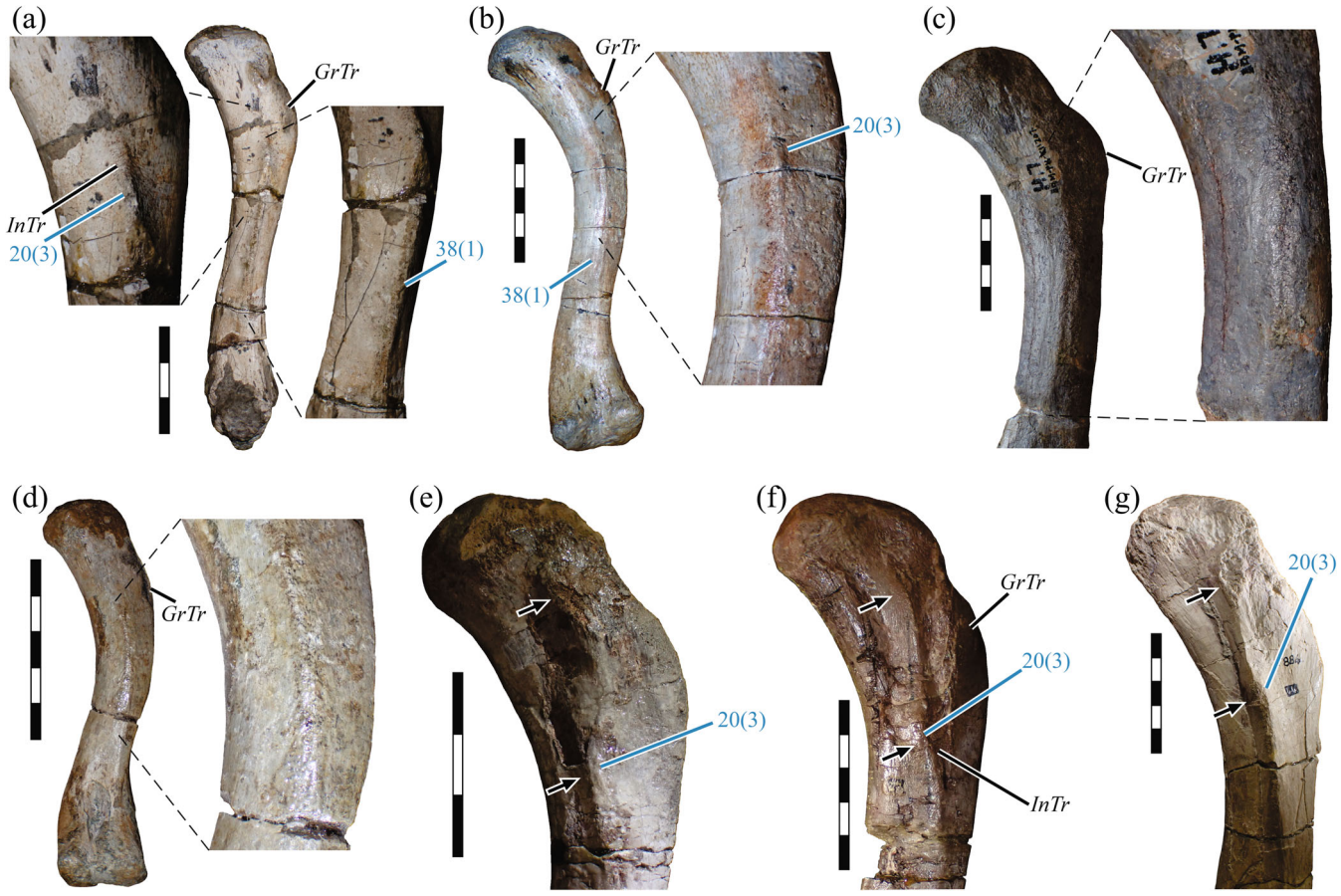

FIGURE 15 Variation in the manifestation of puboischiofemoralis externus musculature insertion on the femur of gorgonopsians. (a) TM 4821 indeterminate taxon. (b) SAM-PK-K8077 indeterminate taxon. (c) SAM-PK-K11207 indeterminate taxon. (d) SAM-PK-K10428 *Cyonosaurus longiceps*. (e) UMZC T.862 indeterminate taxon. (f) UMZC T.883 indeterminate taxon. (g) UMZC T.884 indeterminate taxon. Panels (a)–(d) illustrate a continuum of variation from a well-developed apex on the internal trochanter (a) through to none at all (d). Panels (e)–(g) illustrate the two-apices condition (arrows). All specimens are shown in posterior view.

Remarks—The ILFB is the only crural flexor muscle that derives from the dorsal muscle mass during embryonic development (Diogo et al., 2016). Plesiomorphically, it is the only such muscle to insert on the extreme lateral crus (i.e., exclusively on the fibula), although its insertion is deep into the bellies of the peronei. Curiously, along the line to mammals it was topologically (and by inference, functionally) replaced by the ventrally derived flexor tibialis internus 2 (FTI2), which started as a medially inserting muscle (see character 27 below) to become a laterally inserting muscle, the biceps femoris (BICF). Unlike the TEN, the BICF is the most superficial muscle on the lateral crus in extant mammals, superficial even to the peronei and extensor digitorum longus, gaining a primarily fascial rather than an osseous attachment. The rearrangement of muscles attaching to the lateral fibula is likely marked by the loss of the fibular tubercle/ridge, signaling the transition from direct osseous (ILFB/TEN-dominant) to indirect fascial (BICF-dominant) insertions. This would have occurred crownward to Mammaliaformes (Jenkins & Parrington, 1976; Kühne, 1956) but a more precise estimation of its timing is difficult to pinpoint due to the poor preservation of delicate bones like the fibula in most Mesozoic mammal fossils. A fibular tubercle is absent in *Gobiconodon* and multituberculates.

Among noncynodont therapsids, gorgonopsians are remarkable for the large size and distal positioning of the fibular tubercle, which is consistently present on the distal half of the bone (Figure 16i–l; Tatarinov, 2004). A similar, although not quite as distal, insertion also appears to be present in tapinocephalian dinocephalians and some dicynodonts, although in these forms the scarring is frequently less reduced and often only visible in large, well-preserved specimens (Figure 16e,f,h). One notable exception is *Dicynodontoides*, in which multiple specimens possess a large process on the distal third of the bone (Figure 16g; Angielczyk et al., 2009; King, 1985). This would suggest the retention of a well-developed ILFB, despite the pelvis all but lacking any postacetabular iliac process, implying that a shift in muscle

FIGURE 16 Osteological evidence of iliofibularis musculature attachment in synapsids. (a) MCZ VPRA-1035 *Diadectes tenuitectus* (Diadectomorpha) fibula in anterior view. (b) MCZ VPRA-5876 *Ophiacodon retroversus* (Ophiacodontidae) fibula in anterior view. (c) AMNH FARB 24600 Eupelycosauria indet. pelvis in lateral view. (d) MCZ VPRA-1283 *Dimetrodon giganhomogenes* fibula in anterior view. (e) NMQR 2987 *Tapinocaninus pamelae* (Tapinocephalidae) fibula in anterolateral view. (f) AMNH FARB 5551 *Moschops capensis* (Tapinocephalidae) fibula in anterolateral view. (g) NMQR 479 *Dicynodontoides recurvidens* (Dicynodontia) pelvis in lateral view and fibula in medial view. (h) BP/1/4450 *Kannemeyeria* sp. (Dicynodontia) fibula in posterior view. (i) AMNH FARB 5607 cf. *Aelurosaurus felinus* (Gorgonopsia) fibula in lateral view. (j) CGS FI17 *Lycaenops ornatus* (Gorgonopsia) fibula in lateral view. (k) BSPG 1934-VIII-28 *Gorgonops* sp. (Gorgonopsia) fibula in posterior view. (l) SAM-PK-K10585 cf. *Gorgonops torvus* (Gorgonopsia) fibula in posterolateral view. (m) BP/1/1675 cf. *Cynognathus* (Cynognathia) fibula in lateral (left) and anterior (right) view. (n) PVL 2554 *Exaeretodon argentinus* (Cynognathia) ilium and fibula in lateral view. (o) UFGRS-PV-1051-T *Trucidocynodon riograndensis* (basal probainognathian) fibula in medial view (inset in posterolateral view).

origination need not have coincided with its reduction. Remarkably, a highly reduced postacetabular ilium and large, distally positioned fibular tubercle is also observed in the derived cynognathian *Exaeretodon* (Figure 16n); elsewhere among cynodonts, scarring for the ILFB remains proximally sited on the fibula (Figure 16m,o).

3.9 | Flexor tibialis internus (FTI, Figure 17): Characters 23–27

23. Number of heads

0. Absent
1. At least two

Remarks—The FTI of salamanders is absent as a discrete muscle and, along with the flexor tibialis externus, is probably part of the apomorphic "ischioflexorius" complex (Table 1; Diogo & Molnar, 2014); thus, salamanders are coded as state 0 for characters 23–27. Although sauropsids and some extant mammals have three or more heads, it appears that these can be grouped into two general masses that are homologous across amniotes (Jones, 1979): the ancestral amniote probably had two internal flexors, a ventral (FTI1) and a dorsal (FTI2) one, which ultimately evolved (at least in part) into the semimembranosus (SMEM) and biceps femoris (BICF) of mammals, respectively. A more precise relationship of homology between the different heads and their various subdivisions across sauropsids and mammals is currently unclear, and may

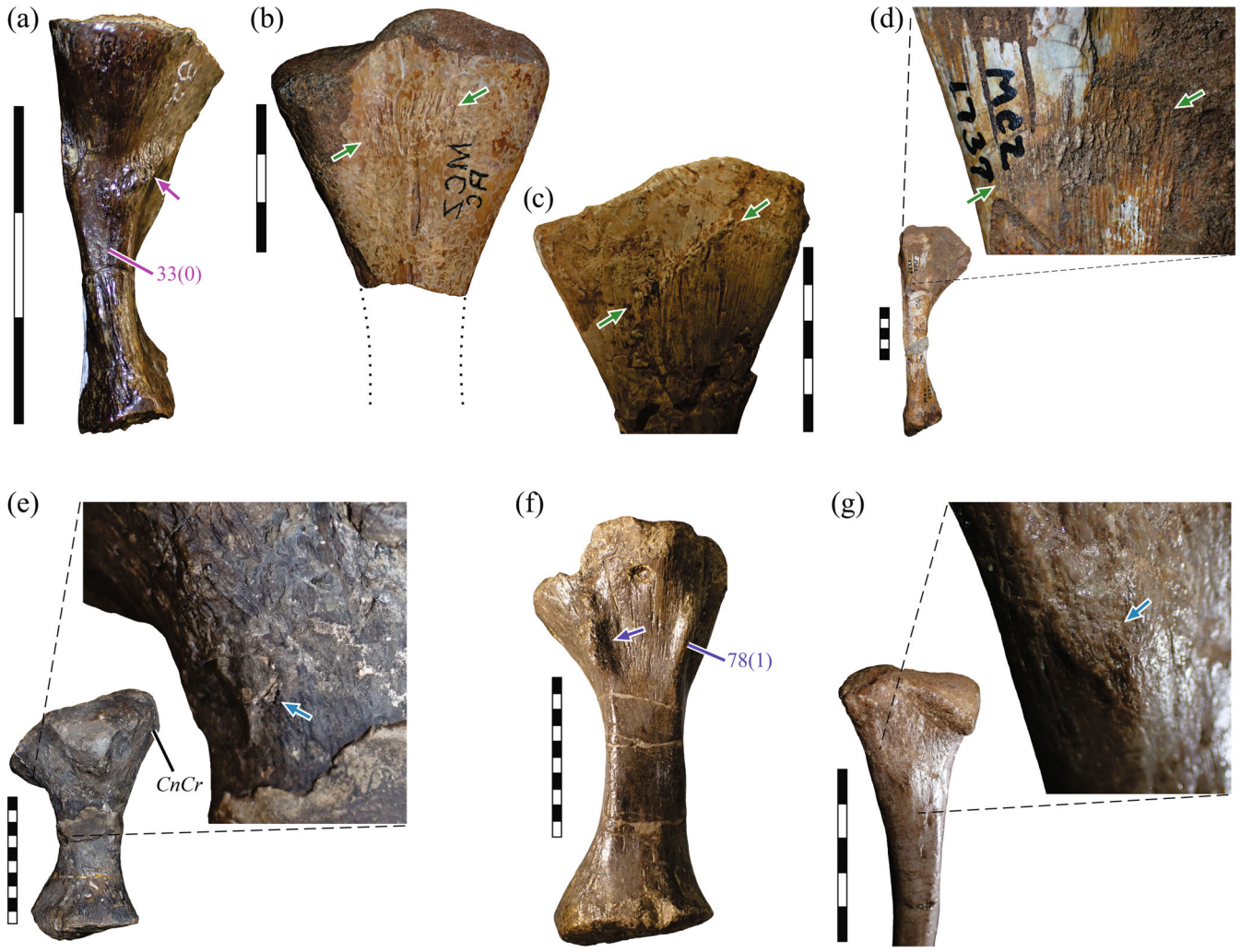

FIGURE 17 Osteological evidence of crural flexor musculature attachment to the tibia in synapsids, in addition to that of the puboischiotibialis (see Figure 18). (a) MCZ VPRA-2045 *Archeria crassidisca* (Embolomeri, stem amniote) in medial view. (b) MCZ VPRA-2930 *Ophiacodon retroversus* (Ophiacodontidae) in posterior view. (c) MCZ VPRA-5669 *Ophiacodon retroversus* in posterior view. (d) MCZ VPRA-1737 *Dimetrodon* sp. (Sphenacodontia) in posterior view E, AMNH FARB 5322 *Moschops capensis* (Tapinocephalidae) in lateral view). (f) UCMP 32447 *Placerias gigas* (Dicynodontia) in posterior view. (g) UMZC T.883 Gorgonopsia indet. in posterolateral view. Arrows signify likely attachment sites for at least one crural flexor muscle, although which one(s) in particular is difficult to resolve.

additionally be entangled with part of the flexor tibialis externus (Diogo & Molnar, 2014; Jones, 1979). Further investigation is needed before a more refined (better split) set of characters and states can be constructed.

24. FTI1 origin

0. Absent as a discrete muscle
1. Posterolateral ischial surface, near ischiocaudalis origin and ilioischiadic ligament attachment [ischiadic tuberosity], possibly also from ilioischiadic ligament

Remarks—Although salamanders are coded as state 0 here, it is worth noting that the "ischioflexorius" originates from the posterolateral corner of ischium, comparable to the situation in amniotes.

25. FTI2 origin

0. Absent as a discrete muscle
1. Apex of posterodorsal ischium [tuberosity] and possibly also transverse processes of posteriormost sacral vertebrae and/or anteriormost caudal vertebrae (BICF)

Remarks—The "short head" of the BICF is apomorphic for a select group of derived placentals, and may in fact be derived from the TEN observed in other therians, including marsupials (Diogo et al., 2016; Green, 1931); it is not considered further here. The posterodorsal corner of the ischium becomes mediolaterally thickened in eucynodonts (and convergently in derived dicynodonts) to form a clearly defined tuberosity (IsTu, see Figure 20d–k). The development of an ischiadic tuberosity on the line to mammals possibly reflects a change in the loading regime (mechanobiological stimulus) experienced by the bone, with a shift from caudal (posterior-pulling) to appendicular (laterally pulling) muscles dominating local bone loading. This may have occurred in association with reduction of tail musculature and increased emphasis on crural flexors for powering femoral retraction.

26. FTI1 insertion

0. Absent as a discrete muscle
1. Posterior proximal tibia [scarring]

27. FTI2 insertion

0. Absent as a discrete muscle
1. Posterior proximal tibia, distal to pubotibialis insertion [scarring], medial to lateral extent variable
2. Superficial aspect of lateral crus; direct osseous attachment either absent or on lateral aspect of proximal fibula and/or tibia and/or patella (BICF)

Remarks—As noted above, the mammalian BICF exhibits a stark topological change compared to its precursor muscle in the ancestral amniote. Uniquely among the crural flexors of all amniotes, this muscle passes *laterally* behind the thigh to become the most superficial muscle attaching to the lateral crus (including the TEN, when present). Proximally, its origin may also shift somewhat laterally as it gains an attachment to the vertebral column. In placentals, the BICF is the most superficial muscle of the back of the thigh, but laterally it remains deep to the GMAX and FCOC.

Large, well-preserved tibiae of some stem amniotes and nonmammalian synapsids occasionally possess scarring on the posterior to posteromedial aspect of the proximal end, either as a discrete patch of striations or as a rugose bump (Figure 17, arrows). This probably marks the insertion of at least one crural flexor, although which one precisely (FTI1,2 or FTE, or homologues) is difficult to discern.

3.10 | Flexor tibialis externus (FTE): Characters 28–31

28. Number of heads

0. Absent
1. One
2. Two (both forming the semitendinosus, STEN)

Remarks—The FTE of salamanders is absent as a discrete muscle, probably forming part of the "ischioflexorius" (Table 1; Diogo & Molnar, 2014); salamanders are coded as state 0 for characters 28–31.

29. Origin

0. Absent as a discrete muscle
1. Ilioischiadic ligament and fascia covering proximal tail muscles
2. Lateral surface of postacetabular iliac process (deep to posterior IT origin)
3. Lateral aspect of ischiadic tuberosity in close association with BICF origin (ventral head), transverse processes of sacral and/or anteriormost caudal vertebrae (dorsal head)

Remarks—Although salamanders are coded as state 0 here, it is worth noting that the "ischioflexorius" originates from the posterolateral corner of ischium, in the same general location as the FTE of most amniotes. In monotremes, the origin of the dorsal head is expanded anteriorly to include all sacral vertebrae (and in *Ornithorhynchus* it extends even further to the posteriormost lumbar vertebrae), such that this muscle becomes the most superficial of the lateral aspect of the thigh. Although the STEN of mammals is not tightly associated with the ischiadic tuberosity (i.e., has no unambiguous osteological correlate), the topographic shift of the FTE origin on the line to mammals, from a plesiomorphic position dorsal to the ischium to being more directly attached to the ischium itself, may have nonetheless contributed to the development of the tuberosity.

30. Primary insertion

0. Absent as a discrete muscle
1. Posteromedial to medial proximal tibia (extent variable), and possibly surrounding fascia

31. Secondary insertion

0. No, FTE absent as a discrete muscle
1. Yes, via additional tendon to gastrocnemius externus
2. No, FTE only has one insertion

3.11 | Puboischiotibialis (PIT, Figure 18): Characters 32 and 33

32. Origin

0. Much of puboischiadic symphysis, and possibly also posterior aspect of pubic tubercle
1. Proximal lateral ischium (PIT [small scar]) and postacetabular iliac process (FTI2)

Remarks—The general arrangement of the PIT across tetrapods is conservative, as the most superficial of the ventral thigh muscles, covering much of the ventral surface of the thigh. It is generally broad and sheet-like proximally, especially in salamanders and lepidosaurs that retain a long puboischiadic plate, and tends to be undivided. Although mammals have an abbreviated pubis, the PIT (gracilis, GRA) can sometimes extend anteriorly onto the base of the epipubis (where present) or iliopubic ligament. Whereas the PIT also originates from a puboischiadic ligament in extant saurians (Hutchinson, 2001a), both salamanders and mammals apparently lack such a ligament, with the muscle directly attaching to the pelvic midline; the ligament may hence be apomorphic for Sauria or a more inclusive clade. Irrespective of these differences, it is fairly certain that the PIT of nonmammalian synapsids took origin on or near a substantial portion of the ventral pubis and ischium. Crocodylians present a highly modified, bipartite, and fusiform configuration of the PIT, possibly associated with the opening up of the puboischiadic plate in archosaurs (state 1; Hutchinson, 2001b).

33. Insertion

0. Posteromedial to medial tibia, typically in close association with FTI/SMEM and FTE/STEN insertions but medial/superficial to them [scarring or groove]

Remarks—As with its origin, the insertion of the PIT is highly conservative across tetrapods. It is demarcated by scarring that can be traced continuously from stem amniotes through to extant synapsids and sauropsids (Figures 5 and 18). Scarring is plesiomorphically manifested as a longitudinal groove on the anteromedial to posteromedial tibia that "faces" posteromedially (i.e., anterior border more pronounced than posterior), and this basic pattern persists with little modification through to extant mammals. In sauropsids, however, it typically acquires positive relief, forming a tuberosity. Quite remarkably, the PIT insertion is distally extensive in stem amniotes and most nonmammalian synapsids, where scarring typically extends down at least two thirds of the length of the tibia. Many extant quadrupedal mammals retain an extensive insertion of the PIT (GRA) and other crural flexors on the tibia, whereas the crural flexors of sauropsids are generally more proximally restricted in their insertions.

Although many previous studies of nonmammalian synapsid postcrania have described or illustrated this structure in passing (Bonaparte, 1963; Fourie & Rubidge, 2007; Jenkins, 1970, 1971; Kemp, 1978; King, 1985; Orlov, 1958; Romer & Price, 1940; Sues & Jenkins, 2006), little interpretation has been offered by way of soft tissue attachment. Holmes (1984) and Pawley and Warren (2006) interpreted this scar as denoting insertion of the PIT in embolomere stem amniotes and temnospondyl amphibians, respectively, but Sumida (1989) and Holmes (2003) suggested that the scar in captorhinids denoted the origin of the tibialis anterior. However, considering the muscle arrangements observed in extant synapsids and saurians, and the wealth of fossil evidence arguing for strong phylogenetic continuity of both this scar and the origin of the tibialis anterior (see character 68 below),

FIGURE 18 Legend on next page.

the interpretation of a PIT insertion is strongly supported. It cannot be ruled out that other crural flexors may have additionally inserted somewhere on this scar.

3.12 | Pubotibialis (PUT): Characters 34 and 35

34. Origin

0. Anterolateral aspect of pubis, on or near pubic tubercle
1. Absent
2. Two origins—anterolateral aspect of pubis, on or near pubic tubercle including epipubis (pectineus, PECN); and anteroventral pubis and possibly epipubis, ventral to first origin (adductor longus, ADDL)

Remarks—The evolutionary history of this muscle on the line to mammals is complex, starting in the ancestral amniote as a singular crural flexor and ending up as at least two hip adductors. Moreover, it involves one of the few well-supported instances of the "recombination" of disparate muscles to form new muscles (Diogo et al., 2016). Based on topology and innervation patterns, Romer (1922) first suggested that as the ancestral PIFI mass migrated dorsally on the line to mammals (character 16), part of it was "left behind" to form the mammalian PECN, but he assumed that the ancestral PUT was wholly lost. Through embryological study, Jones (1979) found evidence supporting the derivation of the PECN in part from the PIFI, but also recognized a partial derivation from the PUT; moreover, the ADDL of mammals was also homologous with the PUT mass. The dual origin of the PECN is perhaps also evidenced by its bipartite structure in some marsupials (MacCormick, 1887; Reilly et al., 2010; Stein, 1981). Apparently, on the line to mammals, as the PIFI migrated dorsally, part of it fused with part of the PUT to form the PECN (the remaining PIFI mass continued dorsally to form the ILC and PSO), and the remaining PUT retracted its insertion from the proximal tibia to distal femur to become the ADDL (see next character). The PUT was therefore never "lost" on the line to mammals, just recombined.

Examining the PUT's history in the fossil record cannot be undertaken directly, as there are no unambiguous osteological correlates of its origin or insertion. (Similar to the AMB, the pubic tubercle is not taken as an unambiguous indicator of the presence of the PUT, only the general location of the muscle's origin, if it were indeed present.) However, if it is assumed that the above transformational hypothesis is correct, then observation of osteological correlates for the PIFI can help indirectly constrain some aspects of the PUT's history. Dorsal migration of the PIFI is signaled, at least in part, by the reduction of the pubis [character 16(1/2)] and appearance of a discrete surface or fossa on the ventral preacetabular ilium [character 16(3)]. The pubis is evidently reduced in therapsids before the appearance of a surface or fossa on the ilium in advanced cynodonts (Figure 3; Supporting Information Appendix S3), consistent with the aforementioned transformational hypothesis. As noted above, the probainognathians *Prozostrodon* and *Therioherpeton* are the earliest-diverging taxa to exhibit an incipient iliac fossa, suggesting that the reorganization of the PIFI—and

FIGURE 18 Osteological evidence of puboischiotibialis musculature attachment to the tibia from stem amniotes to extant mammals [character 33(0)]. (a) MCZ VPRA-2045 *Archeria crassidisca* (stem amniote). (b) MCZ 1948 *Limnoscelis paludis* (Diadectomorpha). (c) MCZ VPRA-1035 *Diadectes tenuitectus* (Diadectomorpha). (d) USNM PAL 768797 cf. *Captorhinus* (Captorhinidae). (e) AMNH FARB 4394 *Labidosaurus hamatus* (Captorhinidae). (f) MCZ VPRA-1443 *Ophiacodon retroversus* (Ophiacodontidae). (g) MCZ VPRA-1926 *Varanops* sp. (Varanopidae). (h) MCZ VPRA-4324 *Edaphosaurus boanerges* (Edaphosauridae). (i) MCZ VPRA-2944 *Secodontoaurus* sp. (Sphenacodontia). (j) AMNH FARB 5322 *Moschops capensis* (Tapinocephalidae). (k) NMQR 2987 *Tapinocaninus pamelae* (Tapinocephalidae). (l) UFRGS-PV-1051-T *Tiarajudens eccentricus* (basal anomodont). (m) NMQR 479 *Dicynodontoides recurvidens* (Dicynodontia). M, SAM-PK-2348 cf. *Dicynodon* sp. (Dicynodontia). (o) NMQR 3940 *Lystrosaurus mccaigi* (Dicynodontia). (p) UMZC T.883 Gorgonopsia indet. (q) SAM-PK-K11200 Scylacosauridae indet. (r) NMQR 3351 *Moschorhinus kitchingi* (Eutherocephalia). (s), BP/1/5394 *Regisaurus jacobi* (Eutherocephalia). (t) UMZC T.837 *Scaloposaurus constrictus* (Eutherocephalia). (u) NHMUK PV R.37054 *Procynosuchus delaharpeae* (Cynodontia). (v) BP/1/2752 *Thrinaxodon liorhinus* (Cynodontia). (w) BP/1/1675 cf. *Cynognathus* (Cynognathia). (x) NMQR 1208 cf. *Cynognathus crateronotus*. (y) NHMUK PV R.3581 *Diademodon tetragonus* (Cynognathia). (z) PVL 2162 *Exaeretodon* sp. (Cynognathia). (aa) MCZ VPRA-3691 *Massetognathus pascuali* (Cynognathia). (ab) UFRGS-PV-1051-T *Trucidocynodon riograndensis* (basal probainognathian). (ac) MCZ VPRA-8838 cf. *Kayentatherium wellesi* (Tritylodontidae). (ad) MCZ VPM-19956 *Eozostrodon parvus* (Mammaliaformes). (ae) MCZ VPM-19965 *Gobiconodon ostromi* (Theriiformes). (af) MCZ 25461 *Tachyglossus aculeatus* (Monotremata). (ag) MCZ 104 *Didelphis marsupialis* (Theria). All panels are shown in medial view, except for (e) which is shown in both anterior (left) and medial (right) views, and (f) which is shown in medial (left) and posterior (right) views. These illustrate a highly conserved manifestation of the muscle's attachment (longitudinal groove or scar, between arrows), which can be traced continuously from stem amniotes through to extant therians. Note the great distal extent of the scar in many instances.

by extension the PUT—was more or less complete by that stage in synapsid evolution.

35. Insertion

0. Posteromedial to posterolateral proximal tibia, generally more proximal to FTI, FTE, and PIT insertions
1. Absent
2. Two insertions—medial to posteromedial aspect of middle of femoral shaft (PECN); and anteromedial to posterior aspect of distal femur (ADDL)

3.13 | Adductor femoris (ADD, Figure 19): Characters 36–38

36. Number of heads

0. One
1. Two

Remarks—Monotremes are coded as possessing a single head, as the "adductor brevis" of Gambaryan et al. (2002) is reinterpreted here as a subdivision of the OBEX (see character 19 above).

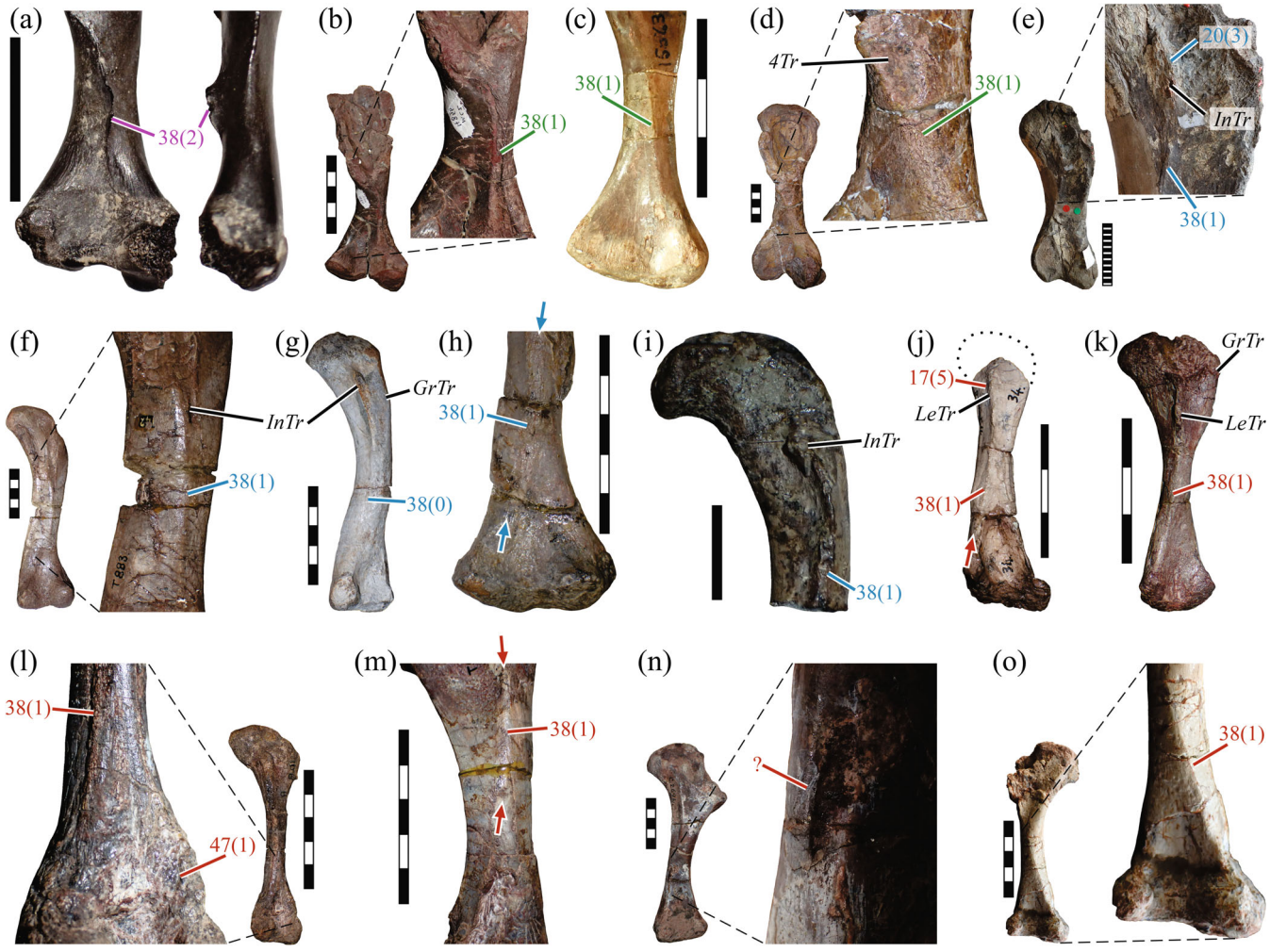

FIGURE 19 Osteological evidence of adductor musculature attachment to the femur in synapsids. (a) USNM PAL 768796 cf. *Captorhinus* (Captorhinidae). (b) MCZ VPRA-4856 *Ophiacodon mirus* (Ophiacodontidae). (c) USNM V 15563 *Varanosaurus acutirostris* (Ophiacodontidae). (d) AMNH FARB 4006 *Lupeosaurus kayi* (Edaphosauridae). (e) NHMUK PV R.49368 *Titanosuchus ferox* (Titanosuchidae). (f) UMZC T.883 Gorgonopsia indet. (g) SAM-PK-K11200 Scylacosauridae indet. (h) SAM-PK-K7809 *Glanosuchus macrops* (Scylacosauridae). (i) NMQR 3375 *Theriognathus microps* (Eutherocephalia). (j) NHMUK PV R.37054 *Procynosuchus delaharpeae* (Cynodontia). (k) TM 83 *Galesaurus planiceps* (Cyodontia). (l) UMZC T.975 *Scalenodon* sp. (Cynognathia). (m) UMZC T.863 Cynognathia indet. (n) NMQR 1206 *Diademodon tetragonus* (Cynognathia). (o) UFRGS-PV-1051-T *Trucidocynodon riograndensis* (basal probainognathian). All bones are shown in posterior view.

37. Origin

0. Ventral and anterior aspect of anterolateral pubis
1. Puboischiadic ligament and surrounding aponeurosis, deep to PIT, and crural flexors
2. Anterior and posterior aspects of lateral ischium
3. Ventrolateral aspect of ischium and/or pubis

Remarks—Although unambiguous osteological correlates are wanting for this character, a puboischiadic ligament may be apomorphic for saurians (as noted above), and the ischial origin in Crocodylia is probably apomorphic for Archosauria due to the opening up of the ventral pelvis (state 2; Hutchinson, 2001b).

38. Insertion

0. Posterior to posteromedial aspect of distal femoral shaft [smooth surface]
1. Posterolateral aspect of femoral shaft [faint longitudinal ridge or rugosity(ies), leading distally from InTr and/or fourth trochanter]
2. Posterolateral aspect of femoral shaft [deep longitudinal crest, leading distally from InTr and/or fourth trochanter]
3. Posterior aspect of distal femoral shaft [two discrete scars]

Remarks—In reality, states 0–2 are ostensibly a discretization of a continuous trait, especially since some "pelycosaur" clades exhibit multiple states across their history. Whether the expression of these states correlates with body (or femur) size, or the expression of other scars on the femur, remains to be investigated. As a general rule throughout the stem and early crown amniotes, the scarring manifested as states 1 or 2 tracks from a more medial side of the femur proximally, diagonally across the posterior shaft toward the lateral condyle distally (e.g., Holmes, 2003; Romer & Price, 1940; Sumida, 1997). One notable exception is the "pelycosaur" genus *Ophiacodon*, where scarring has shifted to lie entirely along the lateral aspect of the shaft (Figure 19b); in the large species *O. retroversus*, it forms a massive posterolateral flange along the entire shaft (Romer & Price, 1940), capped with scarring texture along its apex. This is presumably correlated with the autapomorphic condition of the fourth trochanter in the genus (4Tr, see character 44 below).

Compared to "pelycosaurs," putative scarring for the ADD is less commonly observed in therapsids (Figure 19e–i). Scarring is exceedingly rare among non-mammalian cynodonts, but some exceptions to this generality are illustrated in Figure 19j–o. Aside from *Procynosuchus* (Figure 19j), these instances are so uncommon that they do not bear on the coding for their respective OTUs in the current study.

3.14 | Ischiotrochantericus (ISTR, Figures 20 and 21): Characters 39–41

39. Number of heads

0. One
1. Two (obturator internus [OBIN], gemellus [GEM]) or more

Remarks—Monotremes possess a single head that lacks any origin from the medial (inner, dorsal) surface of the ischium, which would correspond to the OBIN of therians. It is not currently possible to discern whether this reflects the plesiomorphic single-headed condition (with just a restricted origin), or instead is apomorphic, with the OBIN having differentiated prior to crown Mammalia, and subsequently becoming lost in extant monotremes (i.e., they possess just the GEM). Study of embryological development may clarify the matter.

40. Origin

0. Posterolateral and/or posterodorsal (internal/medial) aspects of ischium [shallow depression facing dorsomedially]
1. Dorsolateral ischium posterior to acetabulum [shallow, longitudinal depression/groove facing dorsolaterally], plus medial surface of ischium
2. Dorsolateral ischium posterior to acetabulum, plus medial surface of ischium, pubis, and obturator fenestra membrane

Remarks—The frequently extensive invasion of the medial surface of the ischium and pubis by the ISTR in extant therians is only possible because this region had already been vacated by the PIFI, which pleisomorphically occupied much of the same area (see character 16). If dorsal migration of the PIFI was indeed a "prerequisite" for an extensive medial origin of the ISTR (specifically, OBIN), then medial expansion of the ISTR could have been well underway even within probainognathian cynodonts (see character 34).

As the single-headed ISTR of monotremes takes origin from the dorsolateral aspect of the ischium

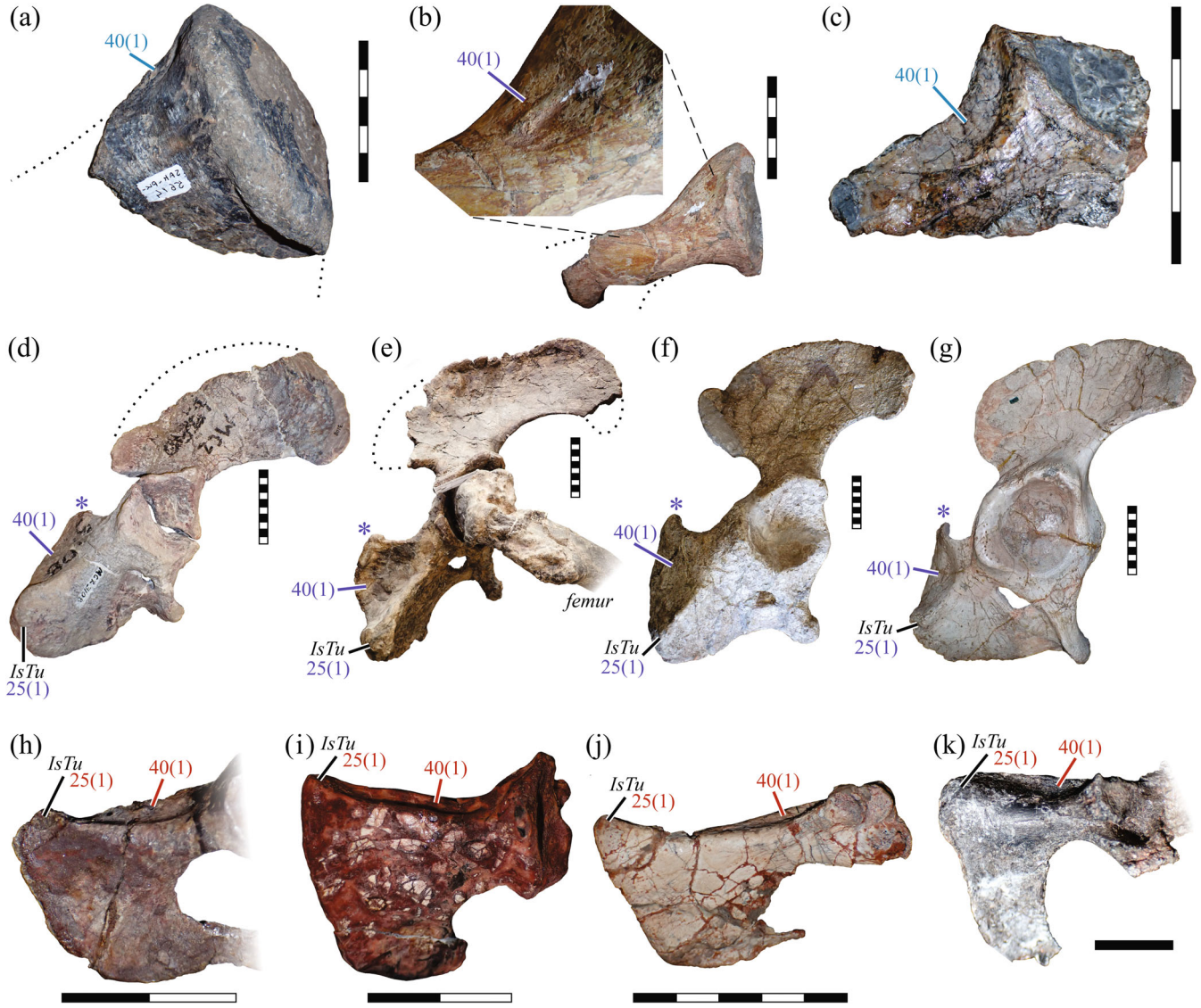

FIGURE 20 Osteological evidence of ischiotrochantericus musculature origin from the pelvis in synapsids. (a) SAM-PK-5614 *Anteosaurus magnificus* (Anteosauridae) proximal ischium. (b) SAM-PK-2348 cf. *Dicynodon* sp. (Dicynodontia) ischium. (c) SAM-PK-K10591 *Gorgonops torvus* (Gorgonopsia) ischium. (d) MCZ VPRA-3018 *Dinodontosaurus tener* (Dicynodontia) pelvis. (e) GPIT-PV-30792 *Stahleckeria potens* (Dicynodontia) pelvis. (f) PVL 3807 *Ischigualastia jenseni* (Dicynodontia) pelvis. (g) UFRGS-PV-0150-T *Jachaleria candelariensis* (Dicynodontia) pelvis. (h) PVL 4442 *Massetognathus pascuali* (Cynognathia) ischium. (i) MCZ VPRA-3616 *Chiniquodon* sp. (basal probainognathian) ischium. (j) UFRGS-PV-1051-T *Trucidocynodon riograndensis* (basal probainognathian) ischium. (k) MACN-N 09 *Vincelestes neuquenianus* (cladotherian, i.e., stem therian) ischium. All specimens are shown in lateral view. Note the large medially projecting flange of the ischium (*) in (d)–(g).

(despite no contact with the medial surface), monotremes are coded as state 1 here. Elsewhere, state 1 is only recognizable among extinct species; a subtle dorsolateral depression or groove is occasionally observed in some noncynodont therapsids (Figure 20a–c), but it becomes widespread and well developed in cynodonts and mammaliaforms (Figure 20h–j), and persists even in some stem therians (Figure 20k). The dorsolateral groove is separated from the medial surface of the ischium by a sharp dorsal margin to the bone, and from the more ventral lateral surface of the ischium by a longitudinal ridge; collectively this gives the proximal ischium near the acetabulum a somewhat triangular cross-section. The groove is situated exactly where the GEM of extant therians originates, and its presence may indicate some level of subdivision of the ISTR mass in many nonmammalian species. (If so, this would suggest apomorphic loss of the OBIN in monotremes.) The presence of a large obturator fenestra in cynodonts cannot be taken as an unambiguous

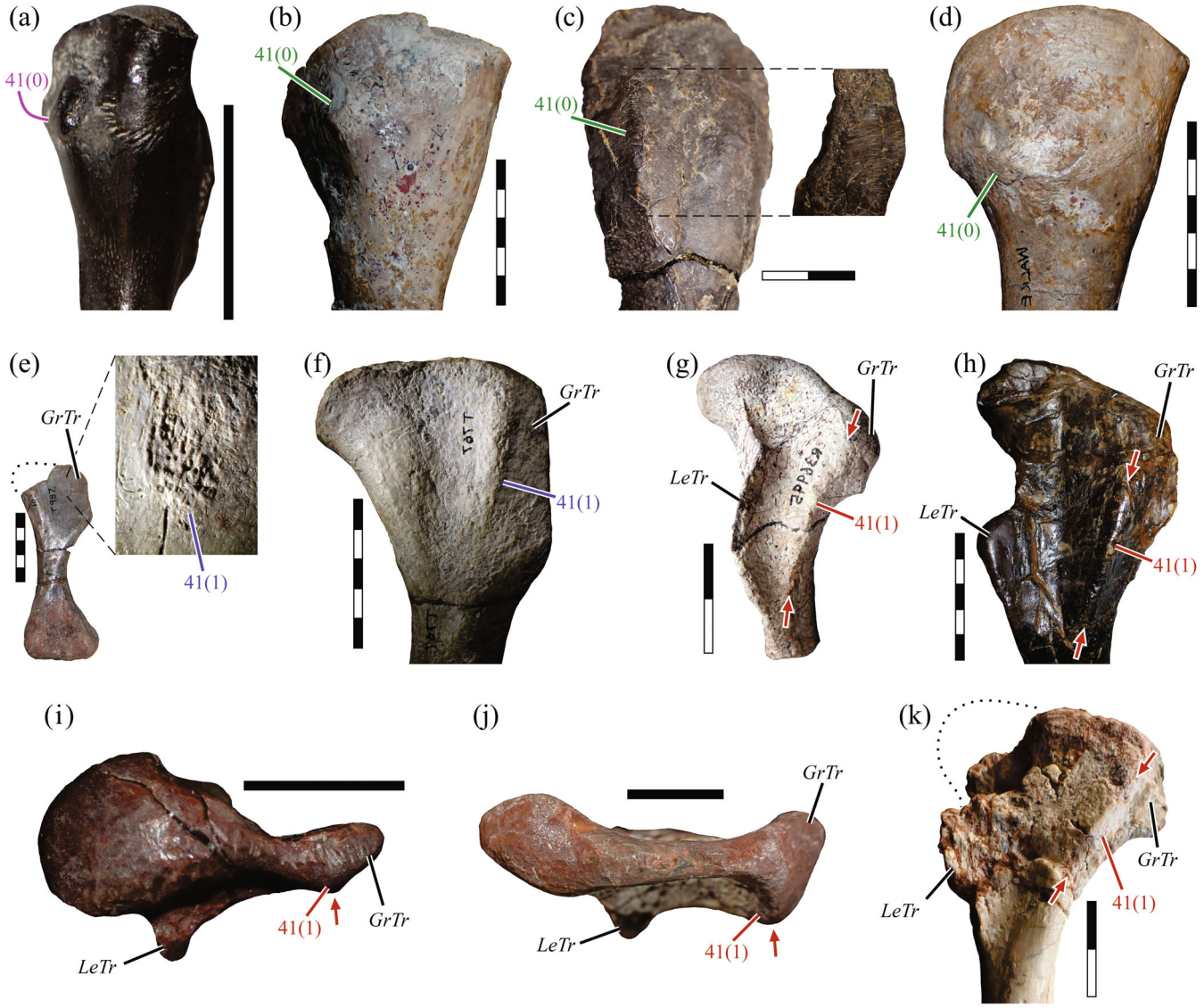

FIGURE 21 Osteological evidence of ischiotrochantericus musculature insertion on the femur in synapsids. (a) USNM PAL 768796 cf. *Captorhinus* (Captorhinidae), in anterior view. (b) MCZ VPRA-4812 *Ophiacodon retroversus* (Ophiacodontidae), in anterior view. (c) FMNH UR 733 *Edaphosaurus boanerges* (Edaphosauridae), in anterior view; inset shows profile of muscle scar in lateral view. (d) MCZ VPRA-2937 *Dimetrodon limbatus* (Sphenacodontia), in anterior view. (e) UMZC T.987 *Oudenodon* sp. (Dicynodontia), in posterior view. (f) UMZC T.767 *Lystrosaurus* sp. (Dicynodontia), in posterior view. (g) NHMUK PV R.36995 *Luangwa drysdalli* (Cynognathia), in posterior view. (h) PVL 2554 *Exaeretodon argentinus* (Cynognathia), in posterior view. (i) MCZ VPRA-3801 *Massetognathus pascuali* (Cynognathia), in proximal view. (j) MCZ VPRA-3616 *Chiniquodon* sp. (basal probainognathian), in proximal view. (k) UFRGS-PV-1051-T *Trucidocynodon riograndensis* (basal probainognathian), in posterior view.

correlate of extensive medial invasion of the ISTR. In kannemeyeriiform dicynodonts, the ischium develops a medially projecting plate from the dorsal margin (Figure 20d–g, asterisk) that can be almost as large as the main ischial body itself, forming an L-shaped cross-section (Kammerer et al., 2013; Pearson, 1924; Ray, 2006). This medial plate ostensibly served as an increased attachment area for the ISTR (Walter, 1988a, 1988b).

41. Insertion

0. Lateral to anterolateral proximal femur, near PIFI insertion, and proximal to IF insertion [tuberosity]
1. Posterolateral proximal femur, posteromedial to apex of GrTr [trochanter], proximal to insertion of PIFE/OBEX

Remarks—The transition from (known) "pelycosaurs" to therapsids involved a marked reorganization of muscle

attachments on the proximal femur, including the loss of a prominent anterolateral tuberosity (Figures 4 and 21a–d). It is reasonable to infer that at this point the insertion of the ISTR acquired a more "mammalian" condition and became associated with the GrTr. In cynognathian and basal probainognathian cynodonts, the posterior aspect of the GrTr frequently exhibits an expanded longitudinal "keel," likely demarcating the insertion of the ISTR (Figure 20g–k, arrows). Superficially similar scarring has also been observed in a few rare dicynodont specimens as well (Figure 21e,f).

3.15 | Caudofemoralis (CF, Figure 22)—Characters 42–45

42. Number of heads

0. One
1. Two, one long and deep (longus/CFL), the other short and superficial (brevis/CFB)

Remarks—This muscle is absent in several marsupial and derived placental groups, but when it is present it comprises a single head only. Assuming homology between the therian CF and the same-named muscle of nontherians, it is reasonable to infer that a single-headed muscle was the ancestral condition for Theria as a whole (state 0), and that groups lacking the muscle represent instances of secondary loss.

43. Origin

0. Transverse processes of anteriormost caudal vertebrae
1. Centra, ventral aspect of transverse processes and haemal arches of anteriormost caudal vertebrae, possibly also posterior ilium and/or transverse processes of sacral vertebrae
2. Anteriormost caudal vertebrae and/or sacral vertebrae
3. Fascia surrounding proximal tail

44. Insertion

0. Posterolateral proximal femur, lateral to InTr [tuberosity]
1. Posterolateral to caudomedial proximal femur, distal to apex of InTr
2. Posterior proximal femur, proximal end of ridge/crest [rugosity (4Tr), distinct and separate from InTr]
3. Strong ridge and pit on posterior proximal femur [4Tr]
4. Posterior to posterolateral femoral shaft [smooth surface]

Remarks—Among stem amniotes, the large region of scarring located proximal to the longitudinal "adductor ridge" on the posterior femur (cf. character 38) and partially enveloping the proximal fossa may variously manifest as a single, rugose projection (e.g., Berman et al., 2004; Holmes, 1984; White, 1939; Williston, 1911), or alternatively as two discrete eminences (Figure 22a; Holmes, 2003; Romer, 1922, 1956; Sumida, 1997). In the latter case, the proximal scar consistently forms a proximally directed, flange-like projection comparable to the InTr of salamanders, lepidosaurs, and testudines, and can be recognized as such (see character 20 above); the distal scar has thence been named the 4Tr (Romer, 1922). The double-scarred morphology remains a consistent feature throughout "pelycosaurs" (Figures 4a, 22b–d), although in caseid caseasaurs and many varanopids, the 4Tr is subsequently reduced or lost (Campione & Reisz, 2010; Romer & Price, 1940; Sumida et al., 2014). In the genus *Ophiacodon*, the 4Tr is no longer situated purely distal to the InTr in the middle of the posterior aspect, but rather has shifted laterally and somewhat proximally to lie on the lateral edge of the proximal fossa, forming a rugose eminence with a central pit (Figure 22c,d; Romer & Price, 1940). Regardless of variations in osteological expression, the core topology of these muscle insertions remains conserved throughout stem and early crown amniotes, and is consistent with the topology of insertion observed in extant salamanders, lepidosaurs, and testudines. This similarity means that the 4Tr of early amniotes (including "pelycosaurs") can be confidently reconstructed as the insertion site of the CF.

However, it remains uncertain as to whether the 4Tr of early amniotes is strictly homologous with the 4Tr of archosaurs (Hutchinson, 2001a; Nesbitt, 2011), even if both served as the insertion of the CF. Notably, the femora of early sauropsids consistently possess only a single process on the posterior face of the proximal femur, which typically has been referred to as the InTr (Simões et al., 2022). This may in part be due to the generally small size of many early sauropsids, as a distinct 4Tr is sometimes not recognizable in small or immature "pelycosaurs." The currently available body of evidence does not help distinguish whether the archosaurian 4Tr is simply a distally displaced InTr, or whether the two are distinct, nonhomologous structures as they are in "pelycosaurs."

In contrast to its near-ubiquitous presence in "pelycosaurs," the 4Tr is exceedingly rare among known therapsids. In biarmosuchians, a 4Tr has only been reported in an indeterminate taxon (Sigogneau & Tchudinov, 1972, fig. 20). A subtle 4Tr is present in the

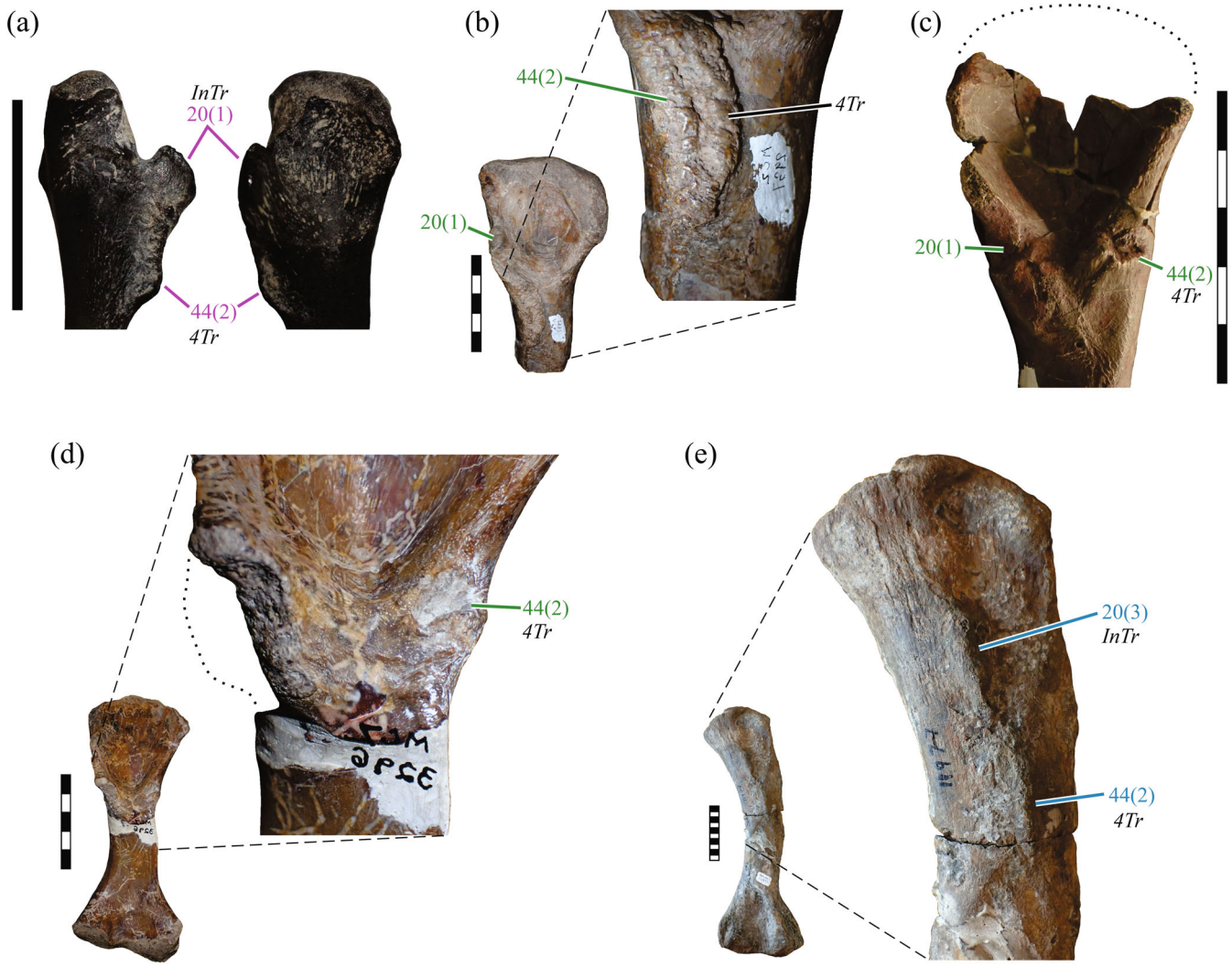

FIGURE 22 Osteological evidence of caudofemoralis musculature attachment to the femur in synapsids. (a) USNM PAL 768796 cf. *Captorhinus* (Captorhinidae), in medial (left) and posterior (right) views. (b) MCZ VPRA-2937 *Dimetrodon limbatus* (Sphenacodontia) in posterior view, with inset highlighting fourth trochanter. (c) MCZ VPRA-4856 *Ophiacodon mirus* (Ophiacodontidae) in posterior view. (d) MCZ VPRA-3296 *Ophiacodon retroversus* (Ophiacodontidae) in posterior view. (e) SAM-PK-11977a *Anteosaurus magnificus* (Anteosauridae) femur in posterior view. Note the pit-like appearance and lateral position of the fourth trochanter in *Ophiacodon* spp.

dinocephalian *Anteosaurus* (Figure 22e); in the closely related *Titanophoneus*, Orlov (1958) did not recognize such a scar but King (1988) claimed that it was present, albeit poorly developed. The rarity of a 4Tr in therapsids coincides with an apparent shortening of the tail in most taxa (comparable to the pattern noted for nonavian theropod dinosaurs and birds; Gatesy, 1990), although this must be viewed with caution due to the current paucity of well-preserved, complete tails of basal therapsid taxa.

45. Secondary tendon to lateral knee region

0. Absent
1. Present

3.16 | Gastrocnemius group (Figures 23 and 24): Characters 46–54

46. Gastrocnemius externus (GE), number of heads

0. Absent
1. One
2. Two
3. Three

Remarks—The gastrocnemii and flexor digitorum longus of salamanders are not present as discrete muscles; rather, there is a single muscle (flexor primordialis communis) that collectively replaces them in topology, which

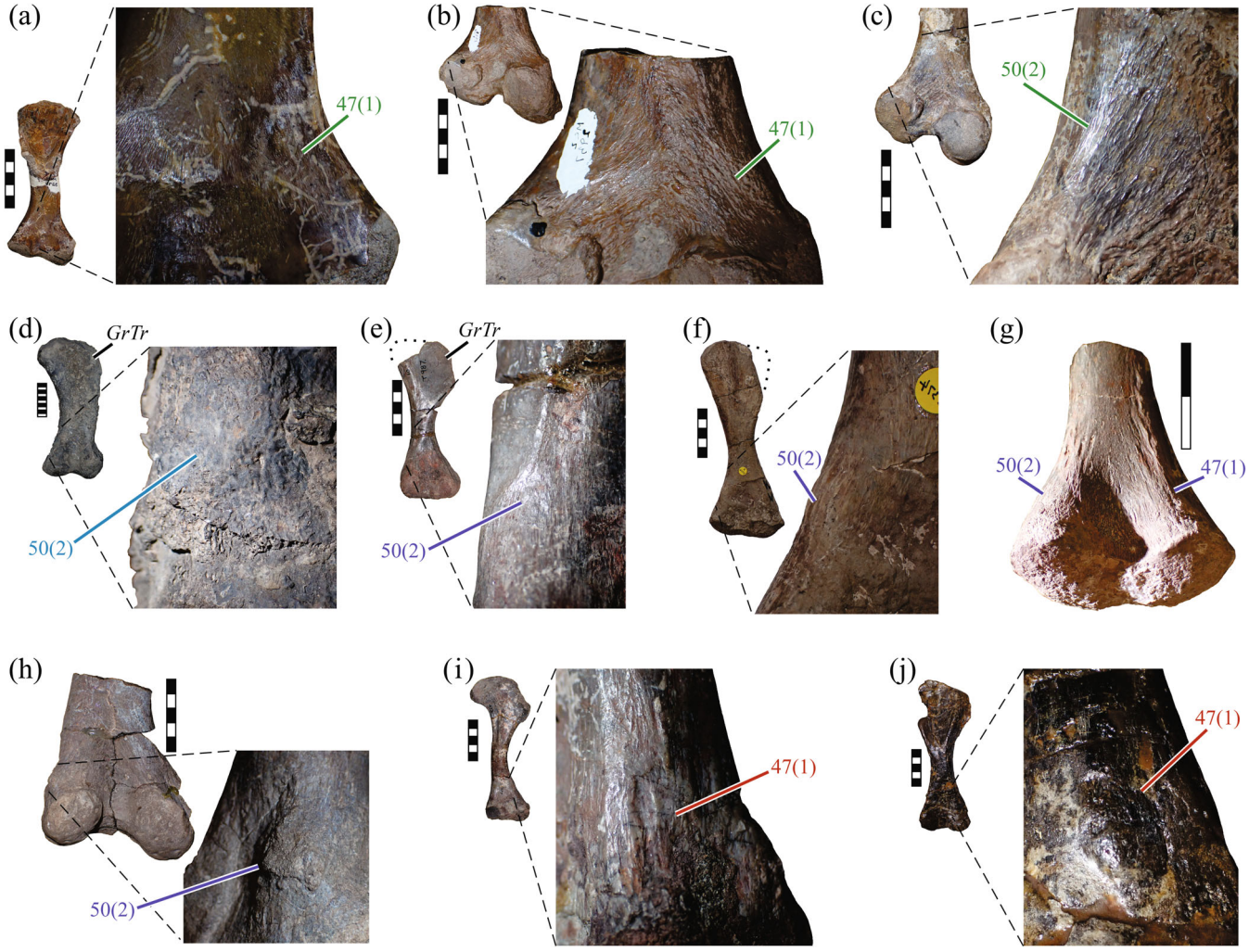

FIGURE 23 Osteological evidence of gastrocnemii attachment to the distal femur in synapsids. (a) MCZ VPRA-3926 *Ophiacodon retroversus* (Ophiacodontidae). (b) MCZ VPRA-2937 *Dimetrodon limbatus* (Sphenacodontia). (c) MCZ VPRA-1108 *Dimetrodon* sp. (Sphenacodontia). (d) SAM-PK-12041 *Moschops* sp. (Tapinocephalidae). (e) UMZC T.987 *Oudenodon* sp. (Dicynodontia). (f) NHMUK PV R.37374 Dicynodontia indet. (g) UMZC T.427 *Lystrosaurus* sp. (Dicynodontia). (h) MCZ VPRA-3455 *Dinodontosaurus brevirostris* (Dicynodontia). (i), BP/1/1675 cf. *Cynognathus* (Cynognathia). (j) PVL 2554 *Exaeretodon argentinus* (Cynognathia). All images are shown in posterior view, with the exception of insets in (h, posteromedial view) and (i, posterolateral view).

is likely homologous with all or part of these muscles in amniotes (Diogo & Molnar, 2014). Although lepidosaurs may possess superficial and deep subdivisions, this often is only partial, and for the purposes of this study are coded as state 1. In contrast, the mass in extant mammals is clearly divided into multiple heads, forming the gastrocnemius lateralis (GL), plantaris (PLA), and, in therians, the soleus (SOL), although the latter is not always fully distinct from the GL, especially in marsupials.

47. GE origin

0. Absent; not present as a discrete muscle
1. Posterolateral distal femur, proximal to lateral condyle [tubercle or scarring]
2. Posterolateral aspect of apex of parafibula

Remarks—Additional attachments can be gained in therians, including the posterolateral aspects of the proximalmost tibia and fibular head, but these nuances are secondary to the overall phyletic patterns examined here. Among extant amniotes, monotremes are remarkable in that the superficial lateral muscle of the posterior crus does not take origin from the femur, but rather the apex of the parafibula (state 2), thus not crossing the knee. In turn, some authors have described the muscle in question as the SOL (see character 49 below), regarding the GL as absent. On topological grounds, Gambaryan et al. (2002) argued that this muscle was indeed the GL, and that the SOL is an apomorphy of therians (or a more inclusive group); their argument is followed here.

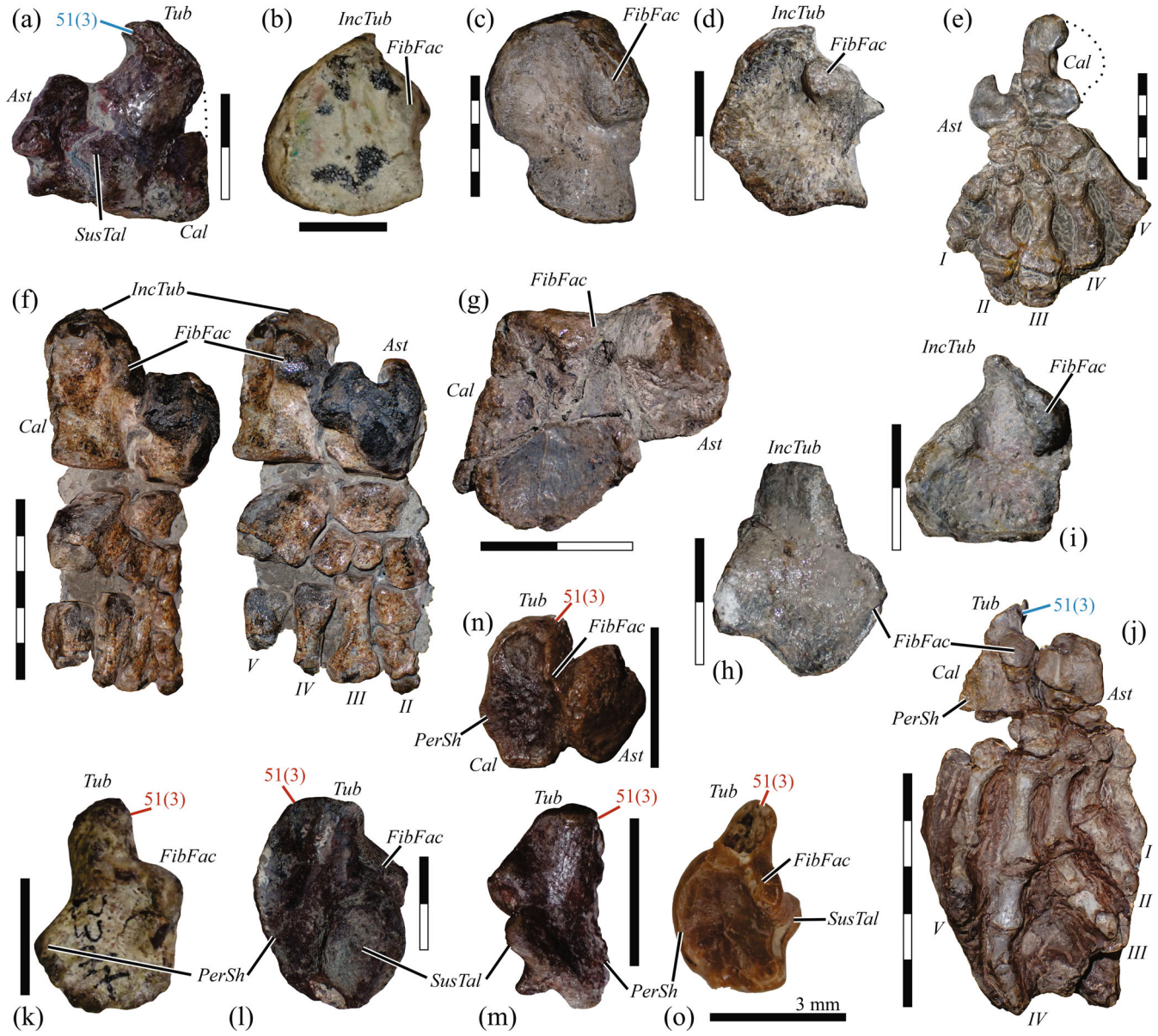

FIGURE 24 Osteological evidence of gastrocnemii attachment to the pes in synapsids. (a) SAM-PK-8950 *Hipposaurus boonstrai* (Biarmosuchia) astragalus and calcaneum in ventral view. (b) NMQR 479 *Dicynodontoides recurvidens* (Dicynodontia) calcaneum in dorsal view. (c) BP/1/2167 *Dinogorgon* sp. (Gorgonopsia) calcaneum in dorsal view. (d) SAM-PK-K10585 cf. *Gorgonops torvus* (Gorgonopsia) calcaneum in dorsal view. (e) BSPG 1934-VIII-28 *Gorgonops* sp. (Gorgonopsia) pes in ventral view. (f) SAM-PK-K4441 Gorgonopsia indet. pes in dorsolateral (left) and dorsal (right) views. (g) SAM-PK-K12051 *Alopecognathus* sp. (Scylacosauridae) astragalus and calcaneum in dorsal view. (h) SAM-PK-K7808 *Glanosuchus macrops* (Scylacosauridae) calcaneum in dorsal view. (i) SAM-PK-K7809 *Glanosuchus macrops* (Scylacosauridae) calcaneum in dorsal view. (j) AMNH FARB 5622 *Bauria cynops* (Eutherocephalia) pes in dorsal view. (k) BP/1/5394 *Regisaurus jacobi* (Eutherocephalia) calcaneum in dorsal view. (l) BP/1/1675 cf. *Cynognathus* (Cynognathia) calcaneum in dorsal view. (m) MCZ-VPRA 4018 *Massetognathus pascuali* (Cynognathia) calcaneum in ventral view. (n) MCZ VPRA-4021 *Probainognathus jenseni* (basal probainognathian) astragalus and calcaneum in dorsal view. (o) MCZ VPM-19959 *Eozostrodon parvus* (Mammaliaformes) calcaneum in dorsal view.

48. PLA origin

0. Absent; not divided
1. Posterior aspect of [parafibula], medial to GL origin
2. Lateral aspect of fibular head and/or lateral fabellar sesamoid and/or lateral femoral condyle (deep to GL)

Remarks—The development of a parafibula is quite common throughout Mesozoic mammals, although it is typically reduced or lost entirely in therians, in concert with the reduction of the proximal fibula and appearance of the lateral fabellar sesamoid. It is possible that the parafibula was a functional precursor to the lateral fabellar

sesamoid (see also Barnett & Lewis, 1958), and its presence is indicative of a more differentiated GE mass, including a distinct PLA (state 1). Morganucodontids (Jenkins & Parrington, 1976), at least one tritylodontid (Kühne, 1956), and the triconodont mammal *Gobiconodon* (Jenkins & Schaff, 1988) possess a small, spatulate flange on the posteroproximal fibular head, level with or projecting proximally above the articular surface. This is interpreted as an incipiently developed parafibula, and hence these taxa are coded as state 1 here.

49. SOL origin

0. Absent; not divided
1. Lateral fabellar sesamoid and/or posterior fibular head and/or lateral femoral condyle (deep to GL)

50. Gastrocnemius internus (GI), origin

0. Absent; not present as a discrete muscle
1. Proximomedial tibia
2. Posteromedial distal femur (proximal to medial condyle) and/or posteroproximal tibia and/or popliteal fossa of femur

Remarks—In testudines, the GI originates purely from the medial tibia (Walker, 1973; Zug, 1971), as does the GI of *Sphenodon*, whereas the GI origin extends to the medial femur in squamates. In mammals, the origin of the muscle (as the gastrocnemius medialis, GM) also extends to the distal femur. Maximum likelihood ASR suggests that an origin from the femur was ancestral for Amniota (Supporting Information Appendix S3), but circumstantial evidence from extant anatomy suggests that an origin from the tibia may have actually been the ancestral condition. This is because the femoral origin in squamates has a different topology with respect to the crural flexors compared to that observed in mammals: in squamates, the GI divides the [FTI1, FTE, PUT] from the [FTI2, PIT], whereas the GI is lateral to all the crural flexors in mammals except the BICF (but this muscle has an apomorphic insertion; see characters 22, 27). The contrasts between squamates and mammals could be explained by the GI having a plesiomorphic origin from just the tibia, which subsequently migrated proximally over the knee via different topological pathways.

In some large, well-preserved femora of edaphosaurids and sphenacodontids, the posterior femur immediately distal to the medial condyle shows a fibrous surface texture indicative of soft tissue attachment (Figure 23c); yet, as this texture is often broadly continuous across much of the popliteal fossa, it may not signify the attachment of just the GI, and so cannot be unambiguously interpreted as such. In contrast, the femora of tapinocephalids (Figure 23d) and large dicynodonts (Figure 23e–h) sometimes possess a small tubercle on the posteromedial aspect of the distal femur, consistent with a GI origin.

51. GE insertion

0. Absent; not present as a discrete muscle
1. Plantar aponeurosis of the pes, attaching to ventral aspect of metatarsal V and tarsals and then to distal phalanges
2. Plantar aponeurosis attaching to metatarsal V and process on distal tarsal V, and calcaneal tuber [tarsal process and calcaneal tuber present]
3. Calcaneal tuber [roughened apex of tuber]

Remarks—Exactly what constitutes a "calcaneal tuber" is not clear, and its development (and associated shift in muscle insertions) is more likely a continuous trait. Baurioid therocephalians, cynodonts, and mammaliaforms (including extant mammals) typically have a distinct posterior projection on the calcaneum, which is sufficiently long that a definite "handle" can be recognized (Figure 24j–o). Despite this, the morphology of the handle is noticeably varied, with that of baurioids being more cylindrical in construction (paralleling the morphology of theriiform mammals) compared to that of most nonmammalian cynodonts. The calcaneum of nonbaurioid eutherocephalians is poorly known, but appears to lack a handle-like tuber (Attridge, 1956; Huttenlocker & Smith, 2017).

The calcaneum of many gorgonopsians and at least one scylacosaurid possesses a "heel" that extends posterior (proximal) to the facet for the fibula (Figure 24d,f,h,i), or at least extends posterior to the posterior margin of the astragalus when the two bones are in natural articulation (Sidor, 2022; fig. 3) This may be considered an incipiently developed calcaneal tuber. Broili and Schröder (1935) described a large calcaneal tuber in the gorgonopsian *Gorgonops* sp., but examination of their material (BSPG 1934-VIII-28; Figure 24e) shows it to have been broken and somewhat sculpted during preparation. Restoration of the plate-like lateral shelf, often missing in gorgonopsian fossils due to its fragile construction, would result in a morphology with only a small posterior heel. Outside theriodonts, Boonstra (1965) described a well-developed, hook-like tuber in the biarmosuchian *Hipposaurus* (Figure 24a), and King (1985) described a small posterior process on the calcaneum of the

dicynodont *Dicynodontoides* (Figure 24b). As the association between soft tissues and a calcaneal tuber are only observable in extant taxa with a distinct, handle-like morphology, use of the term "tuber" (and associated inferences of soft tissues, i.e., state 3) is restricted here to handle-like morphologies only; incipient heels do not qualify. A naïve application of maximum likelihood or parsimony ASR (Supporting Information Appendix S3) leads to the implausible inference that the tubers of *Hipposaurus* and cynodonts are homologous (i.e., state 3 is plesiomorphic for Therapsida as a whole). The fossil record of therapsids overwhelmingly indicates these structures to be nonhomologous by lack of phyletic continuity, and hence state 3 convergently evolved in biarmosuchians, baurioid therocephalians, cynodonts, and at least one dicynodont.

52. PLA insertion

0. Absent; not divided
1. Plantar fascia then to base of metatarsals IV and V
2. Plantar fascia, and tuber and plantar aspect of calcaneum

53. SOL insertion

0. Absent; not divided
1. Tuber and plantar aspect of calcaneum (typically via common tendon with GE/GL)

54. GI insertion

0. Absent; not present as a discrete muscle
1. Common insertion with GE, involving plantar aponeurosis of pes
2. Plantar aponeurosis of the pes to metatarsal V, calcaneal tuber, and metatarsals II–III
3. Calcaneal tuber and possibly plantar aspect of calcaneum [roughened apex of tuber]

3.17 | Flexor digitorum longus (FDL, Figure 25): Characters 55 and 56

55. Origin

0. Absent
1. Posterolateral aspect of distal femur (proximal to lateral femoral condyle) and/or posterior proximal fibula and/or posteroproximal tibia
2. Lateral aspect of parafibula and proximal fibula
3. Posteromedial aspect of head and proximal shaft of fibula

Remarks—As noted above, the FDL of salamanders is not present as a discrete muscle, instead replaced (with the GE) by the flexor primordialis communis. Squamates frequently possess additional slips that take origin further distal to the knee (Russell, 1993), but these are neglected in the present study for they have no bearing on the broader questions examined here.

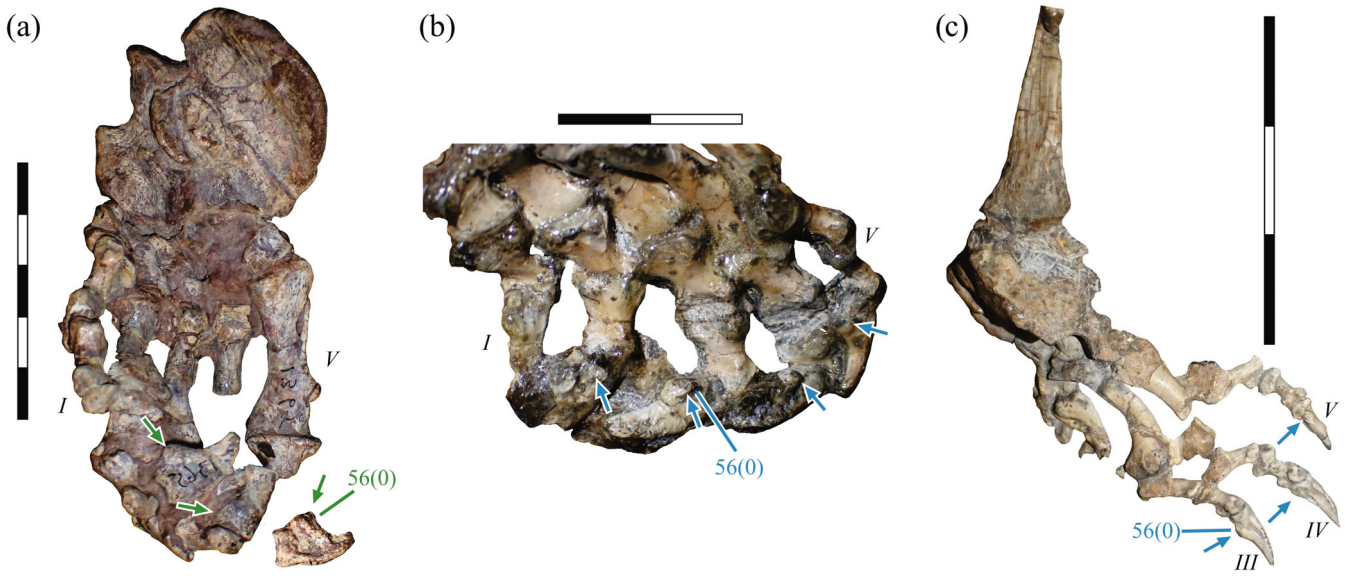

FIGURE 25 Osteological evidence of flexor digitorum longus insertion in the pes of synapsids. (a) MCZ VPRA-1365 *Dimetrodon milleri* (Sphenacodontia) pes in ventral view. (b) SAM-PK-K7580 Gorgonopsia indet. pes in ventral view. (c) UCMP 40467 *Mirotenthes digitipas* (Eutherocephalia) pes in dorsolateral view. Arrows denote flexor tubercles for muscle insertion.

56. Insertion

0. Via plantar aponeurosis of pes, to proximoventral aspect of terminal phalanges of most or all digits [ungual flexor tubercles]
1. Via tendon deep to plantar aponeurosis, to ventral aspect of terminal phalanges [ungual flexor tubercles; calcaneal tuber breaks up plantar aponeurosis]

Remarks—State 0 here incorporates the condition in the flexor primordialis communis of salamanders. It is possible that the progressive development of a calcaneal tuber on the line to mammals was associated with a concomitant breaking up of adjacent soft tissues: the plesiomorphic singular GE mass differentiated to give rise to the PLA, and the ancestral plantar aponeurosis differentiated to give rise to a fully separate passage of the FDL. As currently constructed (and in turn, coded for), this character assumes that the development of a calcaneal tuber leads to a switch from state 0 to state 1. Thus, multiple independent origins of the tuber (cf. character 51) currently would imply multiple origins of a more differentiated GE mass and altered FDL passage.

3.18 | Flexor digitorum brevis (FDB): Characters 57 and 58

57. Origin

0. Dorsal (deep) surface of plantar fascia/aponeurosis
1. Dorsal (deep) surface of plantar fascia/aponeurosis or FDL tendon, and also plantar aspect of some proximal tarsals (especially calcaneum) or metatarsals
2. Tendon or fascia covering posterior surface of belly of FDL, proximal to ankle

Remarks—In some marsupials the FDB is essentially fused with the PLA proximally (e.g., Warburton et al., 2015).

58. Insertion

0. Plantar aspect of metatarsals and/or proximal phalanges (which ones specifically vary)
1. Plantar aspect of unguals [flexor tubercles]

3.19 | Flexor hallucis longus (FHL): Characters 59 and 60

59. Origin

0. Absent, not present as discrete muscle
1. Posterolateral aspect of distal femur, proximal to lateral condyle
2. Posterior to posteromedial aspect of head and shaft of tibia, possibly also posteroproximal fibula

Remarks—Salamanders possess additional flexor muscles—flexores accessorius lateralis et medialis and caput longum musculorum contrahentium—that are apomorphic for the group, but which may be derivatives of the ancestral digital flexor muscle mass, and therefore somewhat equivalent to the FDL and/or FHL of amniotes (Diogo & Molnar, 2014). Further work is required to establish precise homologies. Hutchinson (2002) considered the FHL to be present in lepidosaurs, but neither Russell (1993) nor Russell and Bauer (2008) mentioned it in their detailed surveys of squamates. The condition in *Sphenodon* suggests that the FHL probably never properly differentiated from the various subdivisions of the FDL, but this is of little consequence for the present study's focus.

60. Insertion

0. Absent, not present as discrete muscle
1. Medial plantar aspect of digit I
2. Base of metatarsal I, distal tarsal I (=entocuneiform), plantar fascia or FDL/FDB tendons

3.20 | Extensor digitorum longus (EDL, Figure 26): Characters 61 and 62

61. Origin

0. Anteroproximal border of both femoral condyles
1. Anterior aspect of distal femur, proximal to lateral condyle only [scarring]
2. Anterior aspect of proximal fibula and parafibula
3. Anterior aspect of lateral femoral condyle and/or anterolateral fibular and tibial heads

Remarks—Stem and early crown amniotes are characterized by a distinctly asymmetrical distal femur, wherein the lateral condyle projects further distally than the medial. In well-ossified individuals, a subrectangular shelf projects distally to form an overhang above the lateral condyle (e.g., Holmes, 2003; Romer & Price, 1940). This shelf is often heavily scarred with the texture trending distally (Figure 26), indicating the attachment of the EDL, although the peroneus longus possibly also gained attachment from this region (Romer, 1922; see character 71 below).

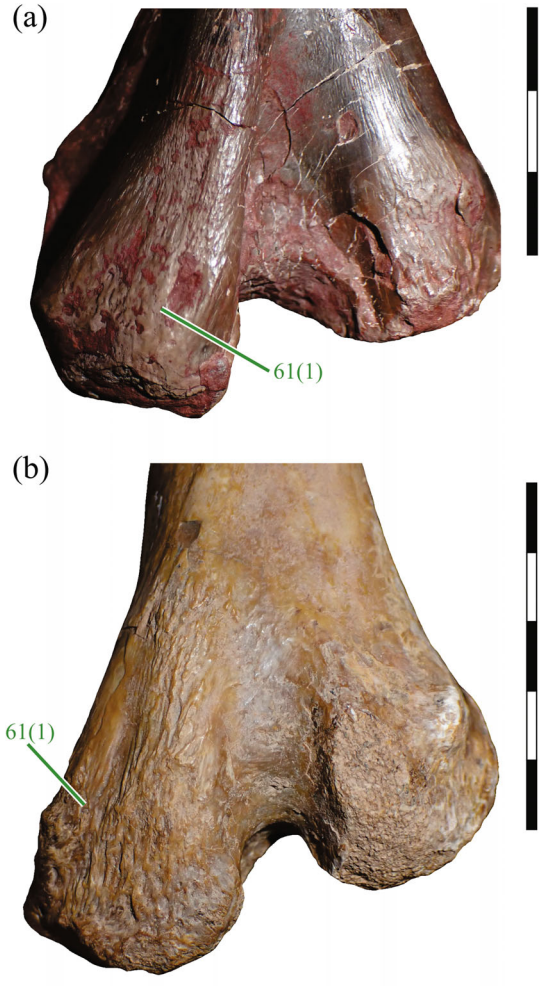

FIGURE 26 Osteological evidence of extensor digitorum longus origin from the anterior aspect of the lateral femoral condyle in "pelycosaurs." (a) MCZ VPRA-4856 *Ophiacodon mirus* (Ophiacodontidae). (b) MCZ VPRA-6003 *Dimetrodon limbatus* (Sphenacodontia). Specimens are shown in anterior view. It is possible that this region also served as the origin of the peroneus longus.

62. Insertion

0. Dorsal aspect of proximal metatarsals (which ones vary)
1. Dorsal aspect of distal phalanges (which ones vary)

3.21 | Extensor digitorum brevis (EDB): Character 63–65

63. Number of heads

0. One
1. More than one (extra "peroneal" heads)

Remarks—Therians possess multiple additional ankle dorsiflexor muscles in the peroneal region of the crus, in addition to the peroneus longus and brevis, including the peroneus tertius, digiti terti, digiti quarti, and digiti quinti. The exact number of these additional heads is variable across therians, and their homology between marsupials and placentals is not clear. Furthermore, contrasting patterns of innervation suggest that, rather than being derivatives of the topologically similar peroneal musculature, the additional heads are actually related to the EDB (Diogo & Molnar, 2014; Greene, 1935). On this basis, they are included here, rather than with characters codifying the peroneal musculature, although future developmental studies could help further clarify homologies.

64. Origin

0. Dorsal aspect of distal tarsals
1. Dorsal aspect of proximal tarsals (principally astragalus and calcaneum)
2. Dorsal aspect of calcaneum, anterodistal fibular shaft, and/or soft tissues surrounding ankle
3. Anterior aspect of proximal fibula, parafibula (when present)

65. Insertion

0. Dorsal aspect of middle to terminal phalanges, which ones vary [extensor processes]

3.22 | Extensor hallucis longus (EHL): Characters 66 and 67

66. Origin

0. Absent, not present as discrete muscle
1. Anteromedial to anterolateral aspect of distal fibula
2. Medial aspect of fibular shaft, proximodistal extent variable
3. Anteromedial aspect of proximal fibula and surrounding tissues (including parafibula or medial tibia)

67. Insertion

0. Absent, not present as discrete muscle
1. Dorsomedial aspect of metatarsal I
2. Dorsal aspect of digit I ungual [extensor process]

3.23 | Tibialis anterior (TA, Figure 27): Characters 68 and 69

68. Origin

0. Anteroproximal border of medial femoral condyle
1. Anterolateral to medial surface of much of tibial shaft, distal to tuberosity on cnemial crest
2. Anterior to anterolateral aspect of proximal third of tibia [fossa and cnemial crest], and possibly surrounding tissues (including fibula) as well

Remarks—This muscle is bipartite in salamanders (extensores cruris et tarsi tibialis), but otherwise its topology remains unaltered. The somewhat contrasting locations of the tibial origin observed in extant sauropsids (more medial) and synapsids (more lateral) would render inference of the ancestral amniote condition uncertain, were it not for the observation that stem and early crown amniotes possess the characteristic association of a cnemial crest and lateral fossa (Figure 27a–e). Some temnospondyl amphibians also exhibit these structures, albeit in a more subdued fashion (Pawley, 2007; Pawley & Warren, 2006). These structures can be continuously traced through the fossil record from stem amniotes through to crown mammals (Figures 5 and 27f–n), supporting their homology and suggesting that a more lateral tibial origin of the TA was the ancestral condition for amniotes (and synapsids).

69. Insertion

0. Anterior aspect of distal tibia and dorsal aspect of medial proximal tarsal (tibiale/astragalus)

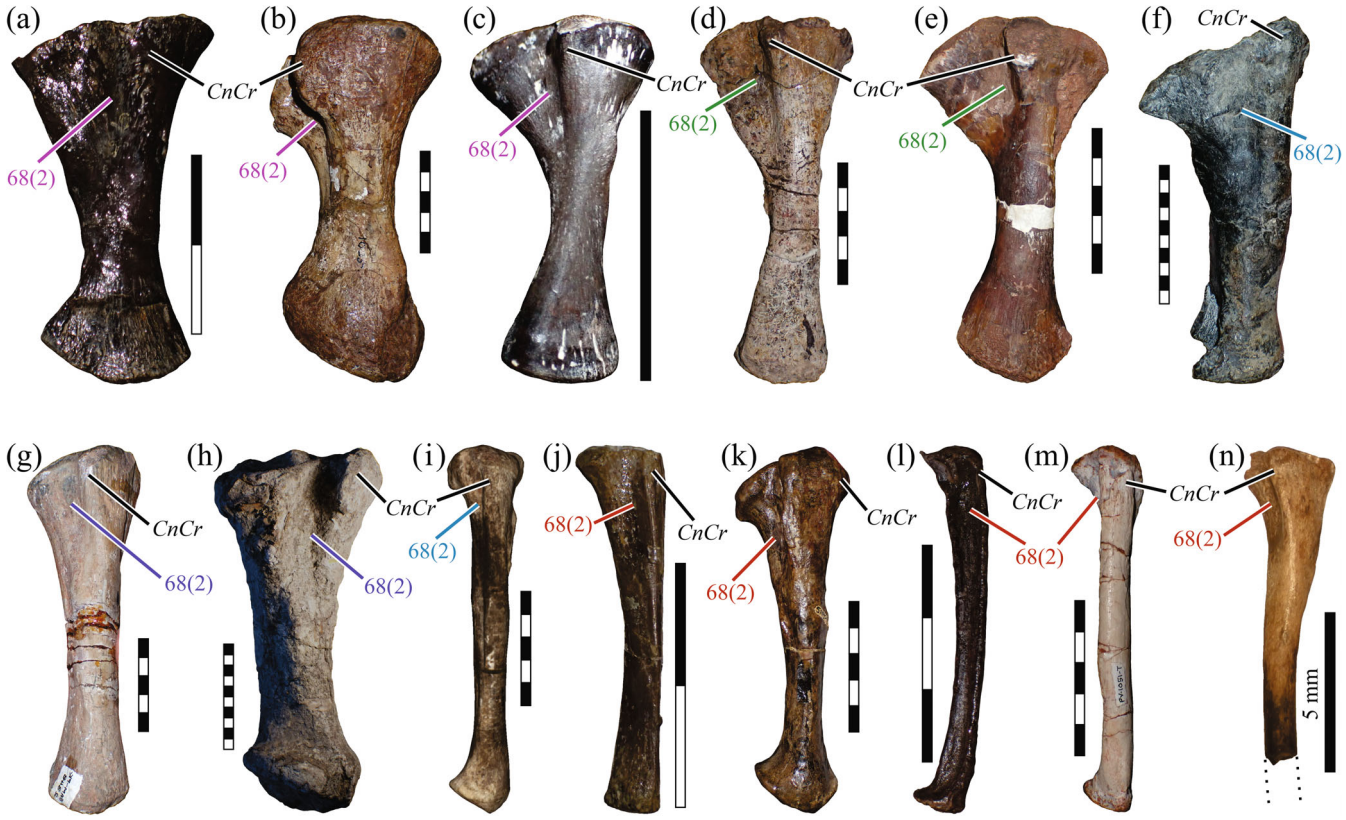

FIGURE 27 Osteological evidence of tibialis anterior musculature attachment to the tibia in synapsids. (a) MCZ VPRA-2045 *Archeria crassidisca* (Embolomeri, stem amniote) in anterior view. (b) MCZ VPRA-1035 *Diadectes tenuitectus* (Diadectomorpha) in anterior view. (c) AMNH FARB 19383 *Captorhinus* sp. (Captorhinidae) in anterior view. (d) MCZ VPRA-1203 *Ophiacodon retroversus* (Ophiacodontidae) in anterior view. (e) MCZ VPRA-1351 *Edaphosaurus* sp. (Edaphosauridae) in anterior view. (f) NMQR 2987 *Tapinocaninus pamelae* (Tapinocephalidae) in lateral view. (g) SAM-PK-2348 cf. *Dicynodon* sp. (Dicynotontia) in anterior view. (h) PVL 3807 *Ischigualastia jenseni* (Dicynodontia) in lateral view. (i) UMZC T.883 Gorgonopsia indet. in anterior view, image rendered from a digital model acquired via a GoSCAN 20 laser surface scanner (Creaform, USA). (j), SAM-PK-1395 *Thrinaxodon liorhinus* (Cynodontia) in lateral view. (k) PVL 2162 *Exaeretodon* sp. (Cynognathia) in anterior view. (l) MCZ VPRA-4021 *Probainognathus jenseni* (basal probainognathian) in lateral view. (m) UFGRS-PV-1051-T *Trucidocynodon riograndensis* (basal probainognathian) in anterior view. (n) MCZ VPM-19956 *Eozostrodon parvus* (Mammaliaformes) in anterior view. See also annotations on other figures for further illustrations of muscle attachment in other taxa.

1. Dorsomedial aspect of metatarsal I
2. Dorsolateral aspect of proximal metatarsals I–IV, principally metatarsal I
3. Dorsomedial aspect of distal tarsal I (entocuneiform) or metatarsal I

3.24 | Peroneus group (Figure 28): Characters 70–74

70. Number of heads

0. One
1. Two

Remarks—Salamanders lack readily identifiable peroneal muscles. The apomorphic "extensor cruris et tarsi fibularis" has a markedly different topology from the peroneus group of amniotes, but Diogo and Molnar (2014) tentatively suggested that the two are homologous, at least in part. This correspondence is assumed here, as there are no other appropriate muscles in this part of the crus.

71. Peroneus longus (PL), origin

0. Anteroproximal border of femoral condyles, especially lateral condyle
1. Anterolateral to lateral aspect of fibula, distal to ILFB insertion
2. Anterolateral aspect of distal femur, proximal to lateral condyle
3. Posterolateral proximal fibula, and possibly lateral condyle of tibia and surrounding soft tissues

Remarks—In monotremes, the origin also extends onto the parafibula. Scarring on the anterior aspect of the lateral femoral condyle shelf in early amniotes, including "pelycosaurs" may indicate attachment of the PL here (see also character 61 above).

72. Peroneus brevis (PB), origin

0. Absent, not differentiated from PL
1. Lateral to anterolateral fibular shaft
2. Anterolateral distal fibula, distal to PL origin
3. Anterolateral proximal fibula, anterior to PL origin when PL also originates from fibula

Remarks—The PB was not recognized explicitly for monotremes by Gambaryan et al. (2002), but they described a muscle ("peroneus digiti quinti") which shows a very similar topology to that in therians, especially proximally, suggesting that this is in fact the PB.

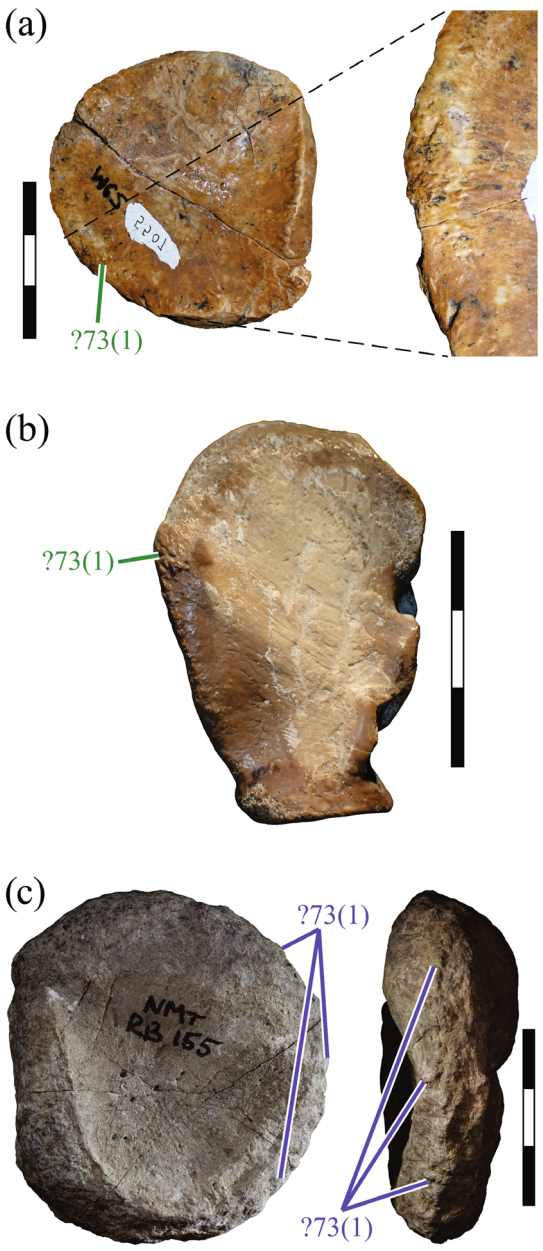

FIGURE 28 Osteological evidence of peroneus musculature attachment to the calcaneum in synapsids. (a) MCZ VPRA-5507 *Ophiacodon retroversus* (Ophiacodontidae) in dorsal view. (b) USNM PAL 407938 *Dimetrodon* sp. (Sphenacodontia) in dorsal view. (c) NMT RB155 *Angonisaurus* sp. (Dicynodontia) in ventral (left) and lateral (right) views.

73. PL insertion

0. Anterolateral fibula and dorsal fibulare

1. Lateral aspects of calcaneum and base of metatarsal V [process(es)]
2. Lateral aspect of distal metatarsal V
3. Plantar aspect of calcaneal [tuber] and lateral aspect of metatarsal V
4. Plantar aspect of metatarsal I, and possibly also entocuneiform

Remarks—The calcaneum of early amniotes forms a thin plate of bone laterally, a basic structure that persisted (albeit reduced in size) on the line to mammals to form the "peroneal shelf" (Luo & Wible, 2005; Panciroli et al., 2021). The margin of this plate in large, well-preserved "pelycosaur" calcanei often preserve fine rugosities or a striated surface texture indicative of soft tissue attachment (Figure 28a,b), possibly at least in part the insertion of the PL (state 1). A similar manifestation has also been observed in a few rare dicynodont specimens (Figure 28c). Additionally, the appearance of a calcaneal tuber in cynodonts, in association with a well-developed peroneal shelf (Figure 24k–o, PerSh) suggests that states 1 and/or 3 can be recognized in these taxa as well. These interpretations remain tentative, however, since the PL of extant mammals inserts on the medial side of the pes, the calcaneum only serving to help guide the tendon on its way toward insertion. Indeed, mammals are distinctive among extant tetrapods in possessing a medial insertion (ASR supports a lateral insertion as the plesiomorphic state for Amniota). It is possible that transfer of the PL to the medial side of the pes occurred alongside the ventral superposition of the calcaneum under the astragalus (in tandem with mediolateral narrowing of the calcaneum), but osteological data does not provide any distinguishing evidence one way or the other at present.

74. PB insertion

0. Absent, not differentiated from PL
1. Lateral aspect of base of metatarsal V [process]
2. Posterolateral aspect of metatarsal V
3. Dorsal aspect of ungual of digit V
4. Base of metatarsal V, possibly also metatarsal IV

3.25 | Pronator profundus (PP)

75. Origin

0. Posterior to medial fibular shaft, superficial to popliteus
1. Posterior fibular and tibial shafts, superficial to popliteus

Remarks—In monotremes, the origin also extends onto the posterior aspect of the parafibula; it is possible that this was also the case in other extinct mammals that possessed a parafibula.

76. Insertion

0. Distolateral tibia (superficial to interosseus cruris), tibiale/astragalus and base of metatarsal I
1. Plantar aspect of astragalus, distal tarsals, and first phalanx of digit I
2. Plantar aspect of distal tarsals and base of metatarsals I–III
3. Plantar aspect of tarsals, especially astragalus and/or calcaneum and/or navicular

3.26 | Popliteus (POP, Figure 29): Characters 77 and 78

77. Origin

0. Proximomedial fibular shaft [scarring]
1. Posterior fibular head and/or popliteal fossa of lateral femoral condyle

Remarks—In monotremes, the origin also extends onto the posteromedial parafibula; it is possible that this was also the case in other extinct mammals that possessed a parafibula. Within "pelycosaurs," scarring on the proximomedial fibula typically manifests as a discrete patch of often very rugose bone (Figure 29c,f,h), but it is usually more diffuse in therapsids (Figure 29j) and cynodonts (Figure 29t), forming a longitudinal ridge instead.

78. Insertion

0. Lateral distal tibia
1. Posterolateral tibial shaft, usually distal to crural flexor and gastrocnemius attachments [scarring]
2. Posterior aspect of medial femoral condyle

Remarks—Whereas the manifestation of scarring on the posterolateral to lateral tibia can be variable across "pelycosaurs," it is more conservative across therapsids and cynodonts (Figure 29i,k,l,o–s,u,v). Here it generally forms an elongate, roughened depression on the proximal half of the tibia that trends anterodistally, and which typically merges distally with a narrower, more subdued groove that continues down toward the distal end. The

FIGURE 29 Legend on next page.

larger, rougher scar proximally is interpreted as demarcating the POP, whereas the narrower scar distally likely marks the insertion of the interosseous cruris (see below). The large, basal probainognathian *Trucidocynodon* exhibits a discrete patch of rugose scarring distally instead of a shallow groove (Figure 29w, see character 80 below), but the small size and often sub-ideal preservation of other known basal probainognathian fossils currently precludes assessment of whether this feature is unique to *Trucidocynodon* or not.

3.27 | Interosseus cruris (IC, Figure 29): Characters 79 and 80

79. Origin

0. Absent, not differentiated from POP
1. Medial distal fibular shaft, distal to POP origin [line of scarring]

Remarks—In mammals, where the tibia and fibula are fused distally, this muscle is inseparable from the POP, or absent altogether. Well-preserved fibulae of "pelycosaurs," especially of larger individuals, sometimes exhibit a line of scarring along their medial or posteromedial margin; likewise, the apposing lateral margin of the tibia typically exhibits a similar line of scarring or rugosities (see next character). Scarring on the distal fibula is far less frequently observed among therapsids or cynodonts (Figure 28n,t; Jenkins, 1971; Kemp, 1980b).

80. Insertion

0. Absent, not differentiated from POP
1. Lateral to posterolateral distal tibia [line of scarring]

Remarks—In some specimens, the character of scarring observed on the lateral tibia or medial fibula varies proximodistally, which probably indicates that the attachments of multiple muscles are recorded [i.e., IC and POP; Figure 28d,g,s,t].

4 | DISCUSSION

Using extensive first-hand observation of fossils and an explicit phylogenetic framework, this study sought to trace the evolution of hindlimb musculature from early amniotes through to crown mammals. The identification of homologous (and nonhomologous) structures across disparate extant and extinct taxa has helped clarify several important aspects of how and when the mammalian hindlimb was assembled. As explored below, several anatomical traits usually regarded as characteristically "mammalian" actually have far greater antiquity, having a long history prior to the origin of Mammalia. Not only do these challenge the concept of "what makes a mammal a mammal," but they also challenge the paradigm of using extant sprawling sauropsids as analogs for early amniotes, including early synapsids. Lastly, the anatomical and phylogenetic framework assembled here will also provide a new, more rigorous basis for the future reconstruction of musculature, limb biomechanics, and organismal biology in extinct species (Bishop et al., 2021, and references cited

FIGURE 29 Osteological evidence of popliteus and interosseus cruris musculature attachment to the tibia and fibula in synapsids. (a) MCZ VPRA-1035 *Diadectes tenuitectus* (Diadectomorpha) fibula in posterior view (left inset in medial view). (b) MCZ VPRA-1203 *Ophiacodon retroversus* (Ophiacodontidae) tibia in posterior view, inset in lateral view. (c) MCZ VPRA-5876 *Ophiacodon retroversus* fibula in posterior view. (d), MCZ VPRA-1351 *Edaphosaurus* sp. (Edaphosauridae) tibia in posterior view; scarring for IC inferred to be along the line between arrows (distinct from tuberosity). (e) MCZ VPRA-4324 *Edaphosaurus boanerges* tibia in posterior view, inset in lateral view. (f) MCZ VPRA-1652 *Edaphosaurus pogonias* fibula in posterior view (left inset in medial view). (g) MCZ VPRA-6480 *Secodontosaurus* sp. (Sphenacodontia) tibia in lateral view, arrow indicates change in the form of muscle scarring between proximal and distal ends. (h) MCZ VPRA-1737 *Dimetrodon* sp. (Sphenacodontia) fibular head in posterior view. (i) NMQR 2987 *Tapinocaninus pamelae* (Tapinocephalidae) tibia in lateral view. (j) AMNH FARB 5552 *Moschops capensis* (Tapinocephaliade) fibula in posterior view. (k) NMQR 1478 *Aulacephalodon bainii* (Dicynodontia) tibia in lateral view. (l) SAM-PK-2348 cf. *Dicynodon* sp. (Dicynodontia) tibia in lateral view. (m) AMNH FARB 5649 *Dicynodon* sp. (Dicynodontia) tibia in lateral view; scarring for IC between arrows. (n) NHMUK PV unnumbered *Kannemeyeria simocephalus* (Dicynodontia) fibula in posteromedial view; scarring for IC between arrows. (o) SAM-PK-K1676 Gorgonopsia indet. tibia in lateral view. (p) UMZC T.883 Gorgonopsia indet. tibiae in lateral view (right image is of left tibia mirrored). (q) SAM-PK-K10465 *Galesaurus planiceps* (Cynodontia) tibia and fibula in lateral view. (r) NMQR 1208 cf. *Cynognathus crateronotus* (Cynognathia) tibia in lateral view. (s) BP/1/1675 cf. *Cynognathus* tibia in lateral view. (t) BP/1/1675 cf. *Cynognathus* fibula in medial view. (u) MCZ VPRA-3691 *Massetognathus pascuali* (Cynognathia) tibia in lateral view. (v) PVL 2554 *Exaeretodon argentinus* (Cynognathia) tibia in lateral view. (w) UFRGS-PV-1051-T *Trucidocynodon riograndensis* (basal probainognathian) tibia in lateral view (see also Figure 16o for apposing aspect of fibula).

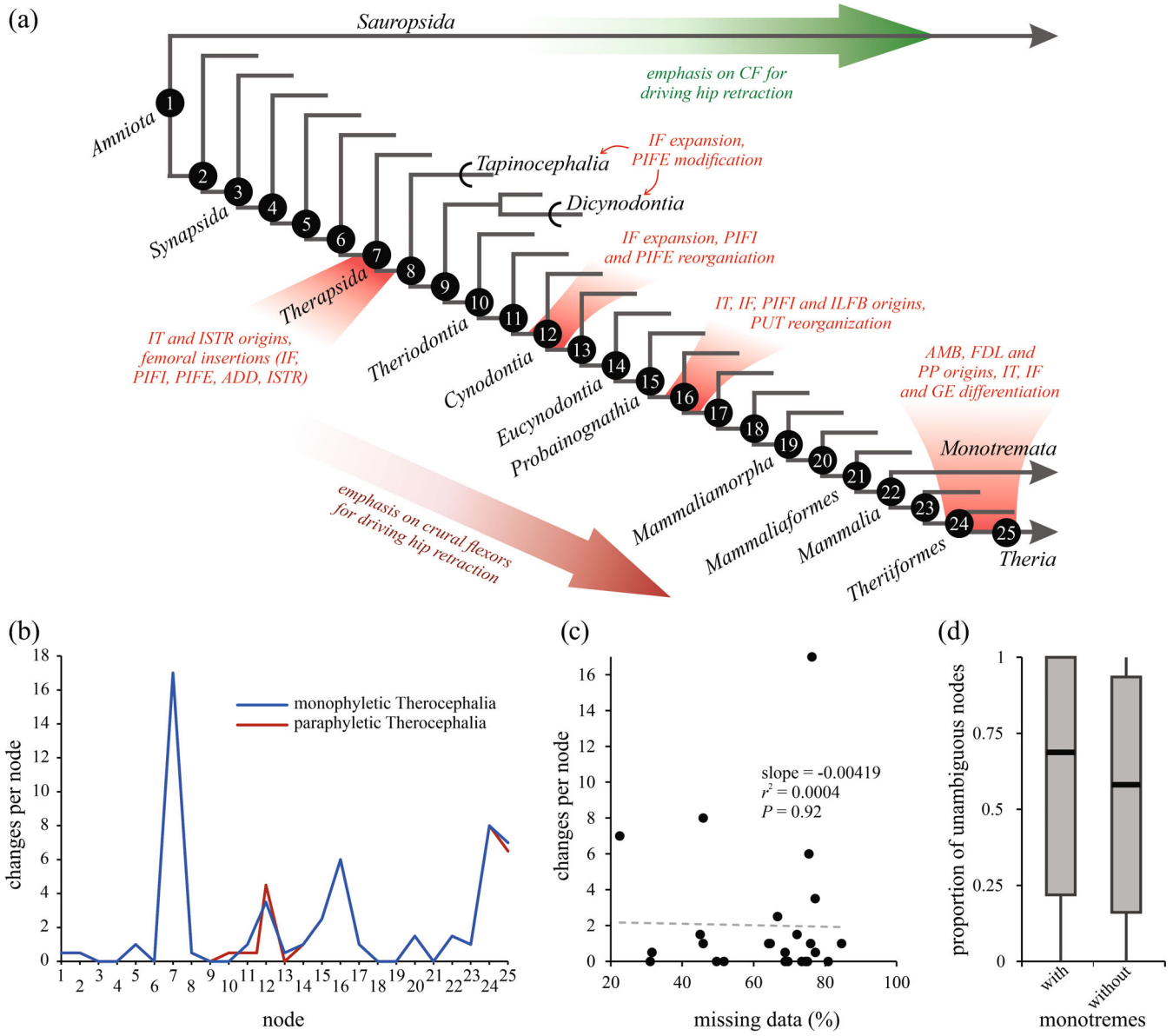

FIGURE 30 Major trends in hindlimb muscle evolution along the mammalian stem lineage. (a) Phylogeny of all crown amniote groups examined in this study, with major phases of muscular reorganization indicated. (b) the pattern of character evolution along the mammalian stem lineage, quantified as the number of state changes inferred for each node by maximum likelihood ancestral state reconstruction. Node numbers correspond to those indicated in (a). Values are the average across root-to-tip and tip-to-root sequential comparisons, and are reported for both tree topologies (mono- and paraphyletic Therocephalia). (c) Comparison of the number of state changes for each node on the stem lineage versus the amount of missing data pertinent to that node; the absence of a significant correlation implies that the patterns in a and b are likely reflective of the true pattern of evolution. (d) Boxplot summary of the proportion of all internal nodes within the phylogeny whose state could be reconstructed unambiguously by maximum likelihood, across all hindlimb characters, both with and without the inclusion of monotremes.

therein), and will help to address questions of postural and functional evolution within Synapsida.

4.1 | Major trends along the stem lineage

The history of hindlimb muscle evolution on the line to mammals involved several large shifts in topology and relative importance (i.e., size) of various muscle groups (Figure 30a), and was altogether considerably more complex compared to that inferred for the forelimb (see Bishop & Pierce, 2023). This stands in contrast with the evolution of the underlying skeleton wherein that of the forelimb and especially pectoral girdle underwent more dramatic reorganization. Overall, synapsid hindlimb muscle evolution was characterized by a progressive shift in emphasis from ventral to dorsal hip

musculature, as well as by a progressive increase in the number of muscle bellies, largely through the differentiation of ancestrally singular muscle masses. Much of the latter appears to have occurred late in synapsid evolution, within crown Mammalia, although it is important to recognize that missing data in fossil species (especially when unambiguous osteological correlates are absent) may bias assessments of the timing of muscle differentiation. A ventral-to-dorsal shift and differentiation of hindlimb muscle groups are also inferred to have characterized the evolution of birds, the other dominant lineage of erect-stance tetrapods (Hutchinson, 2001a, 2001b, 2002). However, while the evolution of avian hindlimb musculature involved numerous instances of muscle loss, few such losses are inferred for mammals, with the two most notable being the ILFB (TEN) and CF. Even then, these were not total phyletic losses, as some extant groups retain vestiges of one or both of these muscles, including notoryctid, peramelid, dasyurid and phalangeriid marsupials, tupaiids, and rodents.

In a similar fashion to the forelimb (Bishop & Pierce, 2023), the number of state changes inferred by ASR for each node of the stem lineage reveals a fluctuating pattern, with at least four pulses of character evolution (Figure 30b). The assumption of therocephalian mono- or paraphyly does not significantly alter the recovered pattern, and there is no significant correlation between the inferred number of state changes at a given node and the proportion of missing data pertinent to that node (Figure 30c; $p = 0.981$, determined using ordinary least squares in PAST 3.01; Hammer et al., 2001). The recovered pattern may hence be cautiously interpreted as genuine. As with the forelimb, the largest shift is concentrated at the origin of therapsids, likely amplified by the long ghost lineage separating Therapsida from Sphenacodontidae (Sidor & Hopson, 1998). Major changes in hindlimb musculature associated with the origin of therapsids revolve around muscles crossing the hip, and include dorsal migration of the IT origin to the margin of the iliac blade (characters 2, 3; accommodating a larger area of origin for the IF), development of a GrTr and lateral shift of IF and ISTR insertions (characters 14, 41), changes to the PIFI and PIFE arrangements (characters 17, 19, and 20), reduction in the prominence of ADD scarring on the femoral shaft (character 38) and a shift in ISTR origin (character 40). The next pulse of character evolution occurred at the base of Cynodontia, involving marked anterior expansion of the iliac blade (character 13) and major reorganization of the PIFI and PIFE, especially in terms of the femoral insertions (characters 16, 17, and 20). A second major shift within cynodonts occurred around the appearance of *Prozostrodon*, revolving around the transformation of the iliac blade into a more mammalian trihedral structure, affecting the origins of the IF and PIFI (characters 13, 16), and also those of the IT and ILFB (characters 3, 21) as the postacetabular ilium was lost. This is also inferred to coincide with the completion of PUT reorganization (characters 34, 35). The final major pulse of character evolution occurred within Theriiformes, involving a shift in the origin of the AMB proximally (character 6), and FDL and pronator profundus (PP) distally (characters 55, 75), as well as the differentiation and subsequent reorganization of several muscle masses, including the IT, IF, and GE (characters 1, 12, 46, 48, 49, 52, and 53). To this list may also be added the ISTR (characters 39, 40), although caution is warranted as monotremes may have instead secondarily lost the OBIN. As with the forelimb, the pattern of character evolution inferred here documents a protracted, step-wise, and mosaic assembly of modern mammalian traits.

It is noteworthy that two traits typically thought of as characteristically mammalian also evolved convergently outside the stem lineage. A greatly expanded anterior iliac blade (character 13, state 2) evolved in cynodonts (eventually transforming into a trihedral shape), dicynodont anomodonts, and tapinocephalian dinocephalians, and beyond therapsids in the varanopid *Mycterosaurus* (Romer & Price, 1940) and even some nonsynapsids such as *Petrolacosaurus* (Peabody, 1952) and pareiasaurs (Turner et al., 2015; Van den Brandt et al., 2021). The homoplasy in this part of the pelvis mirrors that observed in early archosaurs, including dinosaurs, which has in the past been loosely correlated with the use of more erect limb postures (Carrano, 2000; Parrish, 1986). Alternatively, or additionally, expansion of the anterior iliac blade in dicynodonts and tapinocephalians may be related to the evolution of larger body sizes in these groups. Previously, Griffin and Angielczyk (2019) showed that the number of sacral vertebrae is positively correlated with body size in dicynodonts; given that sacralization of vertebrae tended to occur at the anterior end of the sacrum, this would offer an explanation for increased length of the anterior iliac blade in this group. It remains to be determined whether a similar correlation existed in dinocephalians.

In the distal hindlimb, the development of a distinct calcaneal tuber, and associated modification of the gastrocnemii insertions (characters 51, 54, state 3), appeared no later than eucynodonts, but similar structures also evolved in baurioid eutherocephalians (Kemp, 1978, 1986; Schaeffer, 1941b; Watson, 1931), at least one dicynodont (King, 1985) and the biarmosuchian *Hipposaurus* (Boonstra, 1965). Superficially similar, but more subdued, "heels" are also observed in the calcanei of several gorgonopsians and scylacosaurids (Figure 24c–i). It is possible

that the gastrocnemii of the ancestral therapsid had already attained a more direct connection to the calcaneum, and was somewhat dissociated from the plantar aponeurosis, predisposing further change in subsequent lineages and culminating in the development of the tendon-and-tuber arrangement that persisted from eucynodonts to extant mammals. A third notable convergence in hindlimb anatomy was the substantial reduction and partial retroversion of the pubis in dicynodonts, especially more derived members, which preceded that observed in cynodonts (King, 1981a; Ray, 2006; Watson, 1960). Presumably, this reduced the sizes of certain ventral hip muscles, such as the PIFE mass. However, given the disparate suite of anatomical features observed elsewhere in the hindlimb of each of the aforementioned groups (especially the femur), it remains uncertain if the instances of convergence noted here resulted in convergence of musculoskeletal function.

Lastly, in the companion study, the relevance of monotremes to reconstructing forelimb muscular anatomy in extinct synapsids was explored by running a phylogenetic analysis and ASR to their exclusion. There it was found that the proportion of internal nodes whose state could be reconstructed unambiguously (defined as likelihood $\geq$0.75) was, overall, slightly lower when monotremes were taken into consideration (Bishop & Pierce, 2023, Figure 24d). However, performing the same test with the hindlimb dataset here shows that the proportion of unambiguous internal nodes is modestly higher when monotremes are taken into consideration (Figure 30d). The contrast in results between fore- and hindlimbs may in part be a reflection of the semi-fossorial or semi-aquatic lifestyle of extant species, in which phylogenetic signal has been more strongly "overprinted" by a functional signal associated with modified forelimb use. Irrespective of their various adaptations toward specialized lifestyles, extant monotremes have demonstrable utility for understanding anatomical evolution within Synapsida because they possess a suite of transitional states, in both the forelimb (Bishop & Pierce, 2023; characters 9, 21, 22, and 31) and hindlimb (this study; characters 5, 6, 12, 36, 49, 53, 59, 60, and 63, also a well-developed parafibula). Considering these transitional states will improve the precision with which inferences about character evolution can be made, especially when such inferences employ an explicit phylogenetic framework and take into consideration data from fossils.

4.2 | Reorganization of synapsid hip musculature

The number and arrangement of muscles surrounding the mammalian hip are radically different from what is observed in other extant tetrapod clades. The fossil record documents numerous aspects of how this distinctive anatomy was assembled along the mammal stem lineage. Not only does it indicate that certain "mammalian" traits are characteristic of a more inclusive group, it also collectively illustrates a remarkable set of muscle migrations and differentiations (Figure 31). This stands in contrast to the history of synapsid shoulder musculature, where major changes in topology were limited to the supracoracoideus mass, from procoracoid to scapula and clavicle, and the triceps coracoideus, from metacoracoid to latissimus dorsi (see Bishop & Pierce, 2023). The contrast is all the more noteworthy considering that it was the pectoral, not pelvic, girdle that underwent a more radical transformation, with near total loss of dermal bones and the coracoid plate, development of a novel sternal complex, and restructuring of the scapular blade (Bendel et al., 2022; Kemp, 1982; Luo, 2015). The consequences of these differing modes of musculoskeletal transformation for fore- and hindlimb function and locomotor evolution remain to be explored in quantitative detail.

4.2.1 | Iliofemoralis

The transformation of the iliofemoralis (IF) into the mammalian gluteal musculature has featured as a key element in studies of locomotor evolution in synapsids (Gregory, 1926; Kemp, 1978, 1980b; King, 1981a; Ray & Chinsamy, 2003; Romer, 1922; Sullivan et al., 2013; Walter, 1988b). Although no radical transformation in origin or insertion occurred, the relevance of this muscle mass to synapsid evolution lies in its importance as the main hip abductor in most extant mammals. Stages in the transformation of the IF are also readily recognized from osteological correlates in fossils, although evidence of its progressive subdivision into various gluteal heads is currently lacking. The expansion of the IF, in tandem with iliac expansion and the appearance of a novel greater trochanter (GrTr), has always been *correlated* with the evolution of a "more erect" posture (how erect though, in terms of specific joint angles, is frequently not detailed), but very little by way of a *causative* relationship between IF evolution and locomotor evolution tends to be articulated. Iliofemoral expansion and differentiation make for a tidy qualitative narrative, but the dearth of more quantitative, mechanistic analyses has rendered it difficult to evaluate the functional value of various stages of IF evolution as it relates to locomotor biomechanics. More recently, however, Sullivan et al. (2013) suggested a scenario of functional transformation on the line to mammals: in early sprawling synapsids (e.g., "pelycosaurs") the IF functioned as a hip abductor (elevator) during the *swing* phase (cf. Dick & Clemente, 2016; Gatesy, 1997);

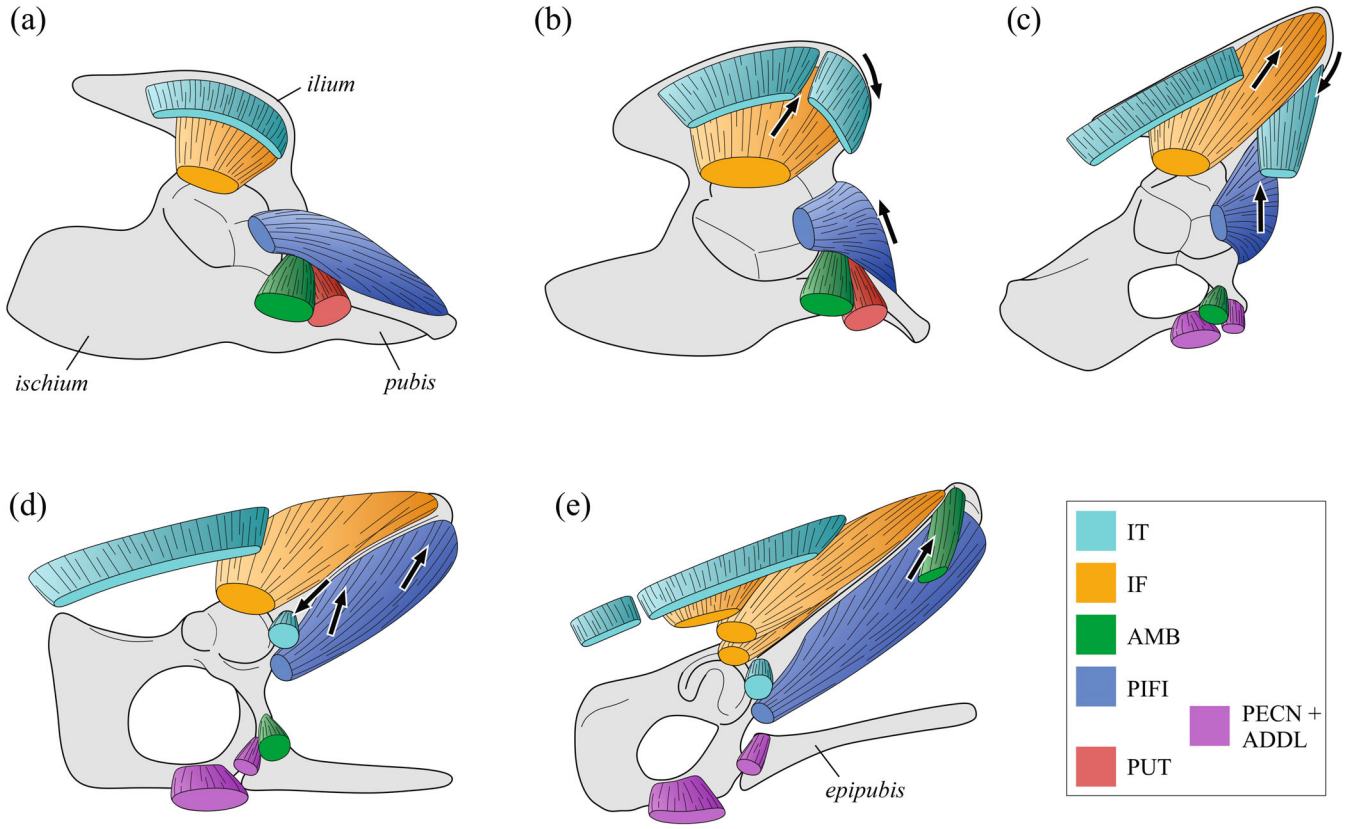

FIGURE 31 Schematic summary of the reorganization of hip musculature on the line to mammals, shown with reconstructions of certain hip muscles at key stages in synapsid evolution. (a) "Pelycosaur". (b) Therapsid. (c) Eucynodont. (d) Crown mammal. (e) Therian. Arrows show inferred paths of migration of muscle origins relative to the previous (more stemward) stage of evolution. Note that, although illustrated here for Eucynodontia, the timing of recombination of the PUT and PIFI is not well constrained; it is only certain that it would have been effectively complete prior to the appearance of *Prozostrodon* (see text).

later in therapsids with the development of the GrTr and a more erect posture, the IF functioned as a hip abductor during the *stance* phase (cf. Hutchinson & Gatesy, 2000); and later in cynodonts with a proximally expanded GrTr, the IF helped confer hip retraction during late stance, while also functioning as a stance phase abductor. As a partial alternative to this scenario, the IF may have remained active in the swing phase in some therapsids, aiding the elevation and protraction of a hindlimb that had not yet acquired a fully erect configuration (cf. Fröbisch, 2006; King, 1981a), in addition to the novel acquisition of stance phase activity. Indeed, such a biphasic recruitment pattern could form an evolutionarily intermediate condition between swing-only and stance-only functions. These mechanistic interpretations are amenable to explicit quantitative testing in the future (e.g., Bishop et al., 2021; Brocklehurst et al., 2022).

4.2.2 | Iliotibialis

In extant nonmammalian tetrapods, the iliotibialis (IT) is the most superficial muscle mass of the dorsal thigh. Yet in mammals, the disposition of its anterior head (IT1 = RF), originating from the base of the ilium near the acetabulum, places it as *deep* to the gluteal musculature (IF homologue, inserting on GrTr) but *superficial* to the iliacus/psoas musculature [PIFI partial homologue, inserting on the lesser trochanter (LeTr)]. This indicates that the evolutionary migration of the IT1's origin took a long course along the anterior-then-ventral perimeter of the ilium (clockwise for the right ilium when viewed laterally; Figure 31a–d), rather than a simple ventral shift. Such a migration was complete by the appearance of tritylodontids, and roughly coincides with the loss of the postacetabular iliac blade and acquisition of a trihedral iliac morphology, at which point the posterior head of the iliotibialis (IT2) would have originated wholly from the vertebral column. Moreover, migration of the IT1 must have preceded the dorsal migration of the PIFI mass making contact with the ventrolateral iliac surface, as signified by the appearance of an iliac fossa. It is in fact possible that migration occurred substantially earlier in synapsid evolution than a dorsal PIFI shift, while the preacetabular iliac blade was still only modestly developed, with a discrete osteological correlate of origin (rectus

tubercle) appearing only later. The proximate reason(s) driving the migration of the IT1 may be related to the sustained dorsal and anterior expansion of the IF musculature in nonmammalian therapsids and cynodonts (Romer, 1922). Paralleling IT1 migration, the posterior iliotibial head differentiated (forming the GMAX and FCOC) and retracted its insertion from the proximal tibia to the lateral femur. Differentiation appears to be a therian apomorphy (Figure 31e), whereas a proximal shift in insertion would have at least been underway by the appearance of crown Mammalia, as indicated by the presence of a subdued third trochanter [character 5(1)] in the docodontan *Haldanodon* (Martin, 2005).

4.2.3 | Ambiens

A geometrically more straightforward solution to the change in IT1 origin would be provided if the mammalian RF were homologous to the nonmammalian AMB (Gregory & Camp, 1918), but evidence from innervation (Romer, 1922) and embryology (Jones, 1979) strongly argues against this. Instead, the origin of the AMB shifted dorsally to ultimately occupy the anterior apex of the preacetabular ilium (Figure 31e), becoming the SART. Extant monotremes retain the plesiomorphic condition of an origin from the anteroventral pubis [near the iliopectineal process; character 6(1)], indicating that the shift occurred within crown mammals. Furthermore, since the proximal AMB of extant nontherian tetrapods is ventral to the PIFI mass (or its homologue; Figure 31a–d), this implies that dorsal migration of the former's origin could not have taken a bony route (i.e., the iliacus/psoas would get in the way). Romer (1922) hypothesized that the change in origin occurred via the muscle "sliding" up along the iliopubic ligament, lateral to the iliacus/psoas, an inference indirectly supported by the observation that the muscle sometimes still takes origin from the ligament in some therians (e.g., tupaiids; George, 1977; Le Gros Clark, 1924, 1926). It is quite remarkable that, from a functional perspective, the IT1/RF and AMB/SART played "musical chairs" on the line to therians: plesiomorphically the IT1 is dorsally located and the AMB ventrally located, with the situation switched in therians. As exhibited by extant monotremes, for a period of time there would have been two muscles adjacent to each other at the anterior base of the ilium or proximal pubis, divided by the passage of the iliacus/psoas mass (Gambaryan et al., 2002; Walter, 1988a). Both muscles have remained knee extensors, so why they would effectively trade places over the course of synapsid evolution defies the current explanation.

4.2.4 | Puboischiofemoralis internus

In extant nonmammalian, nonarchosaur tetrapods, the PIFI mass originates from the medial (inner) surface of the pubis and ischium, but its homologues in mammals, the iliacus and psoas major, originate from the ventral ilium and adjacent vertebrae (Figure 31d,e). A marked contrast also occurs in these muscles' insertion on the femur, predominantly on the anterior surface in nonmammals compared to predominantly on the posterior surface in mammals, but this aspect is dealt with in the next section. Insofar as the origin is concerned, evolution along the mammalian stem lineage involved a dorsal migration off the (progressively shrinking) puboischiadic plate and onto the (progressively expanding) preacetabular iliac blade. In contrast to the AMB, the dorsal shift in origin could have tracked a bony route, along the medial dorsal pubis and medial ventral ilium, as is observed in the "PIFI1" of extant crocodylians. The precise timing of this shift is not clear, but the development of an incipient iliac fossa in *Prozostrodon*, *Therioherpeton*, and tritylodontids indicates that it would have been largely completed by the time these taxa evolved. The dorsal migration of the PIFI, and proliferation and differentiation of the IF, on the line to mammals together show parallels with the inferred history of hip musculature in archosaurs on the line to birds (Hutchinson, 2001a, 2001b; Hutchinson & Gatesy, 2000), and raise interesting questions about functional convergence during the evolution of erect limb posture. Unlike archosaurs, not all the PIFI mass moved dorsally in synapsids, with part of it remaining behind to merge with part of the PUT to form the PECN and ADDL (Figure 31c). Presumably, this recombination was already completed by the time the PIFI mass reached its terminal destination on the preacetabular ilium.

4.3 | Femoral trochanter evolution and homology

Part of the reorganization of hip musculature involved a translocation of insertions on the proximal femur. As in the avian stem lineage (Hutchinson, 2001a; Hutchinson & Gatesy, 2000), much of this is documented through shifts in the location and expression of various scars and trochanters. The GrTr of mammals first appeared in therapsids, and its identity as the major insertion of the iliofemoral/gluteal musculature has never been doubted. In contrast, disagreement has persisted over the homology of two other trochanters recognized in nonmammalian synapsid femora, the internal

trochanter (InTr) and lesser trochanter (LeTr). This fundamentally stems from the fact that the InTr serves as the locus of insertion for the *ventrally* derived PIFE in salamanders, lepidosaurs, and testudines, whereas the LeTr serves as the locus of insertion for the *dorsally* derived PIFI homologue (iliacus/psoas) in mammals. "Pelycosaurs" typically possess two trochanters, the proximally projecting InTr and the more distally sited fourth trochanter (4Tr). To date, almost all known nonmammalian therapsids possess a single trochanter somewhere on the posterior surface of the femur, the only exception being rare dinocephalian and biarmosuchian specimens (Figure 22e; King, 1988; Sigogneau & Tchudinov, 1972); the condition in these few instances indicates that the distally positioned 4Tr was lost within therapsids. Considering these observations, the question is therefore raised as to whether the InTr of nonmammalian, nonarchosaur tetrapods and the LeTr of extant mammals are homologous or not, and if not, what is their differential history on the line to mammals.

Although recognizing the stark contrast in muscular attachments, Gregory and Camp (1918) and Romer (1922) accepted the homology of the InTr and LeTr due to their similar location. However, with additional material, Romer (1924) reversed his opinion and outlined a scenario of synapsid femoral evolution involving (a) lateral migration along the posterior surface, reduction and eventual loss of the InTr, and (b) posterior and subsequently posterolateral migration of scarring from the anteromedial femur, simultaneously developing into a large process, the LeTr (Figure 32a). That is, Romer suggested progressive "rotation" of muscle attachments, where the LeTr came to replace the InTr as the sole trochanter on the posterior femur. Later, Parrington (1961) supported Romer's transformational hypothesis, and posited that the replacement of the InTr by the LeTr occurred between Therocephalia and Cynodontia (Figure 32a). Importantly, Parrington also presented conclusive evidence of an *additional* process for muscle attachment on the proximal femur of certain therapsids (Figure 12l). This process occurs on the anteromedial surface, just distal to the femoral head, in the same general position of the PIFI insertion of extant salamanders, lepidosaurs, and testudines [and as inferred for early amniotes; character 17(2)], and was interpreted as such by Parrington.

Citing a scarcity of supporting fossil evidence, particularly within cynodonts, Jenkins (1971) critiqued Romer's and Parrington's studies, questioning the generality of Romer's observations and suggesting that the therocephalians studied by Parrington may be apomorphic and not related to the line leading to mammals. Although Jenkins remarked (p. 183) that "the internal trochanter of reptiles is not the homologue of the mammalian lesser trochanter," he nevertheless inferred that an "anteroventral trochanter" (AvTr) has always existed. Furthermore, the differing muscular relations observed between extant salamanders, lepidosaurs, and testudines on the one hand, and mammals on the other, were hypothesized to have arisen through the PIFE shifting *off* the AvTr and the PIFI shifting *onto* it on the line to mammals (Figure 32b). That is, whereas Romer (1924) hypothesized shifting (and differential expansion or reduction) of trochanters, carrying the muscle attachments with them, Jenkins (1971) hypothesized shifting of the attachments only, with a single AvTr remaining effectively static in its location. In the subsequent decades, Jenkins' claim of scarce fossil evidence has been rectified, with the recognition of Parrington's additional process in a wider diversity of noncynodont therapsids (Boonstra, 1964; Fourie & Rubidge, 2007; Kemp, 1978; Rubidge et al., 2019). Firsthand examination in the present study indicates that it is in fact a near-ubiquitous feature on the anteromedial femur of dinocephalians, gorgonopsians, scylacosaurids, and eutherocephalians [character 17(4); Figure 12d–o], present alongside the GrTr on the lateral aspect and an AvTr on the middle posterior surface.

An important piece of the puzzle derives from early-diverging cynodonts. The first line of evidence concerns *Charassognathus*, the oldest and most primitive known cynodont (Botha et al., 2007), the holotype of which includes an articulated femur and crus (Figures 12p and 33a). Aside from a small fragment missing from the GrTr and some minor cracking proximally, the femur is otherwise well preserved. On its anteromedial aspect is a distinct longitudinal ridge just distal to the head, in the same position as observed in noncynodont therapsids [Figure 33a, arrow; character 17(4)]; even though minor brittle deformation has occurred in the proximal femur, the pronounced topographic high on the anteromedial aspect is clearly genuine. The femur is not fully exposed ventrally, with a layer of matrix remaining on the specimen. Superimposing a high-resolution surface scan of the specimen with digital models of the femur of other basal cynodonts (Figure 33b; see Supporting Information Appendix S4 for details) shows that were a large, cynodont-like LeTr present, it should be poking clear through the matrix by a few millimeters, but nothing is visible. On the other hand, a smaller InTr positioned in the middle of the posterior surface, in the manner typical of therocephalians [character 20(3); Figure 14j–m], could still be concealed by the matrix. (Of course, this interpretation assumes that the posterior femoral surface is undamaged, but the quality of preservation elsewhere in the specimen suggests significant damage to be unlikely.) These observations are taken to indicate that the femur of *Charassognathus* was more like that of (eu)

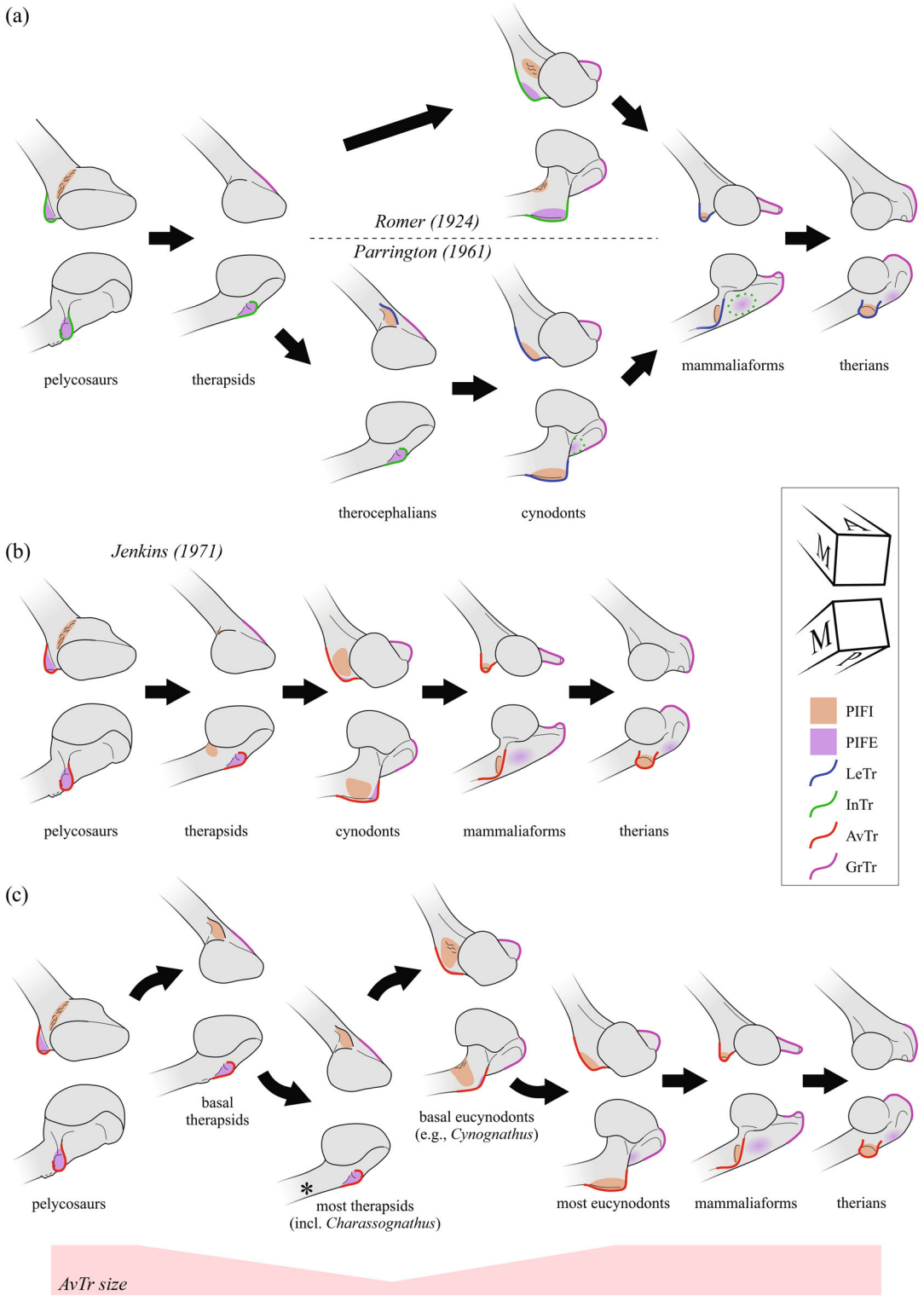

FIGURE 32 Hypotheses of femoral trochanter homology and the evolution of PIFI and PIFE muscle attachments to the proximal femur in synapsids. (a) The scenario outlined by Romer (1922) and Parrington (1961), involving trochanter rotation; specific differences between the two authors' hypotheses are indicated. (b) The scenario outlined by Jenkins (1971), involving shifting of muscle attachments. (c) The scenario of Jenkins (1971) as refined here with new observations of fossil evidence, with greater detail as to the precise sequence and timing of changes: the InTr, LeTr, and AvTr are one and the same entity. Asterisk at the third stage in (c) signifies loss of the 4Tr within therapsids. Each stage is illustrated with the femur shown in two oblique proximal views, anteromedial and posteromedial; see schematic illustration in the legend ("A" = anterior, "M" = medial, "P" = posterior). Bones are not shown to scale. For each scenario, the interpreted areas of PIFI and PIFE musculature attachment are indicated (shading), as are structures interpreted to be homologous (bold lines). Note that this figure does not account for variation in femoral head anteversion, which increases in therapsids and cynodonts prior to the evolution of a distinct neck; instead, for purposes of illustration, femora are oriented with a similar disposition to the imaginary plane passing through the head and GrTr.

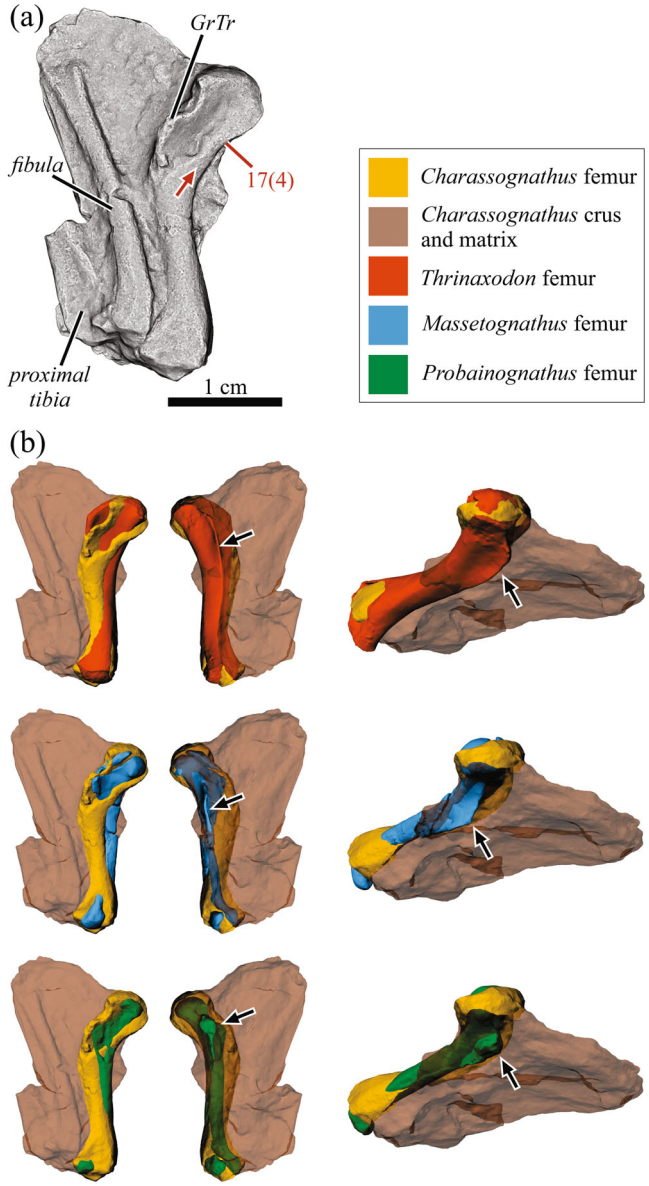

FIGURE 33 Development of trochanters on the femur of the basalmost cynodont *Charassognathus gracilis*. (a) Photogrammetric model of the articulated femur and crus of SAM-PK-K10369 (holotype), rendered with Lambertian radiance scaling to emphasize the topographic features of the specimen. Despite slight damage to the proximal femur, there is clearly a well-developed longitudinal ridge on the anteromedial corner just distal to the femoral head [arrow, character 17(4)]. (b) Comparison of the femur of *Charassognathus* with three-dimensional digital models of well-preserved femora of other basal cynodonts, *Thrinaxodon liorhinus* (BPI/1/7199; Fernandez et al., 2013), *Massetognathus pascuali* (MCZ VPRA-3691) and *Probainognathus jenseni* (MCZ VPRA-4019). In each comparison, the femora have been scaled and superimposed with one another, and each shows the lesser trochanter of the other cynodonts to clearly stand proud of the matrix encasing the posterior surface of SAM-PK-K10369 (arrows). This indicates that whatever trochanter or process was present in *Charassognathus* (currently occluded by matrix), it would have been proportionately poorly developed.

therocephalians than other cynodonts: the primary locus of insertion of the PIFI was on the anteromedial ridge, whereas that of the PIFE was on a small AvTr on the posterior surface. Tomographic scanning could confirm this interpretation in the future, as could further physical preparation, although the former approach poses less risk of damage to the specimen.

Another line of evidence is given by the femora of the large, basal cynognathians *Cynognathus* and *Diademodon*. Numerous specimens show clear evidence of muscle attachment on the anteromedial femur in the form of fine scarring (Figure 12q–s), but a discrete trochanter or ridge is absent. (A femur of ?*Diademodon* was one of the specimens cited by Romer (1924), but the location of this specimen is now unknown.) The trochanter on the posterior surface of the femur in *Cynognathus* and *Diademodon* is positioned toward the medial side, and while the degree of development of the trochanter is variable (Wynd et al., 2017), its positioning is typical of cynodonts (Jenkins, 1971).

The collective body of evidence currently available from fossil data, extant tetrapod anatomy, and phylogeny provides strong support for the transformational hypothesis of Jenkins (1971): a single AvTr has continually persisted on the femur of synapsids; the PIFI ancestrally inserted on the anteromedial femur, but subsequently shifted posteriorly to occupy the AvTr; and the PIFE ancestrally inserted on the AvTr but subsequently shifted laterally to avail the trochanter for the PIFI (Figure 32c). *Charassognathus*, *Cynognathus*, and *Diademodon* are the only cynodonts thus far known to present clear evidence of muscle attachment on the anteromedial proximal femur. Although *Cynognathus* and *Diademodon* are not on the direct line to mammals, they do suggest that the reorganization of PIFI and PIFE insertions was well underway in the common ancestor of eucynodonts, but with some shred of PIFI still inserting anteromedially (accounting for the attenuated scarring in *Cynognathus* and *Diademodon*). It is predicted that a pattern of muscle scarring similar to that in *Cynognathus* and *Diademodon* should also be observed in early-diverging probainognathians, although the small size of the latter may mean that scarring is less easily recognized compared to the large-bodied *Cynognathus* and *Diademodon*. A reorganization of insertions in early cynodonts also offers an explanation for the re-expansion of the anteroventral trochanter (InTr) into a prominent structure (i.e., the LeTr), which had previously been on a phyletic trajectory of reduction within therapsids (Figure 32c), in association with a reduction in the puboischiadic plate, the origin of the PIFE. The reorganization of the PIFI insertion may have been associated with the recombination of the PIFI and PUT, but definite evidence for this is wanting.

If the InTr of "pelycosaurs" (and sauropsids) and the LeTr of mammals are equivalent entities as hypothesized here, what does this mean for their homology? At a purely structural level, they pass the test of congruence, and also the test of similarity (although the latter is not a true test of homology; Patterson, 1982). Yet, their contrasting muscular attachments beg the question of whether the homology of bone surfaces (i.e., the interface between bone and muscle) can be altered while preserving the underlying developmental mechanisms that result in their formation. In other words, can these structures be homologous at one level of organization but not another; can osteological "correlates" of muscle attachment be interchanged among muscles? The issue of "sliding homology" bears certain resemblances to the frame-shift hypothesis of theropod hand evolution (Wagner & Gauthier, 1999; Xu et al., 2009), and a similar scenario has previously been suggested for the early evolution of the tetrapod humerus (Bishop, 2014; Molnar et al., 2018). Here, the ectepicondyle originally served as the origin of the triceps humeralis musculature, but on the line to crown tetrapods, it shifted anteriorly (preaxially), picking up the origins of the forearm extensors and leaving the triceps behind. (In this case, it is the bony process that moved and the muscular attachments remained static.) A third potential example is the origin of the archosaurian fourth trochanter (Hutchinson, 2001a; Nesbitt, 2011), but this requires further investigation as taxa spanning the crucial interval from nonarchosaur archosauriforms to archosaurs are currently uninformative. It is possible that the evolutionary re-association of muscle attachments and osteological processes may be more common than currently appreciated, and that multiple "levels of homology" may need to be more routinely considered in the analysis of fossil morphology. This is of critical importance to palaeobiological studies that rely on the recognition of homologous osteological correlates to constrain inferences (e.g., reconstructing muscle anatomy), but identifying such instances in the fossil record is difficult. Both of the aforementioned cases were identified through the evaluation of phylogenetic (in)congruence of bony structures and muscle attachments within an explicit framework. Even then, a densely sampled dataset may be required to narrow down the timing of bone–muscle re-association along a stem lineage.

4.4 | Crural flexor musculature

Plesiomorphically, the crural flexors comprise the FTIs, FTE, PIT, and PUT medially (ventrally), and the ILFB laterally (dorsally). Tracing their evolutionary history in Synapsida is overall relatively straightforward, the most radical transformations involving the FTI2 (=BICF, lateral relocation of insertion), PUT (=PECN and ADDL, via recombination with PIFI), and the ILFB (=TEN, reduction or loss). More remarkably, the results of the present study indicate that at least some of the crural flexors had very distally extensive insertions throughout much of synapsid history. On the medial side of the tibia, a longitudinal groove-like scar is near-ubiquitous feature of all nonmammalian synapsids, and can be traced to both stem amniotes and through to crown mammals (Figure 18). This scar can be confidently recognized as the insertion of at least the PIT, and potentially other muscles as well, and in stem amniotes and nonmammalian synapsids it typically extends down at least two thirds of the tibia's length. On the lateral side of the fibula, the tubercle for insertion of the ILFB is quite proximally located in "pelycosaurs," but in some noncynodont therapsids, it acquires a much more distal insertion (Figure 16e–l). A position on the proximal third of the bone is typical of cynodonts (Figure 16m,o), prior to the tubercle's loss crownward of Mammaliaformes.

The abundant osteological evidence for distally extensive crural flexor insertions appears to have hitherto escaped notice, and it warrants a re-evaluation of the life appearance of stem amniotes and many nonmammalian synapsids. In these taxa, the thighs would have appeared very deep and the "crook" of the back of the knee markedly less developed (Figure 34). Independent supporting evidence for this comes from a rare instance of fossilized integument in the varanopid *Ascendonanus*, which clearly shows the posterior margin of the thigh extending down almost to the level of the ankle (Figure 34b; Spindler et al., 2018). The crural flexor muscles were likely also relatively strong, simply by virtue of being more extensive (i.e., greater volume), and in turn, were probably more important to effecting limb retraction. The deep thighs of these animals echo the condition of sarcopterygian fish fins (e.g., Cloutier et al., 2020; Shubin et al., 2006): while functional joints are present within the appendage, the bones are so musclebound that stylopodial and zeugopodial segments are less distinct. A comparable situation appears to have existed in the forelimb of "pelycosaurs" as well (see Bishop & Pierce, 2023, character 32). Given that many extant salamanders also possess distally extensive crural flexor insertions (e.g., Ashley-Ross, 1992; Mivart, 1869), and fossil evidence for this is also observed in stem amniotes (Figure 18a–e), deep thighs are likely ancestral for Amniota, and possibly even Tetrapoda. Early amniotes and nonmammalian synapsids did not possess skinny, "lizard-esque" hindlimbs, which should be regarded as an apomorphic trait. Furthermore, many extant

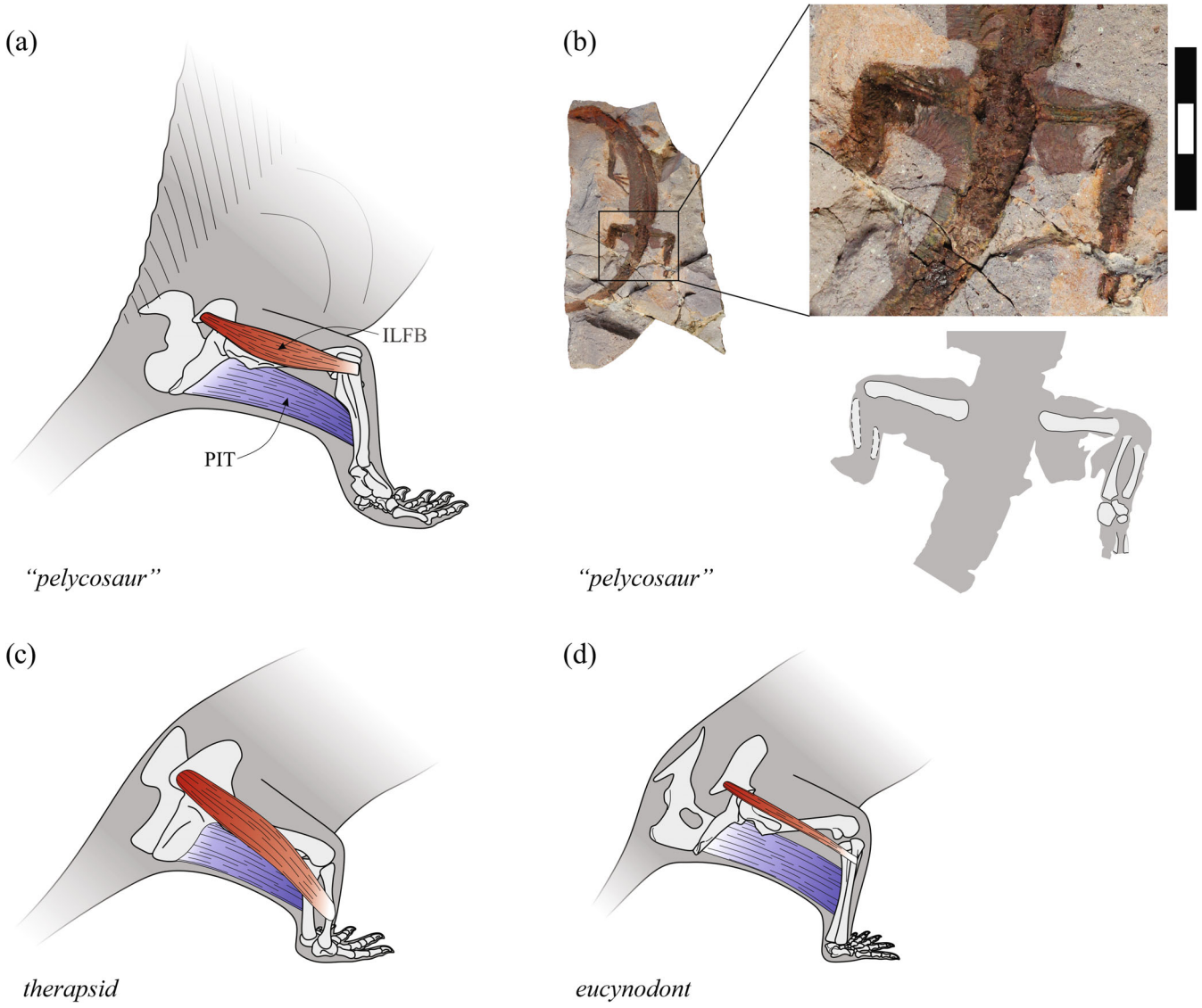

FIGURE 34 Distally extensive crural musculature and deep thighs are plesiomorphic for Synapsida and are retained in crown mammals. (a) Reconstructed life appearance of a "pelycosaur," showing inferred extent of ILFB and PIT musculature and general soft tissue outline with respect to the underlying bones. (b) Specimen of the varanopid *Ascendonanus nestleri* with remarkable soft tissue preservation (MNC-TA1045). This clearly shows the body outline and indicates that the back of the thigh ran down to near the distal end of the crus. (c) Reconstruction of a generic therapsid. (d) Reconstruction of a eucynodont. Reconstructions in (a), (c), and (d) are shown in oblique posterodorsal view; not to scale.

mammals, particularly small or primitive taxa, are notable for their deep thighs and relatively short calves (e.g., monotremes, most marsupials, tupaiids, rodents, lagomorphs, eulipotyphlans), due to distally inserting crural flexors (especially the BICF). This is possibly a retained plesiomorphy, inherited from their very distant ancestors.

4.5 | Evolution of caudofemoral musculature

In addition to transformation of the hip musculature, another key element in the narrative of synapsid locomotor evolution was the reduction of the tail and its consequences for limb mechanics. After all, most extant terrestrial mammals are notable for their diminutive tails, notwithstanding those that have been exapted for novel functions. The relevance of the tail insofar as locomotion is concerned revolves around the CF musculature, and most of what is known about its function during locomotion (e.g., femoral retraction) is based on anatomical and experimental study of extant squamates and crocodylians (Gatesy, 1990; Reilly, 1995; Rewcastle, 1981; Romer, 1922; Snyder, 1954), although some studies have also examined salamanders (Ashley-Ross, 1994; Peters & Goslow, 1983; Pierce et al., 2020). For this and other

reasons, squamates or crocodylians have typically served as analogues in attempts to understand hindlimb function in early amniotes, including "pelycosaurs" (Blob, 2001; Blob & Biewener, 2001; Brinkman, 1981a; Holmes, 1977; Kemp, 1982). The observations and analyses of the present study, however, question the merits of this practice, and suggest that extant-tailed saurians may not necessarily reflect the ancestral amniote condition.

Although almost ubiquitous among extant quadrupedal tetrapods, the CF is a single muscle in salamanders and mammals, but bipartite in lepidosaurs and crocodylians. In testudines, it is singular and apomorphically originates primarily from the sacrum instead of the caudal vertebrae (Walker, 1973). Whereas maximum likelihood ASR is equivocal (Supporting Information Appendix S3), maximum parsimony suggests that the bipartite condition is apomorphic for Sauria or a more inclusive group, and that the CF was singular in early amniotes. Similarly, the existence of a secondary tendon of insertion (to the knee region) is also probably a saurian apomorphy. Only a single head and single insertion probably existed throughout the history of synapsid evolution. The geometry of the CF also appears to have been notably different in early amniotes, in terms of its extent along the tail. Among squamates and archosaurs, the distal extent of caudal vertebrae with transverse processes has traditionally been used as an indicator of the extent of the origin of the CF's long head (Gatesy, 1990). On this basis, a first-order comparison of its extent in different taxa may be made by calculating the ratio of the length of that portion of the tail with transverse processes to the length of the femur. Computing this ratio across a suite of stem amniotes, early synapsids and extant saurians show that it is significantly greater in the latter group (Figure 35; see Supporting Information Appendix S5 for measurements), as determined by a Mann–Whitney two-tailed test (saurians vs. nonsaurians, $U = 1$, $z = -3.0913$, $p < 0.01$; calculated in PAST 3.01). While the distal extent of transverse processes need not fully reflect the extent of origin of the CF (Persons & Currie, 2011), let alone the muscle's actual volume or strength, the pattern observed here is noteworthy, and tentatively suggests that amniotes plesiomorphically had an abbreviated CF compared to extant saurians. Consistent with this inference, the CF of extant salamanders is quite short, its origin extending back only to the fourth or fifth caudal vertebra. Moreover, the "anthracosaurs" *Proterogyrinus* and *Archeria* possess longitudinal ridges for intermuscular septa of the axial musculature starting on the fifth (*Proterogyrinus*) or fourth (*Archeria*) chevrons (Holmes, 1984, 1989). This would imply quite a short CF in these stem amniotes as well.

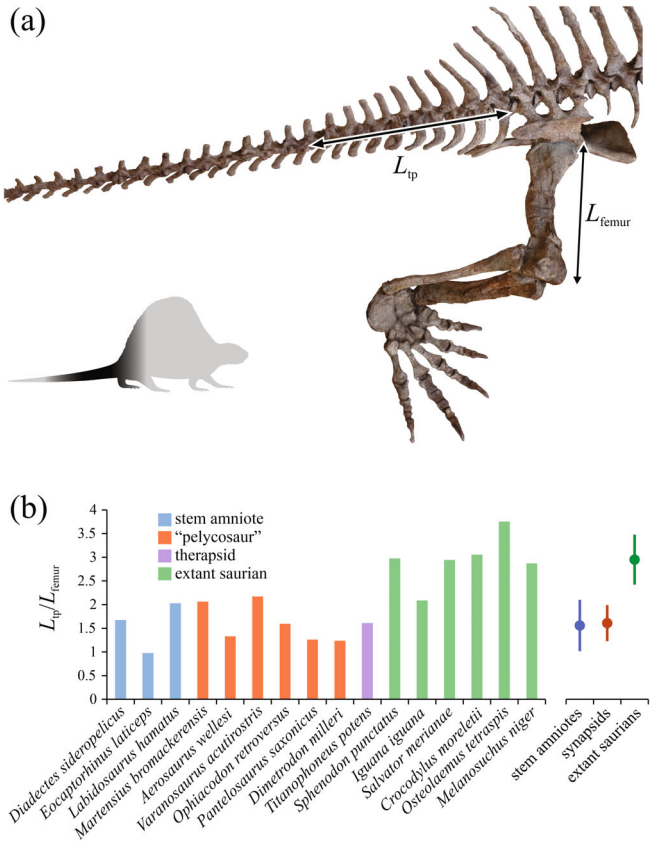

FIGURE 35 The relative extent of caudal vertebrae with ribs or transverse processes, computed for a variety of extant saurians and extinct species where the length and construction of the tail are well preserved and/or adequately documented. (a) The skeleton of *Dimetrodon milleri* (MCZ VPRA-1365) in oblique dorsolateral view, showing the measurements made. The length of the tail with transverse processes was computed from the anterior end of the centrum of the first caudal vertebra to the posterior end of the last caudal vertebra with transverse processes, measured parallel to the axis of the neural canal (rather than measuring along the tips of the neural spines). (b) Plot of the ratio of the two lengths measured, both for individual taxa, as well as the mean ± SD for each main group. Although there is variation, which is expected, the data indicates that extant saurians tend to have a larger ratio (sometimes considerably so) than early synapsids or stem amniotes. This suggests that the caudofemoralis musculature of extant saurians may be apomorphically enlarged. See Supporting Information Appendix S5 for a list of the raw measurements and the sources used to compile the data.

The above considerations further paint a picture of divergent evolutionary trajectories between Synapsida and Sauropsida (Figure 30a), in terms of the mechanics of hindlimb retraction. It is proposed here that amniotes ancestrally had a relatively small, single-bellied CF and well-developed crural flexors (see previous section, Figure 34), and the large size of the latter muscles

possibly meant that they were equally, if not more, important for effecting hip retraction during the stance phase. In Synapsida, this remained the situation for "pelycosaurs," but within therapsids the tail became progressively reduced, sometimes massively so, concurrently reducing the CF's size and firmly shifting emphasis toward the crural flexors. The importance of large, distally extensive crural flexors for locomotion then persisted through to extant mammals. In contrast to synapsids, sauropsids (or a more deeply nested clade, e.g., Sauria) shifted emphasis toward the CF musculature in effecting hip retraction, evolving a hypertrophied, bipartite CF with two insertions. Sizeable crural flexors were retained, but their insertions shifted proximally toward the knee, implying functional specialization for quicker limb movements.

This account of differential emphasis on muscle groups between Synapsida and Sauropsida contrasts with previous narratives. First, it suggests that the magnitude of the shift in CF importance within the former clade was less drastic than previously assumed; indeed, starting with a smaller CF ancestrally may have helped facilitate the shift away from reliance on the CF in synapsids. More importantly, however, the scenario outlined here posits that extant mammals and saurians are *both* apomorphic with respect to the ancestral amniote condition, and in different ways. Mammals' emphasis on crural flexors is suggested to be an exaggeration of a retained plesiomorphy, rather than a wholesale functional shift away from a "reptilian" condition of CF dominance. Likewise, a large, bipartite CF musculature playing a central role in hip retraction is apomorphic for Sauria. That extant saurians are more apomorphic than previously realized further challenges their appropriateness as analogues for early amniotes. Based on vertebral form–function relationships, Jones et al. (2021) recently questioned the paradigm of the "lateral-to-sagittal" transition in synapsids, arguing that extant sauropsids (e.g., squamates) were poor analogues of "pelycosaurs." Also recently, Bishop et al. (2023) showed that shoulder joint function in the sphenacodont *Dimetrodon*, and probably many other early amniotes, was quite unlike that in extant sauropsids, and hence the latter are again poor analogues for "pelycosaurs." The present study raises a similar issue, in a different part of the body, challenging the historical overreliance on certain extant analogues in palaeobiological studies of early amniotes.

5 | CONCLUSION

Analysis of the exceptional fossil record of synapsids, framed within an explicit phylogenetic context, has provided much new insight into hindlimb muscular evolution on the line to mammals. More than the forelimb (Bishop & Pierce, 2023), numerous anatomical traits often considered as characteristic of mammals (especially therians) among extant tetrapods are inferred to be features of a more inclusive group, having been accrued over a protracted period of time prior to the origin of Mammalia. Indeed, certain aspects of the ancestral amniote hindlimb arrangement appear to have been retained in some extant mammals in largely unaltered form. Despite this, changes in hindlimb muscular anatomy in synapsids were overall more numerous and more profound compared to those occurring in the forelimb. This contrast is all the more notable considering that the bones of the synapsid pelvic girdle underwent less marked transformation compared to those of the pectoral girdle, and that it is the forelimb of extant mammals which shows greater anatomical and functional diversity.

The evolution of hindlimb musculature on the line to mammals was, like the forelimb, a complex and nonlinear narrative that involved several pulses of anatomical change and instances of marked convergence; it was also quite protracted, with several important changes not occurring until very late, within crown mammals. In addition to refining the timing and sequence of this transformation, the present study has resolved the homology of trochanters on the proximal femur across Synapsida, and identified a case of dissociation between muscles and their supposed "correlates" of bony attachment. The results of this study also indicate that certain anatomical traits in nonmammalian synapsids (and to a degree, even some extant mammals) are probably a better reflection of the ancestral amniote condition than what is observed among extant saurians, such as a lateral origin of the tibialis anterior, distally inserting crural flexor muscles and deep thighs. Consequently, this suggests a more nuanced scenario of evolutionary divergence (in anatomy and locomotor function) between Synapsida and Sauropsida than has been previously recognized. Not only does this warrant a re-appraisal of the life appearance of many early amniotes and nonmammalian synapsids, but it also questions the prevailing reliance on extant saurians for understanding early amniotes, including basal synapsids (e.g., "pelycosaurs"). The present study did not intend to address all amniotes, but some of the results outlined here can provide a novel perspective to future investigations on this subject, in turn laying the foundation for functional studies addressing contrasting locomotor strategies and how these have evolved through time.

AUTHOR CONTRIBUTIONS

Peter J. Bishop: Conceptualization; methodology; data curation; investigation; formal analysis; funding

acquisition; visualization; writing – original draft; writing – review and editing; validation; software; project administration; resources. **Stephanie E. Pierce:** Conceptualization; methodology; data curation; investigation; formal analysis; funding acquisition; visualization; project administration; writing – original draft; writing – review and editing; validation; software; resources; supervision.

ACKNOWLEDGMENTS

The research documented in the present paper, and its companion paper, would not have been possible without the efforts of countless individuals who have, over the past century and a half, discovered, collected, prepared, and curated the fossil material studied here. The breadth and depth of insights that can now be gained from such an extensive sample of the fossil record are a testament to the dedication and foresight of these people. It is a pleasure to sincerely thank the curatorial and collections staff of all museums that contributed data to this study, for their hospitality, assistance, and access to material in their care. They include C. Mehling and A. Gishlick (AMNH), S. Jirah, B. Rubidge, and B. Zipfel (BP, RC), O. Rauhut (BSPG), N. Mchunu (CGS), K. Angielczyk, W. Simpson, and A. Stroup (FMNH), I. Werneburg and A. Krahl (GPIT), A. Martinelli, J. Escobar, and M. Ezcurra (MACN), C. Byrd, E. Biedron, M. Omura, S. Johnston, and C. Green (MCZ), M. Day (NHMUK), E. Butler and J. Botha (NMQR), P. Ortiz, and R. González (PVL), Z. Skosan and C. Browning (SAM), H. Fourie (TM), P. Holroyd (UCMP), H. Francischini (UFRGS), M. Lowe and R. Stebbings (UMZC), H. Sues, A. Millhouse, and R. Masters (USNM), and C. Sidor (University of Washington, Seattle). The authors benefited from numerous stimulating discussions with many of these people, on various topics, in addition to other colleagues including C. Kammerer, B. Stuart, A. Huttenlocker, M. Van den Brandt, F. Pinheiro, S. Burch, R. Smith, A. Mann, and V. Fernandez. Many colleagues also generously provided permission to examine and photograph (often unpublished) fossil material in their study or care, or shared photographs or important items of literature. M. Sears and R. Broadfoot (Ernst Mayr Library, Harvard University) also facilitated access to important or obscure literature, and their assistance and skill are gratefully acknowledged. The photographs of *Angonisaurus* sp. illustrated in Figure 28c were provided courtesy of K. Angielczyk, and that of *Ascendonanus nestleri* illustrated in Figure 34b was provided courtesy of F. Spindler and the Museum für Naturkunde, Chemnitz. Past and present members of the Pierce Lab are also thanked for their support and feedback, especially M. Wright and R. Brocklehurst for providing laser or computed tomography scans, and T. Simões for assistance with the phylogenetic analyses; T. Barbaro and J. Hughes are also thanked for logistical assistance. The constructive and insightful comments on an earlier version of the manuscript by K. Angielczyk and an anonymous reviewer are also much appreciated, and helped to improve its content and presentation.

FUNDING INFORMATION

This work was financially supported by the United States National Science Foundation, grants DEB-1754459 and EAR-2122115, and the William F. Milton Fund, Harvard University.

CONFLICT OF INTEREST STATEMENT

The authors declare no conflict of interest.

DATA AVAILABILITY STATEMENT

All data relating to this study are provided in the main paper or Supporting Information or are accessioned in registered museum collections (see Materials and Methods).

ORCID

Peter J. Bishop https://orcid.org/0000-0003-2702-0557
Stephanie E. Pierce https://orcid.org/0000-0003-0717-1841

REFERENCES

Abbott, C. P. (2019). *The Dimetrodon dilemma: Reassessing posture in sphenacodontians and related non-mammalian synapsids*. The College of William and Mary.

Alexander, R. M. (2006). *Principles of Animal Locomotion*. Princeton University Press.

Allen, V., Molnar, J., Parker, W., Pollard, A., Nolan, G., & Hutchinson, J. R. (2015). Comparative architectural properties of limb muscles in Crocodylidae and Alligatoridae and their relevance to divergent use of asymmetrical gaits in extant Crocodylia. *Journal of Anatomy*, *225*, 569–582.

Angielczyk, K. D., Sidor, C. A., Nesbitt, S. J., Smith, R. M. H., & Tsuji, L. A. (2009). Taxonomic revision and new observations on the postcranial skeleton, biogeography, and biostratigraphy of the dicynodont genus *Dicynodontoides*, the senior subjective synonym of *Kingoria* (Therapsida, Anomodontia). *Journal of Vertebrate Paleontology*, *29*, 1174–1187.

Anzai, W., Omura, A., Diaz, A. C., Kawata, M., & Endo, H. (2014). Functional morphology and comparative anatomy of appendicular musculature in Cuban *Anolis* lizards with different locomotor habits. *Zoological Science*, *31*, 454–463.

Ashley-Ross, M. A. (1992). The comparative myology of the thigh and crus in the salamanders *Ambystoma tigrinum* and *Dicamptodon tenebrosus*. *Journal of Morphology*, *211*, 147–163.

Ashley-Ross, M. A. (1994). Hindlimb kinematics during terrestrial locomotion in a salamander (*Dicamptodon tenebrosus*). *Journal of Experimental Biology*, *193*, 255–283.

Attridge, J. (1956). The morphology and relationships of a complete therocephalian skeleton from the Cistecephalus zone of South Africa. *Proceedings of the Royal Society of Edinburgh, Series B*, *66*, 59–93.

Bakker, R. T. (1971). Dinosaur physiology and the origin of mammals. *Evolution*, *25*, 636–658.

Barbour, R. A. (1963). The musculature and limb plexuses of *Trichosurus vulpecula*. *Australian Journal of Zoology*, *11*, 488–610.

Barnett, C. H., & Lewis, O. J. (1958). The evolution of some traction epiphyses in birds and mammals. *Journal of Anatomy*, *92*, 593–601.

Bendel, E.-M., Kammerer, C. F., Luo, Z.-X., Smith, R. M. H., & Fröbisch, J. (2022). The earliest segmental sternum in a Permian synapsid and its implications for the evolution of mammalian locomotion and breathing. *Scientific Reports*, *12*, 13472.

Berman, D. S., Henrici, A. C., Kissel, R. A., Sumida, S. S., & Martens, T. (2004). A new diadectid (Diadectomorpha), *Orobates pabsti*, from the Early Permian of Central Germany. *Bulletin of Carnegie Museum of National History*, *35*, 1–36.

Berman, D. S., Maddin, H. C., Henrici, A. C., Sumida, S. S., Scott, D., & Reisz, R. R. (2020). New primitive caseid (Synapsida, Caseasauria) from the early Permian of Germany. *Annals of Carnegie Museum*, *86*, 43–75.

Biewener, A. A., & Patek, S. N. (2018). *Animal Locomotion* (2nd ed.). Oxford University Press.

Bishop, P. J. (2014). The humerus of *Ossinodus pueri*, a stem tetrapod from the carboniferous of Gondwana, and the early evolution of the tetrapod forelimb. *Alcheringa*, *38*, 209–238.

Bishop, P. J., Brocklehurst, R. J., & Pierce, S. E. (2023). Intelligent sampling of high-dimensional joint mobility space for analysis of articular function. *Methods in Ecology and Evolution*, *14*, 569–582.

Bishop, P. J., Cuff, A. R., & Hutchinson, J. R. (2021). How to build a dinosaur: Musculoskeletal modelling and simulation of locomotor biomechanics in extinct animals. *Paleobiology*, *47*, 1–38.

Bishop, P. J., & Pierce, S. E. (2023). The fossil record of appendicular muscle evolution in Synapsida on the line to mammals: Part I—Forelimb. *The Anatomical Record: Advances in Integrative Anatomy and Evolutionary Biology*. https://doi.org/10.1002/ar.25312

Blob, R. W. (2001). Evolution of hindlimb posture in nonmammalian therapsids: Biomechanical tests of paleontological hypotheses. *Paleobiology*, *27*, 14–38.

Blob, R. W., & Biewener, A. A. (2001). Mechanics of limb bone loading during terrestrial locomotion in the green iguana (*Iguana iguana*) and American alligator (*Alligator mississippiensis*). *Journal of Experimental Biology*, *204*, 1099–1122.

Bonaparte, J. F. (1963). Descripción del esqueleto postcraneano de Exaeretodon (Cynodontia–Traversodontidae). *Acta Geológica Lilloana*, *4*, 5–52.

Bonaparte, J. F., & Barberena, C. (2001). On two advanced carnivorous cynodonts from the Late Triassic of southern Brazil. *Bulletin of the Museum of Comparative Zoology at Harvard College*, *156*, 59–80.

Boonstra, L. D. (1934). A contribution to the morphology of the Gorgonopsia. *Annals of the South African Museum*, *31*, 137–174.

Boonstra, L. D. (1955a). The girdles and limbs of the South African Deinocephalia. *Annals of the South African Museum*, *42*, 185–326.

Boonstra, L. D. (1955b). The gorgonopsians, *Aelurognathus microdon* and *Hipposaurus boonstrai*, reconstructed. *Annals of the South African Museum*, *42*, 29–31.

Boonstra, L. D. (1964). The girdles and limbs of the pristerognathid therocephalia. *Annals of the South African Museum*, *48*, 121–165.

Boonstra, L. D. (1965). The girdles and limbs of the Gorgonopsia of the *Tapinocephalus* zone. *Annals of the South African Museum*, *48*, 237–249.

Boonstra, L. D. (1967). An early stage in the evolution of the mammalian quadrupedal walking gait. *Annals of the South African Museum*, *50*, 27–42.

Botha, J., Abdala, F., & Smith, R. M. H. (2007). The oldest cynodont: New clues on the origin and early diversification of the Cynodontia. *Zoological Journal of the Linnean Society*, *149*, 477–492.

Botha-Brink, J., Huttenlocker, A. K., & Modesto, S. P. (2014). Vertebrate paleontology of Nooitgedacht 68: A *Lystrosaurus maccaigi*-rich permo-triassic boundary locality in South Africa. In C. F. Kammerer, K. D. Angielczyk, & J. Fröbisch (Eds.), *Early Evolutionary History of the Synapsida* (pp. 289–304). Springer.

Brannen, T. A. (1979). *The hindlimb myology of the laboratory mouse, Mus musculus, with comparisons to other rodent genera*. Kansas State University.

Brink, A. S., & Kitching, J. W. (1951). On Leavachia, a Procynosuchid Cynodont from the middle Cistecephalus zone. *South African Journal of Science*, *47*, 342–347.

Brinkman, D. (1980a). The hind limb step cycle of *Caiman sclerops* and the mechanics of the crocodile tarsus and metatarsus. *Canadian Journal of Zoology*, *58*, 2187–2200.

Brinkman, D. (1980b). Structural correlates of tarsal and metatarsal functioning in *Iguana* (Lacertilia; Iguanadae) and other lizards. *Canadian Journal of Zoology*, *58*, 277–289.

Brinkman, D. (1981a). The hind limb step cycle of *Iguana* and primitive reptiles. *Journal of Zoology*, *181*, 91–103.

Brinkman, D. (1981b). The structure and relationships of the dromasaurs (Reptilia: Therapsida). *Breviora*, *465*, 1–34.

Brocklehurst, R. J., Fahn-Lai, P., Regnault, S., & Pierce, S. E. (2022). Musculoskeletal modeling of sprawling and parasagittal forelimbs provides insight into synapsid postural transition. *iScience*, *25*, 103578.

Broili, F., & Schröder, J. (1935). Über die Skelettrests einers Gorgonopsiers aus den unteren Baufort-Schichten. In Bayerische Akademie der Wissenschaften, Mathematisch-Physikalische Klasse (Ed.), *Sitzungsberichte der Mathematisch-Naturwissenchaftlichen Abteilung der Baierischen Akademie der Wissenschaften Zu München* (pp. 279–330). München, Die Akademie.

Broom, R. (1947). A contribution to our knowledge of the vertebrates of the Karroo beds of South Africa. *Transactions of the Royal Society of Edinburgh*, *61*, 577–629.

Burch, S. H. (2014). Complete forelimb myology of the basal theropod dinosaur *Tawa hallae* based on a novel robust muscle reconstruction method. *Journal of Anatomy*, *225*, 271–297.

Butler, E., Abdala, F., & Botha-Brink, J. (2019). Postcranial morphology of the Early Triassic epicynodont *Galesaurus planiceps* (Owen) from the Karoo Basin, South Africa. *Papers in Palaeontology*, *5*, 1–32.

Byerly, T. C. (1925). The myology of Sphenodon punctatum. *University of Iowa Studies in Natural History*, *11*, 3–50.

Campione, N. E., & Reisz, R. R. (2010). *Varanops brevirostris* (Eupelycosauria: Varanopidae) from the lower Permian of

Texas, with discussion of varanopid morphology and interrelationships. *Journal of Vertebrate Paleontology*, *30*, 724–746.

Carrano, M. T. (2000). Homoplasy and the evolution of dinosaur locomotion. *Paleobiology*, *26*, 489–512.

Charles, J. P., Cappellari, O., Spence, A. J., Hutchinson, J. R., & Wells, D. J. (2016). Musculoskeletal geometry, muscle architecture and functional Specialisations of the mouse Hindlimb. *PLoS One*, *11*, e147669.

Cloutier, R., Clement, A. M., Lee, M. S. Y., Noël, R., Béchard, I., Roy, V., & Long, J. A. (2020). *Elpistostege* and the origin of the vertebrate hand. *Nature*, *579*, 549–554.

Cluver, M. A. (1978). The skeleton of the mammal-like reptile *Cistecephalus* with evidence for a fossorial model of life. *Annals of the South African Museum*, *76*, 213–246.

Colbert, E. H. (1948). The mammal-like reptile *Lycaenops*. *Bulletin of the American Museum of Natural History*, *89*, 353–404.

Cong, L., Hou, L.-H., & Wu, X.-C. (1998). *The gross anatomy of Alligator sinensis Fauvel*. Beijing Science Press.

Coues, E. (1871). On the myology of the Ornithorhynchus. *Communications of the Essex Institute*, *6*, 127–173.

Coues, E., & Wyman, J. (1872). The Osteology and Myology of Didelphys Virginiana. *Memoirs of the Boston Society of Natural History*, *11*, 11–154.

Cox, C. B. (1959). On the anatomy of a new dicynodont genus with evidence of the position of the tympanum. *Proceedings of the Zoological Society of London*, *132*, 321–367.

Cruickshank, A. R. I. (1967). A new dicynodont genus from the Manda formation of Tanzania (Tanganyika). *Journal of Zoology*, *153*, 163–208.

Cys, J. M. (1967). Osteology of the pristerognathid *Cynariognathus platyrhinus* (Reptilia: Theriodonta). *Journal of Paleontology*, *41*, 776–790.

Davison, A. (1895). A contribution to the anatomy and phylogeny of *Amphiuma means* (Gardner). *Journal of Morphology*, *11*, 375–410.

de Oliveira, T. V., Soares, M. B., & Schultz, C. L. (2010). *Trucidocynodon riograndensis* gen. nov. *et* sp. nov. (Eucynodontia), a new cynodont from the Brazilian upper Triassic (Santa Maria formation). *Zootaxa*, *2382*, 1–71.

de Vis, C. W. (1884). Myology of Chalmydosaurus Kingii. *Proceedings of the Linnean Society of New South Wales*, *8*, 300–320.

DeFauw, S. L. (1986). *The appendicular skeleton of African dicynodonts*. Wayne State University.

Dick, T. J. M., & Clemente, C. J. (2016). How to build your dragon: Scaling of muscle architecture from the world's smallest to the world's largest monitor lizard. *Frontiers in Zoology*, *13*, 8.

Dilkes, D. W. (1999). Appendicular myology of the hadrosaurian dinosaur *Maiasaura peeblesorum* from the late cretaceous (Campanian) of Montana. *Transactions of the Royal Society of Edinburgh*, *90*, 87–125.

Diogo, R., Bello-Hellegouarch, G., Kohlsdorf, T., Esteve-Altava, B., & Molnar, J. (2016). Comparative myology and evolution of marsupials and other vertebrates, with notes on complexity, Bauplan and "Scala Naturae". *The Anatomical Record*, *299*, 1224–1255.

Diogo, R., & Molnar, J. (2014). Comparative anatomy, evolution, and homologies of tetrapod hindlimb muscles, comparison with forelimb muscles, and deconstruction of the forelimb-hindlimb serial homology hypothesis. *The Anatomical Record*, *297*, 1047–1075.

Efremov, I. A. (1954). The terrestrial vertebrate fauna from the Permian copper sandstones of the western fore-Urals. *Trudy Paleontologicheskogo Instituta Akademiya Nauk SSSR*, *54*, 1–416.

Elftman, H. O. (1929). Functional adaptations of the pelvis in marsupials. *Bulletin of the American Museum of Natural History*, *53*, 189–232.

Fernandez, V., Abdala, F., Carlson, K. J., Cook, D. C., Rubidge, B. S., Yates, A., & Tafforeau, P. (2013). Synchrotron reveals early triassic odd couple: Injured amphibian and aestivating therapsid share burrow. *PLoS One*, *8*, e84978.

Fourie, H., & Rubidge, B. S. (2007). The postcranial skeletal anatomy of the therocephalian *Regisaurus* (Therapsida: Regisauridae) and its utilization for biostratigraphic correlation. *Palaeontologia Africana*, *42*, 1–16.

Fourie, H., & Rubidge, B. S. (2009). The postcranial skeleton of the basal therocephalian *Glanosuchus macrops* (Scylacosauridae) and comparison of morphological and phylogenetic trends amongst the Theriodontia. *Palaeontologia Africana*, *44*, 27–39.

Fox, R. C., & Bowman, M. C. (1966). Osteology and relationships of *Captorhinus aguti* (Cope) (Reptilia: Captorhinomorpha). *The University of Kansas Paleontological Contributions, Vertebrata*, *11*, 1–79.

Francis, E. T. B. (1934). *The Anatomy of the Salamander*. Oxford University Press.

Fröbisch, J. (2006). Locomotion in derived dicynodonts (Synapsida, Anomodontia): A functional analysis of the pelvic girdle and hind limb of *Tetragoniaa njalilus*. *Canadian Journal of Earth Sciences*, *43*, 1297–1308.

Fröbisch, J., & Reisz, R. R. (2011). The postcranial anatomy of *Suminia getmanovi* (Synapsida: Anomodontia), the earliest known arboreal tetrapod. *Zoological Journal of the Linnean Society*, *162*, 661–698.

Gaetano, L. C., Abdala, F., & Govender, R. (2017). The postcranial skeleton of the Lower Jurassic *Tritylodon longaevus* from southern Africa. *Ameghiniana*, *54*, 1–35.

Gambaryan, P. P., Aristov, A. A., Dixon, J. M., & Zubtsova, G. Y. (2002). Peculiarities of the hind limb musculature in monotremes: An anatomical description and functional approach. *Russian Journal of Theriology*, *1*, 1–36.

Gatesy, S. M. (1990). Caudofemoral musculature and the evolution of theropod locomotion. *Paleobiology*, *16*, 170–186.

Gatesy, S. M. (1997). An Electromyographic Analysis of Hindlimb Function in *Alligator* During Terrestrial Locomotion. *Journal of Morphology*, *234*, 197–212.

Gatesy, S. M. (1999). Guineafowl Hind Limb function II: Electromyographic Analysis and Motor Pattern Evolution. *Journal of Morphology*, *240*, 127–142.

George, R. M. (1977). The limb musculature of the Tupaiidae. *Primates*, *18*, 1–34.

Gould, S. J., & Lewontin, R. C. (1979). The spandrels of San Marco and the Panglossian paradigm: A critique of the adaptationist programme. *Proceedings of the Royal Society of London. Series B*, *205*, 581–598.

Green, H. L. H. H. (1931). The occurrence of a tenuissinus muscle in a human adult. *Journal of Anatomy*, *65*, 266–271.

Greene, E. C. (1935). Anatomy of the rat. *Transactions of the American Philosophical Society*, *27*, 1–370.

Gregory, W. K. (1926). The skeleton of *Moschops Capensis* Broom, a Dinocephalian reptile from the Permian of South Africa. *Bulletin of the American Museum of Natural History*, *61*, 179–251.

Gregory, W. K., & Camp, C. L. (1918). Studies in comparative myology and osteology. *Bulletin of the American Museum of Natural History*, *38*, 447–563.

Griffin, C. T., & Angielczyk, K. D. (2019). The evolution of the dicynodont sacrum: Constraint and innovation in the synapsid axial column. *Paleobiology*, *45*, 201–220.

Guignard, M. L., Martinelli, A. G., & Soares, M. B. (2018). Reassessment of the postcranial anatomy of *Prozostrodon brasiliensis* and implications for postural evolution of non-mamaliaform cynodonts. *Journal of Vertebrate Paleontology*, *38*, e1511570.

Guignard, M. L., Martinelli, A. G., & Soares, M. B. (2019a). The postcranial anatomy of *Brasilodon quadrangularis* and the acquisition of mammaliaform traits among non-mammaliaform cynodonts. *PLoS One*, *14*, e0216672.

Guignard, M. L., Martinelli, A. G., & Soares, M. B. (2019b). Postcranial anatomy of *Riograndia guaibensis* (Cynodontia: Ictidosauria). *Geobios*, *53*, 9–21.

Hammer, Ø., Harper, D. A. T., & Ryan, P. D. (2001). PAST: Paleontological statistics software package for education and data analysis. *Palaeontologia Electronica*, *4*, 4.

Hattori, S., & Tsuihiji, T. (2021). Homology and osteological correlates of pedal muscles among extant sauropsids. *Journal of Anatomy*, *238*, 365–399.

Haughton, S. H. (1929). On some new therapsid genera. *Annals of the South African Museum*, *28*, 55–78.

Holmes, R. (1977). The osteology and musculature of the pectoral limb of small Captorhinids. *Journal of Morphology*, *152*, 101–140.

Holmes, R. (1984). The Carboniferous amphibian *Proterogyrinus scheelei* Romer, and the early evolution of tetrapods. *Philosophical Transactions of the Royal Society of London, Series B*, *306*, 431–524.

Holmes, R. (1989). The skull and axial skeleton of the Lower Permian anthracosauroid amphibian *Archeria crassidisca* Cope. *Palaeontographica Abteilung A*, *207*, 161–206.

Holmes, R. B. (2003). The hind limb of *Captorhinus aguti* and the step cycle of basal amniotes. *Canadian Journal of Earth Sciences*, *40*, 515–526.

Hurum, J. H., & Kielan-Jaworowska, Z. (2008). Postcranial skeleton of a Cretaceous multituberculate mammal *Catopsbaatar*. *Acta Palaeontologica Polonica*, *53*, 545–566.

Hutchinson, J. R. (2001a). The evolution of femoral osteology and soft tissues on the line to extant birds (Neornithes). *Zoological Journal of the Linnean Society*, *131*, 169–197.

Hutchinson, J. R. (2001b). The evolution of pelvic osteology and soft tissues on the line to extant birds (Neornithes). *Zoological Journal of the Linnean Society*, *131*, 123–168.

Hutchinson, J. R. (2002). The evolution of hindlimb tendons and muscles on the line to crown-group birds. *Comparative Biochemistry and Physiology, Part A*, *133*, 1051–1086.

Hutchinson, J. R., & Gatesy, S. M. (2000). Adductors, abductors, and the evolution of archosaur locomotion. *Paleobiology*, *26*, 734–751.

Huttenlocker, A. K., & Smith, R. M. H. (2017). New whaitsioids (Therapsida: Therocephalia) from the Teekloof formation of South Africa and therocephalian diversity during the end-Guadalupian extinction. *PeerJ*, *5*, e3868.

Jäger, K. R. K., Luo, Z.-X., & Martin, T. (2019). Postcranial skeleton of *Henkelotherium guimarotae* (Cladotheria, Mammalia) and locomotor adaptation. *Journal of Mammalian Evolution*, *27*, 349–372.

Jenkins, F. A., Jr., & Parrington, F. R. (1976). The postcranial skeletons of the Triassic mammals *Eozostrodon*, *Megazostrodon* and *Erythrotherium*. *Philosophical Transactions of the Royal Society of London, Series B*, *273*, 387–431.

Jenkins, F. A., Jr., & Schaff, C. R. (1988). The early Cretaceous mammal *Gobiconodon* (Mammalia, Triconodonta) from the Cloverly formation in Montana. *Journal of Vertebrate Paleontology*, *8*, 1–24.

Jenkins, F. A., Jr. (1970). The Chañares (Argentina) Triassic reptile fauna VII. The postcranial skeleton of the traversodontid *Massetognathus pascuali* (Therapsida, Cynodontia). *Breviora*, *352*, 1–28.

Jenkins, F. A., Jr. (1971). The Postcranial Skeleton of African Cynodonts. *Bulletin of the Peabody Museum of Natural History*, *36*, 1–216.

Jones, C. L. (1979). The morphogenesis of the thigh of the mouse with special reference to tetrapod muscle homologies. *Journal of Morphology*, *162*, 275–310.

Jones, K. E., Dickson, B. V., Angielczyk, K. D., & Pierce, S. E. (2021). Adaptive landscapes challenge "lateral-to-sagittal" paradigm for mammalian vertebral evolution. *Current Biology*, *31*, 1883–1892.

Kammerer, C. F., Fröbisch, J., & Angielczyk, K. D. (2013). On the validity and phylogenetic position of *Eubrachiosaurus browni*, a kannemeyeriiform dicynodont (Anomodontia) from Triassic North America. *PLoS One*, *8*, e64203.

Kemp, T. S. (1978). Stance and gait in the hindlimb of a therocephalian mammal-like reptile. *Journal of Zoology*, *186*, 143–161.

Kemp, T. S. (1980a). Aspects of the structure and functional anatomy of the Middle Triassic cynodont *Luangwa*. *Journal of Zoology*, *191*, 193–239.

Kemp, T. S. (1980b). The primitive cynodont *Procynosuchus*: Structure, function and evolution of the postcranial skeleton. *Philosophical Transactions of the Royal Society of London, Series B*, *288*, 217–258.

Kemp, T. S. (1982). *Mammal-like Reptiles and the Origin of Mammals*. Academic Press.

Kemp, T. S. (1985). A functional interpretation of the transition from primitive tetrapod to mammalian locomotion. In J. Reiss & E. Frey (Eds.), *Principles of Construction in Fossil and Recent Reptiles* (pp. 181–191). University of Stuttgart and University of Tübingen.

Kemp, T. S. (1986). The skeleton of a baurioid therocephalian therapsid from the Lower Triassic (*Lystrosaurus* zone) of South Africa. *Journal of Vertebrate Paleontology*, *6*, 215–232.

Kemp, T. S. (2005). *The Origin and Evolution of Mammals*. Oxford University Press.

Kemp, T. S. (2016). *The Origin of Higher Taxa*. Oxford University Press.

Kielan-Jaworowska, Z., & Gambaryan, P. P. (1994). Postcranial anatomy and habits of Asian multituberculate mammals. *Fossils and Strata*, *36*, 1–92.

King, G. M. (1981a). The functional anatomy of a Permian dicynodont. *Philosophical Transactions of the Royal Society of London, Series B*, *291*, 243–322.

King, G. M. (1981b). The postcranial skeleton of *Robertia broomiana*, an early dicynodont (Reptilia, Therapsida) from the South African Karoo. *Annals of the South African Museum*, *84*, 203–231.

King, G. M. (1985). The postcranial skeleton of *Kingoria nowacki* (von Huene) (Therapsida: Dicynodontia). *Zoological Journal of the Linnean Society*, *84*, 263–289.

King, G. M. (1988). Anomodontia. *Handbuch der Paläoherpetologie*, *17C*, 1–171.

King, G. M. (1996). A description of the skeleton of a bauriid therocephalian from the Early Triassic of South Africa. *Annals of the South African Museum*, *104*, 379–393.

Krause, D. W., & Jenkins, F. A., Jr. (1983). The postcranial skeleton of North American multituberculates. *Bulletin of the Museum of Comparative Zoology at Harvard College*, *150*, 199–246.

Kühne, W. G. (1956). *The Liassic Therapsid Oligokyphus*. British Museum (Natural History).

Lai, P. H., Biewener, A. A., & Pierce, S. E. (2018). Three-dimensional mobility and muscle attachments in the pectoral limb of the Triassic cynodont *Massetognathus pascuali* (Romer, 1967). *Journal of Anatomy*, *232*, 383–406.

Landsmeer, J. M. F. (1990). Functional morphology of the Hindlimb in some Lacertilia. *European Journal of Morphology*, *28*, 3–34.

Le Gros Clark, W. E. (1924). The myology of the tree-shrew (*Tupaia minor*). *Proceedings of the Zoological Society of London*, *31*, 461–497.

Le Gros Clark, W. E. (1926). On the anatomy of the pen-tailed tree-shrew (*Ptilocercus lowii*). *Proceedings of the Zoological Society of London*, *96*, 1179–1309.

Liu, J., & Powell, J. (2009). Osteology of *Andescynodon* (Cynodontia:Traversodontidae) from the Middle Triassic of Argentina. *American Museum Novitates*, *3674*, 1–19.

Liu, J., Schneider, V. P., & Olsen, P. E. (2017). The postcranial skeleton of *Boreogomphodon* (Cynodontia: Traversodontidae) from the Upper Triassic of North Carolina, USA and the comparison with other traversodontids. *PeerJ*, *5*, e3521.

Luo, Z.-X. (2015). Origin of the mammalian shoulder. In K. P. Dial, N. H. Shubin, & E. L. Brainerd (Eds.), *Great Transformations in Vertebrate Evolution* (pp. 167–187). University of Chicago Press.

Luo, Z.-X., & Wible, J. R. (2005). A late Jurassic digging mammal and early mammalian diversification. *Science*, *308*, 103–107.

MacCormick, A. (1887). The myology of the limbs of *Dasyurus viverrinus*. B. Myology of the hind limb. *Journal of Anatomy and Physiology*, *21*, 199–226.

Maddison, W. P., & Maddison, D. R. (2021). Mesquite: a modular system for evolutionary analysis. Version 3.61. http://www.mesquiteproject.org

Maisch, M. W., Matzke, A. T., & Sun, G. (2004). A new tritylodontid from the Upper Jurassic Shishuguo formation of the Junggar Basin (Xinjiang, China). *Journal of Vertebrate Paleontology*, *24*, 649–656.

Martin, T. (2005). Postcranial anatomy of *Haldanodon exspectatus* (Mammalia, Docodonta) from the Late Jurassic (Kimmeridgian) of Portugal and its bearing for mammalian evolution. *Zoological Journal of the Linnean Society*, *145*, 219–248.

Martinelli, A. G., Bonaparte, J. F., Schultz, C. L., & Rubert, R. (2005). A new tritheledontid (Therapsida, Eucynodontia) from the Late Triassic of Rio Grande do Sul (Brazil) and its phylogenetic relationships among carnivorous non-mammalian eucynodonts. *Ameghiniana*, *42*, 191–208.

Mivart, S. G. (1869). Notes on the myology of *Menopoma alleghaniense*. *Proceedings of the Zoological Society of London*, *37*, 254–271.

Mocke, H. B., Gaetano, L. C., & Abdala, F. (2020). A new species of the carnivorous cynodont *Chiniquodon* (Cynodontia, Chiniquodontidae) from the Namibian Triassic. *Journal of Vertebrate Paleontology*, *39*, e1754321.

Molnar, J. L., Diogo, R., Hutchinson, J. R., & Pierce, S. E. (2018). Reconstructing pectoral appendicular muscle anatomy in fossil fish and tetrapods over the fins-to-limbs transition. *Biological Reviews*, *93*, 1077–1107.

Molnar, J. L., Diogo, R., Hutchinson, J. R., & Pierce, S. E. (2020). Evolution of hindlimb muscle anatomy across the tetrapod water-to-land transition, including comparisons with forelimb anatomy. *The Anatomical Record*, *303*, 218–234.

Murie, J., & Mivart, S. G. (1865). On the myology of Hyrax capensis. *Proceedings of the Zoological Society of London*, *33*, 329–352.

Nesbitt, S. J. (2011). The early evolution of archosaurs: Relationships and the origin of major clades. *Bulletin of the American Museum of Natural History*, *352*, 1–292.

Orlov, J. A. (1958). Predatory deinocephalians from the Isheevo Fauna (titanosuchians). *Trudy Paleontologicheskogo Instituta Akademiya Nauk SSSR*, *72*, 1–114.

Osawa, G. (1897). Beiträge zur Anatomie der Hatteria punctata. *Archive of Microscopic Anatomy*, *51*, 481–691.

Otero, A., Gallina, P. A., & Herrera, Y. (2010). Pelvic musculature and function of *Caiman latirostris*. *Herpetological Journal*, *20*, 173–184.

Panciroli, E., Benson, R. B. J., Fernandez, V., Humpage, M., Martín-Serra, A., Walsh, S., Luo, Z.-X., & Fraser, N. C. (2021). Postcrania of *Borealestes* (Mammaliformes, Docodonta) and the emergence of ecomorphological diversity in early mammals. *Palaeontology*, *65*, e12577.

Paradis, E., Claude, J., & Strimmer, K. (2004). APE: Analysis of phylogenetics and evolution in R language. *Bioinformatics*, *20*, 289–290.

Parrington, F. R. (1961). The evolution of the mammalian femur. *Proceedings of the Zoological Society of London*, *137*, 285–298.

Parrish, J. M. (1986). Locomotor adaptations in the hindlimb and pelvis of the Thecodontia. *Hunteria*, *1*, 1–35.

Patterson, C. (1982). Morphological Characters and Homoplasy. In K. A. Joysey & A. E. Friday (Eds.), *Problems of Phylogenetic Reconstruction*. Academic Press.

Pawley, K. (2007). The postcranial skeleton of *Trimerorhachis insignis* Cope, 1878 (Temnospondyli): A plesiomorphic temnospondyl from the lower Permian of North America. *Journal of Paleontology*, *81*, 873–894.

Pawley, K., & Warren, A. A. (2006). The appendicular skeleton of *Eryops megacephalus* Cope, 1877 (Temnospondyli: Eryopoidea). *Journal of Paleontology*, *80*, 561–580.

Peabody, F. E. (1952). *Petrolacosaurus kansensis lane a Pennsylvanian reptile from Kansas* (p. 1). University of Kansas Paleontological Contributions.

Pearson, H. S. (1924). A dicynodont reptile reconstructed. *Proceedings of the Zoological Society of London*, *94*, 827–855.

Perrin, A. (1893). Contributions a l'étude de la myologie comparée: membre postérieur chez un certain nombre de batraciens et de

sauriens. *Bulletin Scientifique de la France et de la Belgique*, *24*, 372–552.

Perrin, A. (1895). Recherches sur les affinités zoologiques de l'Hatteria punctata. *Annales Des Sciences Naturelles Zoologie et Paléontologie*, *20*, 33–102.

Persons, W. S., IV, & Currie, P. J. (2011). The tail of *Tyrannosaurus*: Reassessing the size and locomotive importance of the *M. caudofemoralis* in non-avian Theropods. *The Anatomical Record*, *294*, 119–131.

Peters, S. E., & Goslow, G. E., Jr. (1983). From salamanders to mammals: Continuity in musculoskeletal function during locomotion. *Brain, Behavior and Evolution*, *22*, 191–197.

Pierce, S. E., Lamas, L. P., Pelligand, L., Schilling, N., & Hutchinson, J. R. (2020). Patterns of Limb and Epaxial Muscle Activity During Walking in the Fire Salamander, *Salamandra salamandra*. *Integrative Organismal Biology*, *2*, obaa015.

Polly, P. D. (2007). Limbs in mammalian evolution. In B. K. Hall (Ed.), *Fins into Limbs: Evolution, Development, and Transformation*. University of Chicago Press.

Preuschoft, H., Krahl, A., & Werneburg, I. (2022). From sprawling to parasagittal locomotion in Therapsida: A preliminary study of historically collected museum specimens. *Vertebrate Zoology*, *72*, 907–936.

Ray, S. (2006). Functional and evolutionary aspects of the postcranial anatomy of dicynodonts (Synapsida, Therapsida). *Palaeontology*, *49*, 1263–1286.

Ray, S., & Chinsamy, A. (2003). Functional aspects of the postcranial anatomy of the Permian dicynodont *Diictodon* and their ecological implications. *Palaeontology*, *46*, 151–183.

Reilly, S. M. (1995). Quantitative electromyography and muscle function of the hind limb during quadrupedal running in the lizard *Sceloporus clarki*. *Zoology*, *98*, 263–277.

Reilly, S. M., McElroy, E. J., White, T. D., Biknevicius, A. R., & Bennett, M. B. (2010). Abdominal muscle and Epipubic bone function during locomotion in Australian possums: Insights to basal mammalian conditions and eutherian-like tendencies in *Trichosurus*. *Journal of Morphology*, *271*, 438–450.

Rewcastle, S. C. (1981). Stance and Gait in Tetrapods: An Evolutionary Scenario. *Symposium of the Zoological Society of London*, *48*, 239–267.

Rinker, G. C. (1954). The comparative myology of the mammalian genera *Sigmodon*, *Oryzomys*, *Neotoma*, and *Peromyscus* (Crecetinae), with remarks on their intergeneric relationships. *Miscellaneous Publications Museum of Zoology, University of Michigan*, *83*, 1–124.

Romer, A. S. (1922). The locomotor apparatus of certain primitive and mammal-like reptiles. *Bulletin of the American Museum of Natural History*, *46*, 517–606.

Romer, A. S. (1923). Crocodilian pelvic musculature and their avian and reptilian homologues. *Bulletin of the American Museum of Natural History*, *48*, 533–552.

Romer, A. S. (1924). The lesser trochanter of the mammalian femur. *The Anatomical Record*, *28*, 95–102.

Romer, A. S. (1956). *Osteology of the Reptiles*. University of Chicago Press.

Romer, A. S., & Price, L. I. (1940). Review of the Pelycosauria. *Special Papers of the Geological Society of America*, *28*, 1–538.

Ronquist, F., Teslenko, M., van der Mark, P., Ayres, D. L., Darling, A., Höhna, S., Larget, B., Liu, L., Suchard, M. A., & Huelsenbeck, J. P. (2012). MRBAYES 3.2: Efficient Bayesian phylogenetic inference and model selection across a large model space. *Systematic Biology*, *61*, 539–542.

Rougier, G. W. (1993). *Vincelestes neuquenianus Bonaparte (Mammalia, Theria) un primitivo mamifero del Cretacio Inferior de la Cuenca Neuquina*. Universidad Nacional de Buenos Aires.

Rubidge, B. S., Govender, R., & Romano, M. (2019). The postcranial skeleton of the basal tapinocephalid dinocephalian *Tapinocaninus pamelae* (Synapsida: Therapsida) from the South African Karoo Supergroup. *Journal of Systematic Palaeontology*, *17*, 1767–1789.

Rubidge, B. S., & Hopson, J. A. (1996). A primitive anomodont therapsid from the base of the Beaufort group (Upper Permian) of South Africa. *Zoological Journal of the Linnean Society*, *117*, 115–139.

Rubidge, B. S., King, G. M., & Hancock, J. A. (1994). The postcranial skeleton of the earliest dicynodont synapsid *Eodicynodon* from the Upper Permian of South Africa. *Palaeontology*, *37*, 397–408.

Russell, A. P. (1993). The aponeuroses of the lacertilian ankle. *Journal of Morphology*, *218*, 65–84.

Russell, A. P., & Bauer, A. M. (2008). The appendicular locomotor apparatus of *Sphenodon* and normal-limbed squamates. In C. Gans, A. S. Gaunt, & K. Adler (Eds.), *Biology of the Reptilia 24, Morphology 1* (pp. 1–466). Society for the Study of Amphibians and Reptiles.

Samuels, M. E., Regnault, S., & Hutchinson, J. R. (2017). Evolution of the patellar sesamoid bone in mammals. *PeerJ*, *5*, e3103.

Sargis, E. J. (2002). Functional morphology of the hindlimb of Tupaiids (Mammalia, Scandentia) and its phylogenetic implications. *Journal of Morphology*, *254*, 149–185.

Schaeffer, B. (1941a). The morphological and functional evolution of the tarsus in amphibians and reptiles. *Bulletin of the American Museum of Natural History*, *78*, 395–472.

Schaeffer, B. (1941b). The pes of *Bauria cynops* Broom. *American Museum Novitates*, *1103*, 1–7.

Seeley, H. G. (1894). Researches on the structure, organization, and classification of the fossil Reptilia. VIII. Further evidences of the skeleton in *Deuterosaurus* and *Rhopalodon*, from the Permian rocks of Russia. *Philosophical Transactions of the Royal Society of London, Series B*, *185*, 663–717.

Shubin, N. H., Daeschler, E. B., & Jenkins, F. A., Jr. (2006). The pectoral fin of *Tiktaalik roseae* and the origin of the tetrapod limb. *Nature*, *440*, 764–771.

Sidor, C. A. (2022). New information on gorgonopsian pedal morphology based on articulated material from Zambia. *Journal of African Earth Sciences*, *191*, 104533.

Sidor, C. A., & Hopson, J. A. (1998). Ghost lineages and "mammalness": Assessing the temporal pattern of character acquisition in the Synapsida. *Paleobiology*, *24*, 254–273.

Sidor, C. A., & Hopson, J. A. (2017). *Cricodon metabolus* (Cynodontia: Gomphodontia) from the Triassic Ntawere formation of northeastern Zambia: Patterns of tooth replacement and a systematic review of Trirachodontidae. *Journal of Vertebrate Paleontology*, *37*(suppl. 1), 39–64.

Sigogneau, D., & Tchudinov, P. K. (1972). Reflections on some Russian eotheriodonts (Reptilia, Synapsida, Therapsida). *Palaeovertebrata*, *5*, 79–109.

Sigogneau-Russell, D. (1989). Theriodontia I. *Handbuch der Paläoherpetologie*, *17B*, 1–123.

Simões, T. R., Kammerer, C. F., Caldwell, M. W., & Pierce, S. E. (2022). Successive climate crises in the deep past drove the early evolution and radiation of reptiles. *Science Advances*, *8*, eabq1898.

Simpson, G. G., & Elftman, H. O. (1928). Hind limb musculature and habits of a Paleocene multituberculate. *American Museum Novitates*, *333*, 1–19.

Snyder, R. C. (1954). The anatomy and function of the pelvic girdle and hindlimb in lizard locomotion. *American Journal of Anatomy*, *95*, 1–45.

Spindler, F. (2016). Morphological description and taxonomic status of *Palaeohatteria* and *Pantelosaurus* (Synapsida: Sphenacodontia). *Freiberger Forschungshefte*, *C550*, 1–57.

Spindler, F., Werneburg, R., Schneider, J. W., Luthardt, L., Annacker, V., & Rößler, R. (2018). First arboreal 'pelycosaurs' (Synapsida: Varanopidae) from the early Permian Chemnitz Fossil Lagerstätte, SE Germany, with a review of varanopid phylogeny. *PalZ*, *92*, 315–364.

Stein, B. R. (1981). Comparative limb myology of two opossums, *Didelphis* and *Chironectes*. *Journal of Morphology*, *169*, 113–140.

Stein, B. R. (1986). Comparative limb myology of four Arvicolid rodent genera (Mammalia, Rodentia). *Journal of Morphology*, *187*, 321–342.

Sues, H.-D. (1986). Locomotion and body form in early Therapsids (Dinocephalia, Gorgonopsia, and Therocephalia). In N. H. Hotton, III, P. D. MacLean, J. J. Roth, & E. C. Roth (Eds.), *The Ecology and Biology of Mammal-like Reptiles* (pp. 61–70). Smithsonian Institution Press.

Sues, H.-D., & Jenkins, F. A., Jr. (2006). The postcranial skeleton of *Kayentatherium wellesi* from the lower Jurassic Kayenta formation of Arizona and the phylogenetic significance of postcranial features in Tritylodontid Cynodonts. In M. T. Carrano, T. J. Gaudin, R. W. Blob, & J. R. Wible (Eds.), *Amniote Paleobiology: Perspectives on the Evolution of Mammals, Birds, and Reptiles* (pp. 114–152). Chicago University Press.

Sullivan, C., Liu, J., Roberts, E. M., Huang, T. D., Yang, C., & Zhong, S. (2013). Pelvic morphology of a tritylodontid (Synapsida: Eucynodontia) from the Lower Jurassic of China, and some functional and phylogenetic implications. *Comptes Rendus Palevol*, *12*, 505–518.

Sumida, S. S. (1989). The appendicular skeleton of the Early Permian genus *Labidosaurus* (Reptilia, Captorhinomorpha, Captorhinidae) and the hind limb musculature of captorhinid reptiles. *Journal of Vertebrate Paleontology*, *9*, 295–313.

Sumida, S. S. (1997). Locomotor Features of Taxa Spanning the Origin of Amniotes. In S. S. Sumida & K. L. M. Martin (Eds.), *Amniote Origins: Completing the Transition to Land* (pp. 353–398). Academic Press.

Sumida, S. S., Pelletier, V., & Berman, D. S. (2014). New information on the basal Pelycosaurian-grade synapsid *Oedaleops*. In C. F. Kammerer, K. D. Angielczyk, & J. Fröbisch (Eds.), *Early Evolutionary History of the Synapsida* (pp. 7–23). Springer.

Sun, A., & Li, Y. (1985). The postcranial skeleton of the late tritylodont *Bienotherioides*. *Vertebrata PalAsiatica*, *23*, 135–150.

Suzuki, D., Chiba, K., Tanaka, Y., & Hayashi, S. (2011). Myology of crocodiles III: Pelvic girdle and hindlimb. *Fossils—The Palaeontological Society of Japan*, *90*, 37–60.

Tatarinov, L. P. (2004). A postcranial skeleton of the Gorgonopian *Viatkogorgon ivachnenkoi* (Reptilia, Theriodontia) from the Upper Permian Kotelnich locality, Kirov region. *Paleontological Journal*, *38*, 437–447.

Tchudinov, P. K. (1983). Early therapsids. *Trudy Paleontologicheskogo Instituta Akademiya Nauk SSSR*, *202*, 1–229.

Turner, M. L., Tsuji, L. A., Ide, O., & Sidor, C. A. (2015). The vertebrate fauna of the Upper Permian of Niger—IX. The appendicular skeleton of *Bunostegos akokanensis* (Parareptilia: Pareiasauria). *Journal of Vertebrate Paleontology*, *35*, e994746.

van den Brandt, M. J., Benoit, J., Abdala, F., & Rubidge, B. S. (2021). Postcranial morphology of the South African middle Permian pareiasaurs from the Karoo Basin of South Africa. *Palaeontologia Africana*, *55*, 1367–1393.

Wagner, G. P., & Gauthier, J. A. (1999). 1,2,3 = 2,3,4: A solution to the problem of the homology of the digits in the avian hand. *Proceedings of the National Academy of Sciences*, *96*, 5111–5116.

Walker, W. F. (1973). The Locomotor Apparatus of Testudines. In C. Gans & T. S. Parsons (Eds.), *Biology of the Reptilia*. Academic Press.

Walter, L. R. (1988a). Appendicular musculature in the echidna, *Tachyglossus aculeatus* (Monotremata: Tachyglossidae). *Australian Journal of Zoology*, *36*, 65–81.

Walter, L. R. (1988b). The limb posture of kannemeyeriid dicynodonts: Functional and ecological considerations. In K. Padian (Ed.), *The Beginning of the Age of Dinosaurs* (pp. 89–97). Cambridge University Press.

Walthall, J. C., & Ashley-Ross, M. A. (2006). Postcranial myology of the California newt, *Taricha torosa*. *The Anatomical Record*, *288A*, 46–57.

Warburton, N. M., Malric, A., Yakovleff, M., Leonard, V., & Cailleau, C. (2015). Hind limb myology of the southern brown bandicoot (*Isoodon obesulus*) and greater bilby (*Macrotis lagotis*) (Marsupialia: Peramelemorphia). *Australian Journal of Zoology*, *63*, 147–162.

Watson, D. M. S. (1931). On the skeleton of a bauriamorph reptile. *Proceedings of the Zoological Society of London*, *101*, 1163–1205.

Watson, D. M. S. (1960). The Anomodont skeleton. *Transactions of the Zoological Society of London*, *29*, 131–209.

Werneburg, R., Spindler, F., Falconnet, J., Steyer, J.-S., Vianey-Liaud, M., & Schneider, J. W. (2022). A new caseid synapsid from the Permian (Guadalupian) of the Lodève basin (Occitanie, France). *Palaeovertebrata*, *45*, e2.

Westling, C. (1889). Anatomische untersuchungen über Echidna. *Bihang till Kongl Svenska Vetenskaps-Akademiens Handlingar*, *15*, 1–69.

White, T. E. (1939). Osteology of *Seymouria baylorensis* Broili. *Bulletin of the Museum of Comparative Zoology at Harvard College*, *85*, 325–409.

Wilder, H. H. (1912). The appendicular muscles of *Necturus maculosus*. *Zoologischen Jarbüchern Supplement*, *15*, 383–424.

Williston, S. W. (1911). *American Permian Vertebrates*. University of Chicago Press.

Witmer, L. M. (1995). The extant phylogenetic bracket and the importance of reconstructing soft tissues in fossils. In J. J. Thomason (Ed.), *Functional Morphology in Vertebrate Paleontology* (pp. 19–33). Cambridge University Press.

Wynd, B. M., Peecook, B. R., Whitney, M. R., & Sidor, C. A. (2017). The first occurrence of *Cynognathus crateronotus* (Cynodontia: Cynognathia) in Tanzania and Zambia, with implications for the age and biostratigraphic correlation of Triassic strata in southern Pangea. *Journal of Vertebrate Paleontology*, *37*(suppl. 1), 228–239.

Xu, X., Clark, J. M., Mo, J., Choiniere, J. N., Forster, C. A., Erickson, G. M., Hone, D. W. E., Sullivan, C., Eberth, D. A., Nesbitt, S. J., Zhao, Q., Hernandez, R., Jia, C.-k., Han, F.-I., & Guo, Y. (2009). A Jurassic ceratosaur from China helps clarify avian digital homologies. *Nature*, *459*, 940–944.

Young, C.-C. (1947). Mammal-like reptiles from Lufeng, Yunnan, China. *Proceedings of the Zoological Society of London*, *117*, 537–597.

Yuan, C.-X., Ji, Q., Meng, Q.-J., Tabrum, A. R., & Luo, Z.-X. (2013). Earliest evolution of multituberculate mammals revealed by a new Jurassic fossil. *Science*, *341*, 779–783.

Zaaf, A., Herrel, A., Aerts, P., & De Vree, F. (1999). Morphology and morphometrics of the appendicular musculature in geckoes with different locomotor habits (Lepidosauria). *Zoomorphology*, *119*, 9–22.

Zug, G. R. (1971). Buoyancy, Locomotion, Morphology of the Pelvic Girdle and Hindlimb, and Systematics of Cryptodiran Turtles. *Miscellaneous Publications Museum of Zoology, University of Michigan*, *142*, 1–98.

SUPPORTING INFORMATION

Additional supporting information can be found online in the Supporting Information section at the end of this article.

How to cite this article: Bishop, P. J., & Pierce, S. E. (2024). The fossil record of appendicular muscle evolution in Synapsida on the line to mammals: Part II—Hindlimb. *The Anatomical Record*, *307*(5), 1826–1896. https://doi.org/10.1002/ar.25310